TECHNICAL REPORT 5-6717-01-1
TxDOT PROJECT NUMBER 5-6717-01

Implementation of a Testing Protocol for Approving Alternative Supplementary Cementitious Materials (SCMs): Natural Minerals and Reclaimed and Remediated Fly Ashes

Saif Al-Shmaisani
Ryan Kalina
Michael Rung
Dr. Raissa Ferron
Dr. Maria Juenger

Technical Report Documentation Page

1. Report No. FHWA/TX-18/5-6717-01-1	2. Government Accession No.	3. Recipient's Catalog No.	
4. Title and Subtitle Implementation of a Testing Protocol for Approving Alternative Supplementary Cementitious Materials (SCMs): Natural Minerals and Reclaimed and Remediated Fly Ashes		5. Report Date August 2017; Published February 2018	
		6. Performing Organization Code	
7. Author(s) Saif Al-Shmaisani, Ryan Kalina, Michael Rung, Raissa Ferron, Maria Juenger		8. Performing Organization Report No. 5-6717-01-1	
9. Performing Organization Name and Address Center for Transportation Research The University of Texas at Austin 1616 Guadalupe Street, Suite 4.202 Austin, TX 78701		10. Work Unit No. (TRAIS)	
		11. Contract or Grant No. 5-6717-01	
12. Sponsoring Agency Name and Address Texas Department of Transportation Research and Technology Implementation Office P.O. Box 5080 Austin, TX 78763-5080		13. Type of Report and Period Covered Technical Report; 9/1/2015–8/31/2017	
		14. Sponsoring Agency Code	
15. Supplementary Notes Project performed in cooperation with the Texas Department of Transportation and the Federal Highway Administration.			

16. Abstract

Supplementary cementitious materials (SCMs) provide many benefits to concrete mixtures in terms of cost, long-term strength, and durability. Class F fly ash is the most widely used SCM in Texas, but its availability is dwindling while demand is increasing. Given the importance of Class F fly ash as a means to improve concrete durability, it is important to find alternative materials that can maintain the high quality and durability of concrete required in Texas. TxDOT Project 0-6717: Investigation of Alternative Supplementary Cementing Materials (SCMs), completed in August 2014, identified sources of Class F fly ash alternatives that can be used in Texas concrete and developed best practices for testing these materials. Lower cost sources of materials have been identified since the completion of that project and may present better opportunities for Class F fly ash replacement than those initially tested. These materials include natural mineral byproducts of other industries, reclaimed fly ashes, and remediated fly ashes. The experimental protocols developed in Project 0-6717 were performed on these new sources of materials to determine their suitability for use in Texas concrete. The materials were chemically and physically characterized, and their performance in cement paste, mortar, and concrete mixtures was tested. It was determined that some of the natural minerals were inert; thus, they are not recommended for use in concrete. Natural pumicite performed well as an SCM, including a pumicite that is quarry overburden and could be procured at a relatively low cost. This overburden pumice, however, did not perform as well as expected in testing for sulfate resistance and merits further investigation. It is possible that the overburden pumicite would perform better if used as at a higher replacement level of cement. The reclaimed and remediated fly ashes performed very well, proving their ability to be used as substitutes for "production" Class F fly ash based on the criteria established in this project. In the cases where reduced performance was seen in fly ashes, the problems should be easily managed through the addition of chemical admixtures.

17. Key Words Fly Ash, Pozzolans, Concrete, SCMs, Pumice, Reclaimed, Remediated, Durability		18. Distribution Statement No restrictions. This document is available to the public through the National Technical Information Service, Springfield, Virginia 22161; www.ntis.gov.	
19. Security Classif. (of report) Unclassified	20. Security Classif. (of this page) Unclassified	21. No. of pages 140	22. Price

Form DOT F 1700.7 (8-72) Reproduction of completed page authorized

THE UNIVERSITY OF TEXAS AT AUSTIN
CENTER FOR TRANSPORTATION RESEARCH

Implementation of a Testing Protocol for Approving Alternative Supplementary Cementitious Materials (SCMs): Natural Minerals and Reclaimed and Remediated Fly Ashes

Saif Al-Shmaisani
Ryan Kalina
Michael Rung
Dr. Raissa Ferron
Dr. Maria Juenger

Center for Transportation Research
The University of Texas at Austin
1616 Guadalupe, Suite 4.202
Austin, TX 78701

http://ctr.utexas.edu/

Disclaimers

Engineering Disclaimer

Research Supervisor: Dr. Maria Juenger

Acknowledgments

Table of Contents

List of Figures

List of Tables

Chapter 1. Introduction

1.1 Motivation and Objective

Supplementary cementitious materials (SCMs) are commonly used in concrete mixtures as partial replacements of portland cement, with more than 60% of ready-mixed concrete in the U.S. containing SCMs (Juenger and Siddique, 2015). Currently in Texas, fly ash is the most commonly used SCM and is added to concrete to replace 15–35% of portland cement by weight. Fly ash, as defined by the American Concrete Institute (ACI CT-16, 2016, p.30) is "the finely divided residue that results from the combustion of ground or powdered coal and that is transported by flue gases from the combustion zone to the particle removal system." ASTM C 618 (2015) categorizes fly ash in two different classes: Class C fly ash, containing greater than 50% combined silica, alumina and iron oxide, and Class F fly ash, consisting of greater than 70% of these oxides. Class F fly ash is used predominantly in Texas and most of the U.S. due to its ability to provide resistance to alkali-silica reaction (ASR) as well as sulfate attack (Thomas et al., 2017). Additionally, fly ash is cheaper than portland cement, being a coal combustion by-product, costing approximately $45/ton in Texas, compared to portland cement at $120/ton. Fly ash in concrete is used as a pozzolan, which, as defined by ACI CT-16 (2016, p.50), is "a siliceous or silico-aluminous material that will, in finely divided form and in the presence of moisture, chemically react with calcium hydroxide at ordinary temperatures to form compounds having cementitious properties." Although the use of pozzolans dates back to the ancient civilizations of Greece and Rome where they used volcanic ash in their cementitious mixtures, the potential for using fly ash as a pozzolan was not realized until the early 1900s and still was not widely available until the 1930s (Thomas et al., 2017). The use of fly ash in concrete affects both the fresh state and hardened state properties in positive ways by increasing the workability, reducing bleeding, improving pumpability, reducing the heat of hydration, increasing strength gain at later ages and refining the pore structure to reduce permeability (ACI 232, 2003). Class F fly ash can also improve concrete durability by increasing resistance of concrete to ASR and sulfate attack.

In 2015, the U.S. generated approximately 106.4 million metric tons of coal combustion products, 38% (approximately 40.2 million metric tons) of which was fly ash. Of the 40.2 million metric tons of fly ash, 21.8 million metric tons (54%) of the overall ashes were utilized in other industries (ACAA, 2016). Based on the American Coal Ash Association (ACAA) data, the percentage of fly ash utilized has increased in the past five years because the amount produced has dropped 34%, and the amount utilized has remained relatively stagnant (ACAA 2011; 2016). This can be largely attributed to competing fuel sources for electricity generation, such as natural gas, as well as emission standards issued by the Environmental Protection Agency (EPA) in 2011 requiring coal-fired power plants to install emission control systems, which, in turn, reduces the quality of the fly ash. Natural gas is a cheaper alternative to coal, so as a result, no new coal-fired power plants have been constructed in the U.S. since 2013 even though there are plant retirements forecasted through 2040 (US EIA, 2017). In the last five years, there have been 200 plant closures (about 40%) in the U.S., and the U.K. is set to have its remaining coal-fired power plants retired by 2025 (McCarthy et al., 2017). This will become a problem in regards to concrete production, following a study conducted by the American Road and Transportation Builders Association (ARTBA), which estimates that concrete production will increase more than 50% through 2033 (ARTBA, 2015; Diaz-Loya et al., 2017).

In order to prepare for the upcoming shortage in fly ash supply, the Texas Department of Transportation (TxDOT) funded Project 5-6717-01 with the purpose of testing potential alternatives for "production" Class F fly ash for use in concrete. In this report, the term "production" with respect to fly ashes denotes fly ashes that require no additional modifications after recovery from coal-fired power plant using electrostatic precipitators or mechanical devices such as baghouses. The alternative materials that were tested in this implementation project included reclaimed fly ashes, remediated fly ashes, and natural minerals. Reclaimed fly ashes are fly ashes that are retrieved from disposal sites, while remediated, or beneficiated, fly ashes are those that do not meet the requirements of ASTM C 618 specifications and are treated in order to do so. Beneficiation, as defined by ACI CT-16 (2016, p. 7), is the "improvement of the chemical or physical properties of raw material or intermediate product by the removal or modification of undesirable components or impurities." Natural minerals are raw or calcined natural materials.

1.2 Literature Review

This literature review presents some background information on the SCMs that have been selected for testing as potential low-cost alternatives to production Class F fly ash in concrete used for TxDOT projects. Specifically, the following alternative SCMs are discussed: reclaimed fly ashes, remediated fly ashes, and natural mineral by-products (pumicite, nepheline syenite, dacite, rhyolite). In order for SCMs to be approved for use by TxDOT, they must meet certain requirements. Background information on the composition of the materials, the potential for pozzolanic activity, and the behavior of cementitious mixtures utilizing the materials, when available, is presented.

1.2.1 TxDOT Requirements for SCMs

The permissible SCMs for hydraulic cement concrete mixture designs are designated in Section 421.2.B in Section 4.2.6 of Item 421 in the 2014 edition of the TxDOT Standard Specifications for Construction and Maintenance of Highways, Streets, and Bridges (TxDOT, 2014). This specifies the use of Class C and F fly ashes, ground-granulated blast furnace slag, silica fume, and metakaolin, which is the only natural pozzolan allowed in concrete mixture design. However, the use of other natural minerals is allowed in concrete mixture designs if the materials meet requirements set forth by Section 4.2.6, which outlines eight options for acceptable concrete mixture designs (TxDOT, 2014). Use of SCMs other than those outlined in Section 4.2.6 depends on the ability of the concrete mixture design utilizing that SCM to limit expansion from ASR to 0.08%, per testing procedures in ASTM C1567 (TxDOT, 2014; ASTM 2013).

Besides durability improvements, TxDOT also recognizes other properties of concrete mixtures that are changed with the use of SCMs, such as heat of hydration, setting times, and water demand. Therefore, these properties will also be discussed for the selected materials.

1.2.2 Reclaimed Fly Ash

Of the 40.2 million metric tons of fly ash produced in U.S. in 2015, 21.8 million metric tons (54%) of the overall ashes were utilized (ACAA, 2016). The remaining unused fly ashes are disposed of due primarily to storage space constraints or failure to meet the requirements of ASTM C 618, with landfill disposal and surface impoundments by ponding being the most frequently used waste management methods, accounting for up to 80% of total unused ashes in the U.S. in 2012 (EPA, 2017). Ponding is a process in which unused ash is mixed with significant quantities

of water, sluiced and pumped along pipelines to ponds as a slurry, where it naturally settles (White, 2006; Sobolev and Batrakov, 2007; McCarthy et al., 2017). However, there is pressure to end the use of surface impoundments following the ash dam failure at the Kingston power plant in Tennessee in 2008 along with concerns about groundwater contamination. Many U.S. power plants have or will be converting to landfilled systems for disposal, where the fly ash is conditioned with relatively low levels of water (10–20%), which reduces dusting and optimizes compaction, and is then disposed of in large horizontal cells (Diaz-Loya et al., 2017; McCarthy et al., 2017). In the U.S. in 2012, there were more than 310 active on-site landfills, averaging more than 120 acres in size, and more than 735 active on-site surface impoundments, averaging more than 50 acres in size (EPA, 2017). Landfilled or ponded ashes can be reclaimed, retrieved or recovered, and then beneficiated or treated to improve physical or chemical properties, in order to be reused. Disposal sites run the risk of groundwater contamination and the release of fugitive dust to nearby communities, which can be reduced by reclamation of these materials. Investing in a beneficiation facility can lead to millions of dollars in savings over the life of the plant compared to costs accrued from disposal site development, construction, equipment purchases, operation, closure, and post-closure, as well as a reduction in liability associated with disposal (Fedorka et al., 2015). Although ashes can be reclaimed from both types of disposal sites (landfills or ponds) ponded or hydrated ashes are usually excavated only to be used as artificial aggregates or structural fill material such as in pavement subgrades.

Material characterization data on reclaimed fly ash show comparable values from oxide analysis, x-ray diffraction and scanning electron microscope images to production ashes, showing no major changes in composition and shape (Diaz-Loya et al., 2017; McCarthy et al., 2017). However, McCarthy et al. (2017) showed that fineness and loss-on-ignition (LOI) increased with the increasing length of the wet-storage period. The researchers also noted the differences in fly ashes reclaimed from U.K. ponds and from U.S. ponds and advised to consider storage areas individually when considering reclamation.

Few studies have implemented the use of unmodified reclaimed fly ash. Cheerarot and Jaturapitakkul (2004) tested disposed fly ashes that had been landfilled for 6, 12 and 24 months. They examined the effect of the ashes on mortar compressive strength, replacing 10%, 20% and 30% by mass of cement with these ashes following ASTM C 109 procedures. A decrease of 10-20% of compressive strength for 10% substitution and a larger decrease in strength for higher substitution amounts were observed. No relationship was found between the length of time spent in the landfill and compressive strength (Cheerarot and Jaturapitakkul, 2004). In another study by McCarthy et al. (2017), wet fly ashes from stockpiles were used as a cement replacement in concrete, accounting for moisture conditions in the batching stage, similar to wet aggregates, where the procedure involved includes: measuring the moisture content of fly ash, taking the water content of concrete as that batched plus that in fly ash, and adjusting the fly ash content to allow for water present in the material. Results showed that fresh and hardened properties of concrete containing the reclaimed stockpiled fly ash could be controlled by making mixture adjustments. However, handling issues could occur at ready-mix and precast concrete plants. Drying and grinding of the reclaimed fly ash could prevent this issue (McCarthy et al., 2017).

It is possible to have minimal beneficiation with landfill ashes due to the fly ash in the stockpile remaining relatively homogeneous; however, the ashes are susceptible to agglomeration, which requires additional beneficiation. Ponded ashes have high water levels that disperse rather than agglomerate the particles, so the particles then sort and stratify, resulting in a heterogeneous material (McCarthy et al., 2017). As a result of this, ponded fly ashes must be beneficiated in order

to meet ASTM C 618 (2015) requirements. Beneficiation transforms fly ash from a by-product, "an incidental or secondary product made in the manufacture or synthesis of something else," to a product, "an article or substance that is manufactured or refined for sale," due to the added energy used in refining the material (Oxford Dictionaries, 2017). Ponded fly ash can be beneficiated by particle separation and grinding to meet these requirements. For example, Ranganath et al. (1998) tested ponded ash and evaluated the influence of size fraction by separating the ash into different particle size ranges: <20 μm (F), 20-75 μm (M), and 75-100 μm (C). The C fraction of the ponded ash showed low values of specific gravity, fineness, and strength in lime reactivity testing, all of which adversely affect fly ash properties in concrete. The poorly reactive C fraction was found to be 65% of the ponded ash with the M and F fraction comprising the remaining 35%, making reclaimed fly ash unusable in its "as-disposed" state. Berry et al. (1989) also evaluated beneficiated fly ash with fractions of <10 μm, 10-45 μm, and >45 μm, resulting in a similar conclusion to that of Ranganath et al. (1998), finding that the fly ashes with finer particles were more reactive than the coarser ones. Cheerarot and Jaturapitakkul (2004) also found that grinding or milling the reclaimed fly ash resulted in similar early age strength as production fly ash and an increase in late strength in relation to the OPC control. Diaz-Loya et al. (2017) also performed compressive strength and ASR expansion testing of mortars using a production fly ash and a reclaimed fly ash that had been dried to less than 3% moisture content, then classified by screening to achieve a similar fineness to the production fly ash. The results of the testing showed equivalent performance of the reclaimed fly ash to the production fly ash.

Other forms of beneficiation can and have been done on reclaimed fly ashes, discussed in detail by McCarthy et al. (2017). Preliminary treatment of material includes slurrying of the fly ash in order to wash and de-agglomerate the material followed by screening to remove coarser and unwanted particles. Froth flotation can then be performed to separate carbon char from fly ash by the addition of frothing agent and injection of air causing non-wettable materials (carbon particles) to attach to bubbles. Next, additional screening using wire mesh can be performed followed by hydraulic classification, which separates particles by differential settling, where large particles fall at a faster rate than smaller particles. The fly ash slurries are then thickened to help remove excess water and dried. The materials tested and presented by McCarthy et al. (2017) proved to perform well if the gradation of the reclaimed fly ash was restored to that of the original fly ash.

1.2.3 Remediated Fly Ash

Emission standards issued by the EPA in 2011 requiring coal-fired power plants to install emission control systems has resulted in a reduction in the quality of the fly ash. Fly ashes with high carbon content, improper composition, or improper particle size that do not meet the requirements of ASTM C 618 specifications can be treated in order to meet the specifications; such materials are called remediated or beneficiated. It is important to note that these remediated fly ashes differ from reclaimed fly ashes that have been remediated since they have not been disposed of in landfills or ponds. Air pollution controls focus on reducing emissions from sulfur oxides (SOx), nitrogen oxides (NOx) and mercury. In order to reduce SOx emissions, dry sorbent injection (DSI) is used in several plants (Ladwig and Blythe, 2017). These injections can be either hydrated lime powder or sodium-based such as trona or sodium bicarbonate, which remove SO_3 by a gas-solid reaction (Ladwig and Blythe, 2017). These sorbents, however, contaminate the fly ash with free lime and calcium sulfite/sulfate or sodium carbonate and sulfate, respectively (Diaz-Loya et al., 2017). Selective catalytic reduction (SCR) is used at power plants in the U.S. to control the NOx emissions due to increased air pollution control standards (Howard et al., 2013; Hamley

et al., 2001). SCR uses ammonia to reduce the NOx emissions of coal-fired power plants by converting it to nitrogen gas; excess ammonia collects in the fly ash, which does not affect fly ash performance in concrete, but does pose as a health hazard to workers handling concrete (Diaz-Loya et al., 2017). Activated carbon injection systems use activated carbon to scrub mercury from the flue gases, which can get intermingled with the fly ash (Diaz-Loya et al., 2017). This results in an increased amount of unburned carbon in fly ash, resulting in a failure to meet the ASTM specifications and affecting the stability of air-entrainment agents in concrete mixtures. The amount of carbon present in the ashes is measured by LOI. The LOI in Class C and Class F fly ash used in concrete is limited by ASTM C 618 (2015) specifications to be no more than 6%.

Several methods exist to treat fly ash that do not comply with ASTM specifications, such as (Robl, 2017):
- Blending;
- Selective collection, which involves segregating the fly ash by monitoring LOI and/or fineness, allowing higher quality ash to be recovered from the rest of the batch;
- Chemical passivation, which reduces the activity of carbon in fly ash and avoids the need for large amounts of air entraining admixtures by adding a chemical that will react with the active sites on the carbon, neutralizing them, or by adding a chemical that will encapsulate the carbon;
- Air classification, which uses centrifugal force to selectively separate the coarse particles of the fly ash from the finer particles;
- Electrostatic separation, where interparticle contact or "tirbocharging" charges the particles and causes them to move in opposite directions on a moving open-mesh belt to remove carbon;
- Thermal beneficiation, where combustion is used to reduce carbon content and ammonia as well as improve fineness.

Another method to treat fly ash with high carbon contents includes treatment with supercritical water. Hamley et al. (2001) performed research in which high carbon fly ashes were treated through a process of supercritical water oxidation (SCWO). A supercritical fluid is at temperatures above its vapor-liquid critical point, in which the behavior of the fluid is in between a liquid and a gas. Therefore, the fluid has the solvating property of a liquid and diffusivity of a gas. During the process of SCWO, the oxidation reactions occur in a homogenous phase where carbon is converted to carbon dioxide, hydrogen to water, nitrogen-containing substances to nitrogen, and sulfur-containing substances to sulfuric acid (Hamley et al., 2001). The researchers treated seven fly ashes with high carbon content utilizing the method of SCWO. The treatment process resulted in a reduced LOI in all of the ashes, ranging between a 19.0% and 82.5% reduction. The ashes with higher initial carbon content resulted in a higher removal efficiency.

Fly ash not meeting ASTM specifications based on particle size may be treated by mechanical grinding methods. Grinding aids are utilized to improve grinding efficiency, which reduces energy consumption. Zelinkova et al. (2013) studied the effects of laboratory and industrial grinding, with and without grinding aids, on fly ash particle size distribution. Laboratory grinding was performed for 18, 30, 42 and 60 minutes, while industrial grinding was completed at 30, 45 and 60 minutes with and without grinding aids. In all of the fly ash samples, with or without grinding, the smallest particle size was found to be in the range of 1-20 μm. Grinding for 60 minutes proved to be most effective in increasing the percentage of particles in that size range. Laboratory grinding only increased the percentage of small particles slightly, while industrial

grinding increased the percentage of particles in that range from 46%, without grinding, to up to 80%. It was also found that industrial grinding with and without grinding aids resulted in nearly identical particle ranges. Therefore, there is no negative effect of utilizing grinding aids, which is better for reducing energy consumption (Zelinkova et al., 2013).

1.2.4 Pumicite

Pumice was tested in TxDOT 0-6717 as a natural mineral; the literature on pumice as an SCM was reviewed in that project (Seraj et al., 2014). However, that project did not address pumice blends or low-quality, low-cost pumice by-products from quarrying higher purity pumice. Pumice blends have been implemented in concrete structures in the US including the Friant Dam, Altus Dam, and Glen Canyon Dam (Elfert, 1974). Kabay et al. (2015) compared the properties of concrete using pumice powder (PP), fly ash (FA), and a blend of both materials. Cement was replaced at 10% and 20% by mass of each material and a pumice-fly ash blend that consisted of equal ratios of pumice and fly ash. Mixtures containing PP had a higher water demand and lower slump due to the irregular shape and high porosity of pumice, while the mixes with only FA substitution had results nearly identical to the OPC control. All PP and FA mixes had delayed initial and final setting time, typical of concrete with pozzolanic substitution. A denser microstructure, compared to the control, was also found through the use of both PP and FA, resulting in lower porosity and absorption, which prevents the ingress of deleterious chemicals, improving the durability of the concrete. Compressive strength testing results showed a decrease in early age strength compared to the control mixture; however, later age specimens had strengths similar to the control. The use of pumice in concrete also influenced magnesium sulfate resistance, with the pumice mixtures performing best against magnesium sulfate attack after 360 days of exposure.

1.2.5 Feldspar and Related Minerals

Feldspar is the most abundant mineral group in the earth's crust, accounting for approximately 60% of terrestrial rocks. Feldspar is a group of minerals that are chemically comprised of aluminum silicates, containing sodium, potassium, iron, calcium, barium, or a combination of these elements. Feldspar is used in industrial applications for its alumina and alkali content, with products including glass, fiberglass, floor tiles, shower basins, and tableware (IMANA, 2015).

Nepheline is a feldspar mineral found in intrusive and volcanic rocks that is under-saturated in silica (Spencer, 1911). Syenite is an intrusive igneous rock, having a component of alkali feldspar, with a composition similar to granite, but is lacking in quartz (Lieber, 1856). Nepheline syenite is silica-deficient feldspathic rock, and is primarily composed of nepheline, sodium feldspar (albite), and syenite. The high strength, water resistant, and ultraviolet resistant properties of nepheline syenite make it ideal for roofing granules by preventing degradation of asphalt roofing materials (McLemore, 2006). Additionally, nepheline syenite is utilized in road materials, riprap, fertilizer, paper, ingredients in refractory cement, aggregate for asphalt and concrete, and manufacturing of glass, ceramics, and flatware.

Researchers at the Royal Institute of Technology in Stockholm, Sweden performed testing of cement paste mixtures containing 20% and 40% replacement of nepheline syenite in order to test minerals other than quartz. The nepheline syenite utilized in the testing was comprised of 56.1% SiO_2, 24.3% Al_2O_3, 0.1% Fe_2O_3, 9.0% K_2O, and 8.3% Na_2O. The density of the material was 2.56 g/cm^3. A superplasticizer was utilized to achieve adequate workability of the mixtures

(Vogt, 2010). The 28-day compressive strengths of mixtures containing nepheline syenite ranged between approximately 52 MPa at w/c=0.5 to approximately 39 MPa at w/c=0.8, and mixtures containing nepheline syenite experienced greater amounts of drying shrinkage in comparison to the other materials tested, with a magnitude of 0.7 mm/m at 175 days. The researcher concluded that the high magnitude of shrinkage was likely due to a slow chemical reaction between the cement and nepheline syenite (Vogt, 2010).

Dacite is an igneous volcanic rock, consisting mostly of plagioclase feldspar, with some quartz (Flett, 1911). The composition of dacite is between andesite and rhyolite (Kayali, 2008). This mineral can also be used in roofing material. Research has been conducted utilizing dacite as an aggregate (coarse and fine) in concrete, which is popular in Australia (Kayali, 2008). The composition of the dacite used in research contained 65.7% SiO_2, 15.6% Al_2O_3, 2.1% Fe_2O_3, 2.1% FeO, 2.0% K_2O, and 3.7% Na_2O (Arabani and Azarhoosh, 2012). The bulk densities of the material consisted of 2.650 g/cm^3 as coarse aggregate and 2.657 g/cm^3 as fine aggregate (Kayali, 2008). No research utilizing dacite as a replacement for cement was found at the time of this report.

Rhyolite is an extrusive igneous rock, comprised of quartz, plagioclase, and sanidine, having a high silica content (Geology.com, 2015). This mineral can also be used in roofing material. Research containing rhyolite consisted of utilizing the material as an aggregate for concrete. When used with low-alkali cements with alkali contents ranging between 0.35% and 0.6%, deleterious reactivity of the rhyolite aggregate was found to exist (Farny and Kerkhoff, 2007). No research utilizing rhyolite as a replacement for cement was found at the time of this writing.

1.3 Materials Selected for Testing

Materials were received from multiple entities and are mainly sourced in Texas or neighboring states where the material could be shipped at low cost. The materials were provided by three suppliers, designated as Supplier A through C and materials were designated as "D" for dacite, "NS" for nepheline syenite, "P" for pumicite, "R" for rhyolite, "RC" for reclaimed fly ash, or "RM" for remediated fly ash followed by a single letter, which designates a supplier, plant, or material physical characteristic. Table 1.1 contains a list of the materials and the sources. The materials from Supplier A are byproducts of grinding the natural minerals for use in a commercial, non-concrete product. They are, therefore, available at a low cost relative to other natural minerals used as pozzolans in concrete. The natural minerals from Supplier B are both pumicites. The P-W is a relatively pure pumicite that can be used in many applications. The P-B is quarry overburden and could, therefore, likely be obtained at a lower cost. While most of the fly ashes come from different power plants, the RC-M and RM-M from Supplier C are from the same plant, with the RM-M remediated to improve performance since the ash from that plant was carbon-injected.

Table 1.1: Controls and Materials Procured for this Study

Supplier	Designation	Source	Material Classification
Control	OPC	Texas	Type I (ordinary) Portland Cement
	FA	Texas	Production Class F Fly Ash
	Q	West Virginia	Ground Quartz
A	D-L	California	Natural Mineral
	D-S	California	Natural Mineral
	NS-I	Arkansas	Natural Mineral
	NS-L	Arkansas	Natural Mineral
	NS-S	Arkansas	Natural Mineral
	R-O	Wisconsin	Natural Mineral
B	RM-C	Colorado	Remediated Fly Ash
	RM-L	Texas	Remediated Fly Ash
	RM-S	Oklahoma	Remediated Fly Ash
	P-B	New Mexico	Natural Mineral
	P-W	New Mexico	Natural Mineral
C	RC-G	Texas	Reclaimed Fly Ash
	RC-M	Texas	Reclaimed Fly Ash
	RC-P	Texas	Reclaimed Fly Ash
	RM-M	Texas	Remediated Fly Ash

Chapter 2. Material Characterization

Prior to conducting paste, mortar, and concrete mixture performance testing, the SCMs were characterized in order to be able to correlate performance with material properties. Characterization tests included standardized ASTM C618 (2015) tests and advanced characterization techniques (Table 2.1). In certain cases, where prior testing data were already available, the tests were not duplicated. The control materials, cement, production fly ash, and quartz, were also characterized.

Table 2.1: SCM Characterization Tests

Category	Property	Test Method
ASTM C618/C311	Oxide Composition	X-ray Fluorescence (XRF)
	Moisture Content	Oven Drying
	Loss on Ignition	Oven Drying
	Fineness	No. 325 Sieve (Wet)
	Soundness	Autoclave
	Density	Pycnometer
	Strength Activity Index	Mortar Compression Testing
Advanced Characterization Tests	Particle Size	Laser Particle Size Diffraction
	Particle Shape	Scanning Electron Microscopy (SEM)
	Phase Composition	X-ray Diffraction (XRD)
	Phase Composition	Differential Scanning Calorimetry/Thermal Gravimetric Analysis (DSC/TGA)

2.1 ASTM C618 Characterization Tests

ASTM C618 specifies the property requirements of coal fly ash (Class F and Class C) and raw or calcined natural pozzolans (Class N) for use in concrete. The standard refers to ASTM C311 (2013), which provides the procedures for sampling and testing. The testing was performed at the University of Texas at Austin (UT), unless otherwise noted.

2.1.1 Oxide Composition

The oxide composition of the materials was determined by X-ray fluorescence (XRF) testing, performed by J.C. Montelongo at TxDOT. ASTM C618 specifies that in order for a material to be considered a Class F fly ash or Class N pozzolan, the sum of the silicon dioxide (SiO_2), aluminum oxide (Al_2O_3), and ferric oxide (Fe_2O_3) must be at least 70%. A material is considered a Class C fly ash if the sum of these oxides is greater than 50% and less than 70%. A Class F fly ash can also have a maximum of 5% sulfur trioxide (SO_3). The complete oxide analyses for the reclaimed and remediated fly ashes as well as the control materials, OPC and FA, are

presented in Table 2.2. The sum of SiO_2, Al_2O_3 and Fe_2O_3 is not shown for OPC since it is not required for cement. Based on the results, RC-P does not meet the ASTM specifications for a Class F fly ash. However, RC-P does meet the ASTM specifications for a Class C fly ash.

The remediated fly ashes from Supplier B had similar oxide compositions, with RM-S having a slightly higher Fe_2O_3 content and lower CaO content than the others. From Supplier C, RC-M and RM-M have similar oxide compositions, since they are from the same power plant, as discussed earlier. RC-G is very similar in oxide composition to the production fly ash, FA. The natural minerals had comparable oxide compositions between materials with similar origins (i.e., dacites, nepheline syenites, and pumicites).

Table 2.2: Oxide Analysis from XRF

Supplier	Material	SiO_2 (%)	Al_2O_3 (%)	Fe_2O_3 (%)	CaO (%)	MgO (%)	SO_3 (%)	Na_2O (%)	K_2O (%)	SiO_2+ Al_2O_3+ Fe_2O_3 (%)
Control	OPC	20.36	5.82	2.30	62.49	1.36	3.30	0.15	0.89	--
	FA	50.88	22.79	5.01	10.60	2.45	0.47	0.13	0.86	78.68
A	D-L	66.29	15.57	4.85	3.08	1.22	0.09	3.60	2.85	86.71
	D-S	65.47	15.83	5.15	2.80	1.36	0.07	3.70	3.12	86.45
	NS-I	56.09	18.14	7.26	1.63	0.59	0.17	6.03	5.85	81.48
	NS-L	58.49	18.97	3.69	1.82	0.80	0.16	6.42	6.15	81.15
	NS-S	57.74	19.48	4.05	1.82	0.99	0.19	5.89	5.85	81.27
	R-O	63.26	17.56	4.69	1.69	1.43	0.07	3.60	4.27	85.51
B	RM-C	59.07	14.07	3.16	9.36	1.57	3.41	3.28	2.94	76.30
	RM-L	60.99	13.10	3.08	10.19	0.61	3.92	2.69	3.08	77.17
	RM-S	60.13	14.43	4.65	6.91	1.13	3.22	3.20	3.46	79.21
	P-B	73.69	13.08	2.39	0.75	0.20	0.04	3.65	4.30	89.16
	P-W	73.99	13.08	2.08	0.33	0.00	0.04	4.40	4.27	89.14
C	RC-G	51.50	21.34	4.92	11.33	2.08	2.72	0.17	0.78	77.77
	RC-M	46.95	19.90	8.35	14.05	3.43	0.86	0.77	0.98	75.20
	RC-P	35.73	17.76	5.61	25.69	5.08	2.59	1.64	0.45	59.10
	RM-M	46.95	19.91	8.35	14.06	3.42	0.85	0.77	0.98	75.21

Red text indicates material that does not meet ASTM C618 requirements for Class F fly ash or Class N pozzolan.

2.1.2 Moisture Content and Loss on Ignition

Moisture content (MC) testing and loss on ignition (LOI) testing of the materials were performed in accordance with ASTM C311. ASTM C618 specifies that in order for a material to be considered a Class F fly ash, Class C fly ash, or Class N pozzolan, the MC cannot exceed 3%. In regards to LOI, ASTM C 618 specifies that in order for a material to be considered a Class F

fly ash or Class C fly ash, the LOI cannot exceed 6%; a Class N pozzolan cannot exceed 10%. The results of the MC and LOI testing, including the comparison to the ASTM C 618 specifications, are presented in Table 2.3. The MC and LOI values presented are the average of the results obtained along with the error associated with replicate testing. All of the materials passed the specifications for LOI; however, RC-G and RC-P did not pass the specifications for MC for a Class F fly ash or a Class C fly ash. The supplier has stated that these materials were processed with pilot scale equipment. However, the supplier believes that an industrial-scale processing facility will ensure that the reclaimed fly ashes meet the moisture requirements of ASTM C618.

Table 2.3: Results of MC and LOI Testing

Supplier	Material	MC (%)		LOI (%)	
Control	FA	0.54	+/- 0.06	0.39	+/- 0.09
	Q	0.74	+/- 0.14	0.20	+/- 0.00
A	D-L	1.39	+/- 0.10	1.41	+/- 0.00
	D-S	1.30	+/- 0.10	1.01	+/- 0.10
	NS-I	0.76	+/- 0.05	0.47	+/- 0.25
	NS-L	0.89	+/- 0.00	0.79	+/- 0.00
	NS-S	1.32	+/- 0.06	1.57	+/- 0.15
	R-O	0.94	+/- 0.06	2.91	+/- 0.02
B	RM-C	2.87	+/- 0.01	1.79	+/- 0.16
	RM-L	1.42	+/- 0.55	1.56	+/- 0.16
	RM-S	2.05	+/- 0.06	5.89	+/- 0.10
	P-B	1.95	+/- 0.10	1.16	+/- 0.16
	P-W	2.65	+/- 0.25	2.09	+/- 0.15
C	RC-G	3.89	+/- 0.05	0.87	+/- 0.15
	RC-M	0.87	+/- 0.03	0.73	+/- 0.07
	RC-P	6.96	+/- 0.16	3.42	+/- 0.32
	RM-M	0.87	+/- 0.00	0.59	+/- 0.00

Red text indicates material that does not meet ASTM C618 requirements for Class F fly ash or Class N pozzolan.

2.1.3 Fineness

Fineness of the materials was determined by the amount retained when wet-sieved on a 45 μm (No. 325) sieve as outlined in ASTM C311, and testing was performed in accordance with ASTM C430 (2015). ASTM C618 specifies that in order for a material to be considered a Class F fly ash, Class C fly ash, or Class N pozzolan, the amount retained cannot exceed 34%. The results of fineness testing are presented in Table 2.4. All of the materials passed the specifications for fineness for a Class F fly ash, Class C fly ash, or Class N pozzolan.

Table 2.4: Results of Fineness Testing

Supplier	Material	Percent Retained
Control	OPC	4.93
	FA	25.20
	Q	1.18
A	D-L	16.09
	D-S	6.68
	NS-I	0.17
	NS-L	30.45
	NS-S	4.20
	R-O	7.31
B	RM-C	2.70
	RM-L	15.15
	RM-S	10.10
	P-B	0.00
	P-W	0.04
C	RC-G	10.61
	RC-M	15.30
	RC-P	7.25
	RM-M	15.60

2.1.4 Soundness

Soundness of the materials was determined by measuring the amount of autoclave expansion as outlined in ASTM C311 and performed in accordance with ASTM C151 (2015). ASTM C618 specifies that in order for a material to be considered a Class F fly ash, Class C fly ash, or Class N pozzolan, the autoclave expansion cannot exceed 0.8%. The results of soundness testing are presented in Table 2.5. Results for samples indicated with an asterisk were provided by the suppliers, and, therefore, testing was not duplicated.

Table 2.5: Results of Soundness Testing

Supplier	Material	Expansion (%)
A	D-L*	0.00
	D-S*	0.00
	NS-I*	-0.01
	NS-L*	0.19
	NS-S*	0.19
	R-O*	0.01
B	RM-C*	0.01
	RM-L*	-0.04
	RM-S*	-0.01
	P-B*	0.00
	P-W*	0.00
C	RC-G*	-0.02
	RC-M	0.00
	RC-P*	0.03
	RM-M	0.00

Asterisk (*) indicates test performed by supplier or third party.

2.1.5 Density

Density measurements are performed on materials to ensure uniformity between separate batches of materials, and results must be within a certain variance to comply with ASTM C 618. However, all of the samples studied in this research came from a single batch. Even so, density was still obtained for use in concrete mixture design. The densities of the materials were determined by a gas-comparison pycnometer, performed by J.C. Montelongo at TxDOT. The densities of the materials are presented in Table 2.6.

2.2 Advanced Characterization Tests

2.2.1 Laser Particle Size Analysis

Laser particle size analysis was performed to determine the entire particle size distribution of each material as a supplement to the fineness test. Particle size distribution of the materials can affect reactivity, workability, and cement hydration kinetics due to filler effects. Testing was performed using a Malvern Mastersizer 2000 Laser Diffraction Particle Size Distribution Analyzer. All materials were tested as received, using isopropanol as a dispersant. The results are presented in Table 2.7 and include the particle diameters at 10%, 50% and 90% of the cumulative particle size distribution, designated as d_{10}, d_{50} and d_{90}, respectively. Figures 2.1-2.3 show the particle size distribution of the materials. The particle sizes of the materials were subjectively categorized using a defined range for size, utilizing the median particle size of the materials found

in particle size analysis (Table 2.7). Median particle sizes that ranged from 0 to 10 μm, 10 to 20 μm and 20 to 30 μm were classified as small, medium, and large, respectively.

Table 2.6: Densities of Materials

Supplier	Material	Density (g/cm³)
Control	OPC	3.12
	FA	2.45
	Q	2.63
A	D-L	2.78
	D-S	2.83
	NS-I	2.77
	NS-L	2.72
	NS-S	2.71
	R-O	2.83
B	RM-C	2.45
	RM-L	2.50
	RM-S	2.50
	P-B	2.50
	P-W	2.40
C	RC-G	2.48
	RC-M	2.69
	RC-P	2.54
	RM-M	2.71

Table 2.7: Results of Laser Particle Size Analysis

Supplier	Material	d_{10} (µm)	d_{50} (µm)	d_{90} (µm)	Median Particle Size Category
Control	OPC	2.3	13.9	44.4	Medium
	FA	9.7	26.9	95.7	Large
	Q	4.4	16.2	40.3	Medium
A	D-L	1.9	11.8	62.1	Medium
	D-S	1.6	6.6	40.6	Small
	NS-I	1.4	7.2	27.7	Small
	NS-L	2.4	21.6	97.4	Large
	NS-S	2.1	12.9	48.2	Medium
	R-O	1.6	5.6	38.8	Small
B	RM-C	2.0	6.3	18.7	Small
	RM-L	2.2	9.5	67.0	Small
	RM-S	2.3	9.8	60.6	Small
	P-B	1.5	6.4	23.0	Small
	P-W	1.6	5.2	14.0	Small
C	RC-G	4.3	22.2	63.5	Large
	RC-M	2.6	12.8	59.3	Medium
	RC-P	3.2	17.8	56.9	Medium
	RM-M	2.6	12.6	63.5	Medium
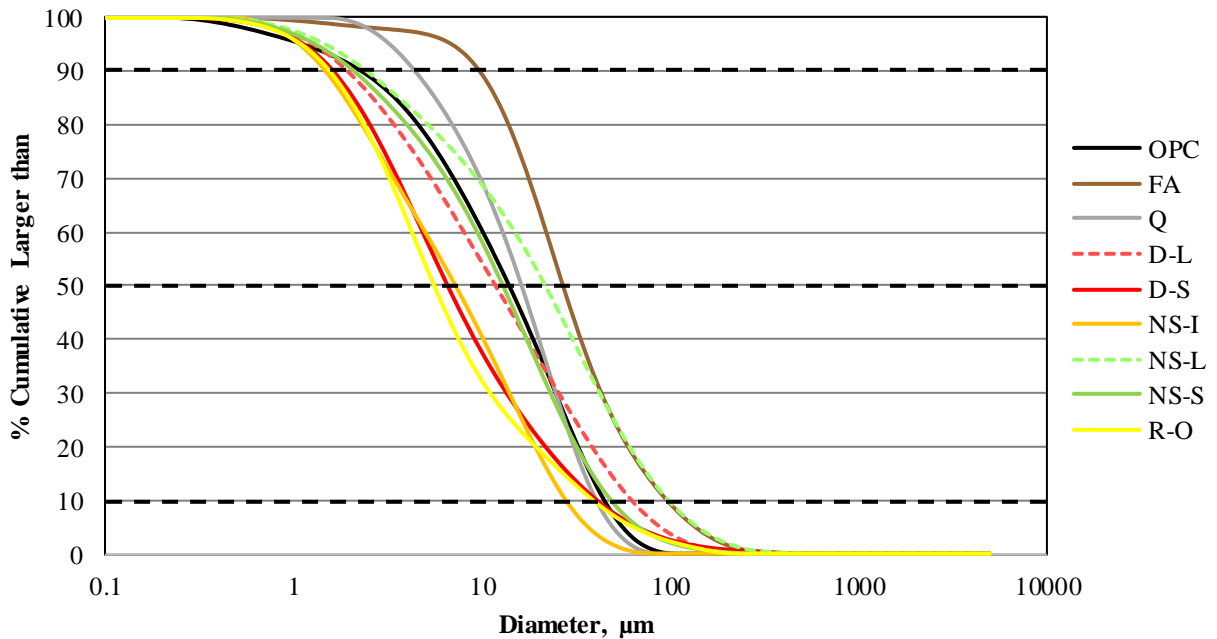
Figure 2.1: Particle size distribution of controls and Supplier A materials
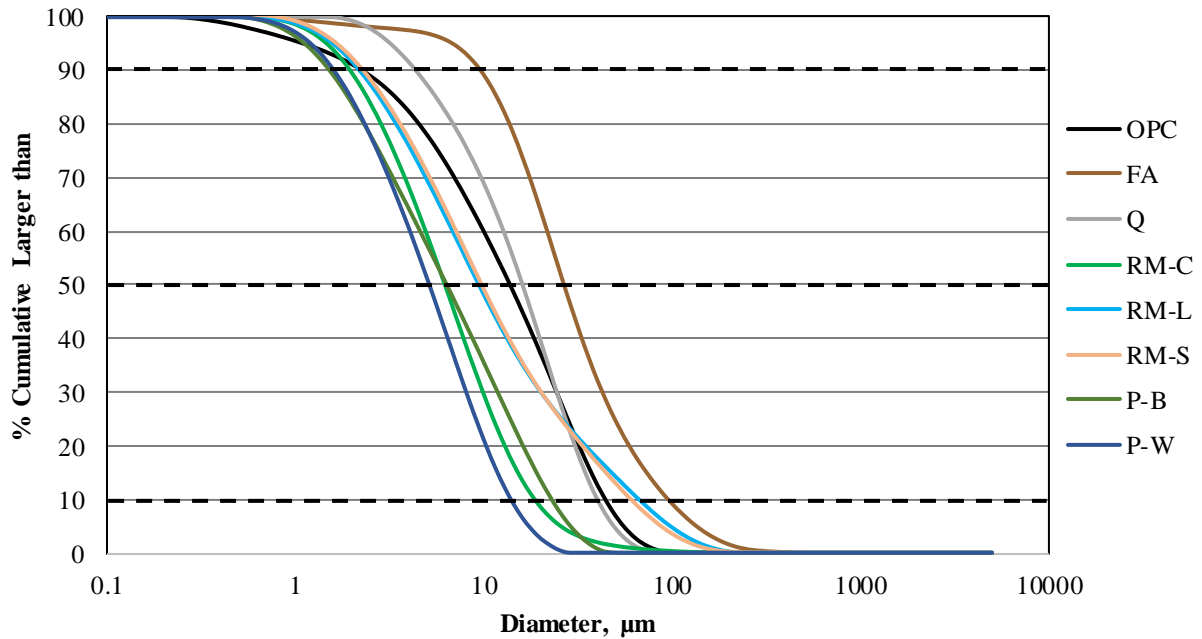
Figure 2.2: Particle size distribution of controls and Supplier B materials
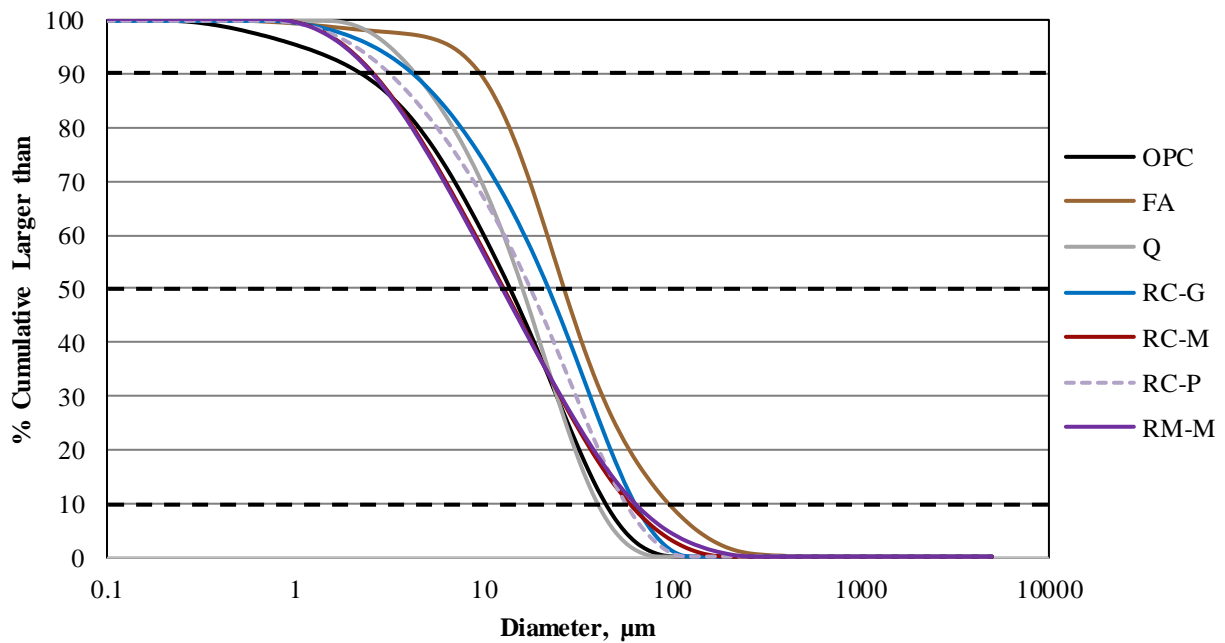
Figure 2.3: Particle size distribution of controls and Supplier C materials

2.2.2 Scanning Electron Microscopy (SEM)

Scanning electron microscopy (SEM) was performed to examine the particle shape of the materials using a Philips/FEI XL30 Environmental Scanning Electron Microscope (ESEM). Samples were mounted on a holder using carbon tape and then lightly blown with compressed air

to remove loose particles. Images were taken in ESEM mode using the Gaseous Secondary Electron (GSE) detector with an accelerating voltage of 20 kV, a spot size of 4, and chamber pressure of 0.2 Torr. Images were taken at three different locations at magnifications of 125, 250, 500, 1000, 2000 and 4000x for each sample.

ESEM images of the materials are shown in Appendix A. Based on the ESEM images, the shapes of the materials were subjectively categorized (Table 2.8). Examples of particles corresponding to the categories are shown in Figures 2.4-2.7. The particle shape categories, as well as the particle size categories shown in Table 2.7, were used to interpret the results from the pastes, mortar, and concrete tests.

The ESEM images shown in Appendix A and particle shape summary in Table 2.8 revealed that the particles for RM-C, RM-L, and RM-S were predominantly angular, which is atypical for fly ashes. This is likely due to the blending process used in remediation. The particles for the natural minerals provided by Suppliers A and B were also predominantly angular. This condition creates the potential for reduced slump in concrete mixtures.

Table 2.8: Particle Shape Categories

Supplier	Material	Particle Shape
A	D-L	Angular
	D-S	Angular
	NS-I	Angular
	NS-L	Angular
	NS-S	Angular
	R-O	Angular
B	RM-C	Partially Angular
	RM-L	Angular
	RM-S	Angular
	P-B	Angular
	P-W	Angular
C	RC-G	Round
	RC-M	Round
	RC-P	Partially Angular
	RM-M	Round
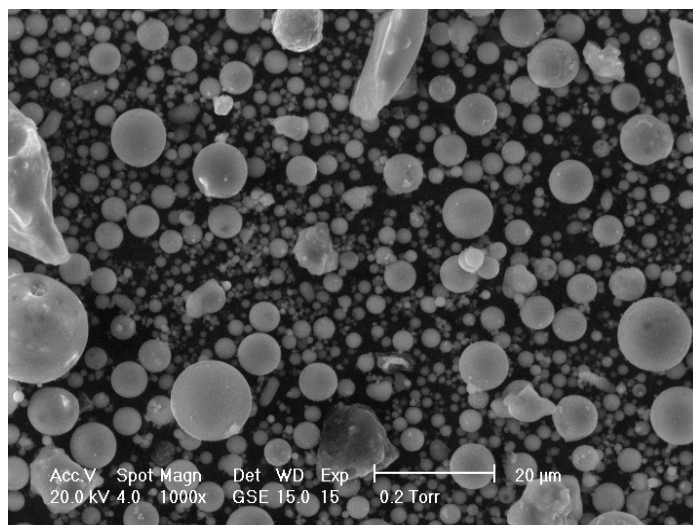
Figure 2.4: ESEM image depicting round particles (RM-M)
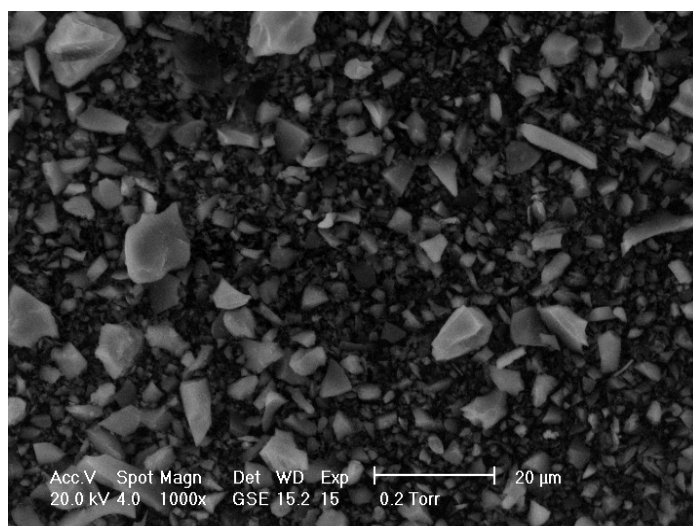
Figure 2.5: ESEM image depicting angular particles (RM-S)
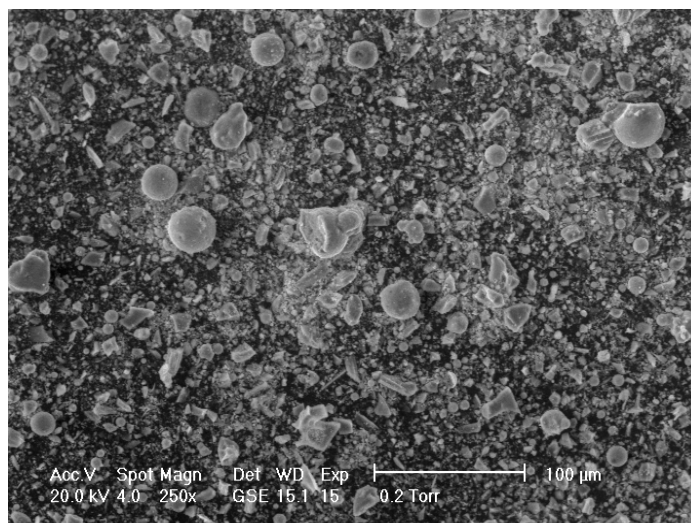
Figure 2.6: ESEM image depicting partially angular particles (RM-C)

2.2.3 X-Ray Diffraction (XRD)

X-ray diffraction (XRD) was performed to determine the main crystalline phases of the materials, which complements the oxide composition results from XRF. The XRD pattern provides a plot (diffractogram) of X-ray intensities at different angles, which was then compared with known crystalline peaks to identify the phases within the materials. These phases are presented in Table 2.9 and X-ray diffractograms can be found in Appendix B. XRD testing was performed using a Rigaku MiniFlex II with the following parameters: a continuous scan at a measurement range of 5º to 75º 2θ, a step size of 0.02º 2θ at a rate of 2º 2θ per second, a tube voltage of 40 kV and a tube current of 15 mA. Prior to performing XRD, the materials were dried at 105 °C and ground to pass through the No. 325 sieve to ensure adequate packing. Samples were then prepared in such a way as to minimize preferential orientation of particles.

2.2.4 Differential Scanning Calorimetry/Thermal Gravimetric Analysis (DSC/TGA)

Differential scanning calorimetry (DSC) and thermal gravimetric analysis (TGA) were performed to assist in determining the composition of the materials. The as-received materials were ground to pass the No. 325 sieve (45 μm) prior to performing the tests. The tests were performed using a Mettler Thermogravimetric Analyzer, Model TGA/DSC 1. The heat flow and mass loss of the samples were recorded as they were heated from 40°C to 1000°C, at a rate of 20 °C/min. The measured mass loss was used to plot the TGA curve and the heat flow was used to plot the DSC curve. The TGA and DSC plots for each material are included in Appendix C. During the test, the chamber gas used was nitrogen and the samples were contained in alumina crucibles. Prior to being tested, the materials were dried at 105°C and ground to pass through the No. 325 sieve.

Table 2.9: Results of XRD

Supplier	Material	Ac	Ah	Al	Ba	Bi	C	Ca	G	He	I	L	Me	Mg	Mi	Mu	Ms	O	Ol	Pr	Q
										Main Crystalline Phases Identified											
A	D-L			X		X															X
	D-S			X		X															X
	NS-I	X		X		X								X	X						
	NS-L	X		X		X															
	NS-S					X					X				X				X		
	R-O			X		X													X		X
B	RM-C						X								X					X	X
	RM-L	X	X									X									X
	RM-S	X	X					X		X						X					X
	P-B	X																	X		X
	P-W	X														X					X
C	RC-G				X											X					X
	RC-M		X							X						X					X
	RC-P							X					X							X	X
	RM-M		X							X						X					X

Ac = Anorthoclase; Ah = Anhydrite; Al = Albite; Ba = Bassanite; Bi = Biotite; C = Celite; Ca = Calcite G = Gehlenite; He = Hematite; I = Iron Oxide; L = Lime; Me = Merwinite; Mg = Magnetite; Mi = Microcline; Mu = Mullite; Ms = Muscovite; O = Orthoclase; Ol = Oligoclase; Pr = Periclase; Q = Quartz

2.2.5 Zeta Potential

Zeta potential (ZP) testing was performed to determine the particle surface charge of the materials. Such information can be insightful in understanding agglomeration mechanisms and admixture interactions. Prior to testing, the material particles were dispersed in water. The tests were performed using a Zetaphoremeter V with the following parameters: a zeta potential range of -150 mV to +150 mV, an electrical conductivity range of 100 µS/cm to 100mS/cm, a temperature range ambient to 40 °C, a cell voltage range of 0 to 255 V, and a cell current range of 0 to 15 mA. The velocity of the electrically charged particles was measured and used to determine the ZP of the particles through the use of the Smoluchowski equation. The results of the ZP testing are presented in Table 2.10. Prior to performing the ZP testing, the materials were passed through the No. 200 (75 µm) sieve, without grinding or drying.

Table 2.10: Results of Zeta Potential Testing

Supplier	Material	Zeta Potential (mV)
	OPC	-4.13
Control	FA	-25.73
	Q	-43.72
	D-L	-27.26
	D-S	-33.28
A	NS-I	-40.36
	NS-L	-39.54
	NS-S	-34.48
	R-O	-25.01
	RM-C	-23.64
	RM-L	-20.52
B	RM-S	-24.08
	P-B	-33.04
	P-W	-39.01
	RC-G	-17.47
C	RC-M	-20.37
	RC-P	-4.65
	RM-M	-13.79

2.3 Conclusions from Characterization Tests

The materials tested were compared against the requirements specified within ASTM C618 for the determination of the suitability of the materials for use in concrete. Table 2.11 is a summary of the results obtained, including whether or not the materials passed ASTM C618 specifications. Based on the results of the testing, RC-G and RC-M did not pass the specifications for Class F fly ash due to excess moisture content. However, the suppliers of these fly ashes maintain that the moisture content will not be a problem when the materials are produced on an industrial scale. RC-P did not pass the specifications for a Class F fly ash due to the sum of silicon dioxide, aluminum oxide, and ferric oxide being less than 70%; however, RC-P did pass specifications for a Class C fly ash.

The fineness testing showed good correlation with the particle size analysis. With typical fly ash having a median particle range from 5 to 20 μm (Thomas et al., 2017), the large particle size of FA ($d_{50} = 26.9$ μm) seems unusual. The large particle size should be considered when evaluating properties of cementitious mixtures made with FA and when comparing the properties of mixtures containing the other SCMs to FA mixtures. It is also interesting to note that the particle size of NS-L ($d_{50} = 26.9$ μm) was also quite large and that the OPC had the third smallest d_{90} of all the materials, indicating that the particle size range is narrower for OPC than for the SCMs.

Based on the results of the characterization tests, testing was discontinued on some materials, which were expected to be low-performing materials:

- D-L: a natural mineral of the same mineralogy as D-S, but with a larger particle size;
- NS-L: a natural mineral of the same mineralogy as NS-S, but with a larger particle size;
- and RC-P: a reclaimed Class C fly ash.

Table 2.11: Summary of ASTM C618 Characterization Tests

Supplier	Material	SiO_2+ Al_2O_3+ Fe_2O_3 (%)	SO_3 (%)	MC (%)	LOI (%)	Fineness (% Retained)	Soundness (%)	Passes ASTM C 618 for F or N?
A	D-L	86.7	0.09	1.39	1.41	16.09	0.00	YES
	D-S	86.4	0.07	1.30	1.01	6.68	0.00	YES
	NS-I	81.5	0.17	0.76	0.47	0.17	-0.01	YES
	NS-L	81.1	0.16	0.89	0.79	30.45	0.19	YES
	NS-S	81.3	0.19	1.32	1.57	4.20	0.19	YES
	R-O	85.5	0.07	0.94	2.91	7.31	0.01	YES
B	RM-C	76.3	3.41	2.87	1.79	2.70	0.01	YES
	RM-L	77.2	3.92	1.42	1.56	15.15	-0.04	YES
	RM-S	79.2	3.22	2.05	5.89	10.10	-0.01	YES
	P-B	89.2	0.04	1.95	1.16	0.00	0.00	YES
	P-W	89.1	0.04	2.65	2.09	0.04	0.00	YES
C	RC-G	77.8	2.72	3.89	0.87	10.61	-0.02	NO
	RC-M	75.2	0.86	0.87	0.73	15.30	0.00	YES
	RC-P	59.1	2.59	6.96	3.42	7.25	0.03	NO
	RM-M	75.2	0.85	0.87	0.59	15.60	0.00	YES
	Criteria in ASTM C618	70% min	4% max	3% max	6% max	34% max	+/- 0.8% max	

Red text indicates materials non-compliant to ASTM C618.

Chapter 3. Paste Testing

Paste, mortar, and concrete testing were conducted on the materials shown in Table 3.1. Paste samples were tested for workability, rate of hydration, pozzolanicity, and admixture interaction by means of rheology, isothermal calorimetry, and $Ca(OH)_2$ (CH) content, as outlined in Table 3.2.

Table 3.1: Remaining SCMs after Material Characterization

Supplier	Designation	Source	Material Classification
A	D-S	California	Natural Mineral
	NS-I	Arkansas	Natural Mineral
	NS-S	Arkansas	Natural Mineral
	R-O	Wisconsin	Natural Mineral
B	RM-C	Colorado	Remediated Fly Ash
	RM-L	Texas	Remediated Fly Ash
	RM-S	Oklahoma	Remediated Fly Ash
	P-B	New Mexico	Natural Mineral
	P-W	New Mexico	Natural Mineral
C	RC-G	Texas	Reclaimed Fly Ash
	RC-M	Texas	Reclaimed Fly Ash
	RM-M	Texas	Remediated Fly Ash

Table 3.2: Paste Tests

Property	Test Method
Workability	Rheology
Admixture Interaction	Rheology and Foam Index
Rate of Hydration	Isothermal Calorimetry
Pozzolanicity	Thermal Gravimetric Analysis

3.1 Paste Rheology

To assess the workability of the SCM-containing pastes, rheological properties were measured using an Anton Paar MCR 301 rheometer. Rheological testing was only performed on the reclaimed and remediated fly ashes along with the controls, OPC and FA. Paste mixtures consisted of 500 g of cementitious materials at a 20% replacement of the cement by mass for each SCM and a water-to-cementitious material (w/cm) ratio of 0.45. Mixing was performed in accordance with ASTM C 1738 (2014) using a temperature-controlled high shear mixer that utilizes chilled water flowing through the wall of the mixing container to keep the temperature of

the paste at 23 ± 2 °C. Similar to the work of Han and Ferron (2016), the mixing water was chilled to 10 °C prior to mixing to assist in keeping the paste within the desired temperature range. The mixing water (de-ionized) was added to the mixing container, which was then covered, and the water was mixed at 4000 rpm. Dry material was then added to the mixture within the timeframe of 60 sec, and then the mixing speed was increased to 10,000 rpm for 30 sec. The paste was then allowed to rest for 150 sec; the paste on the sides of the mixing container was scraped within the first 15 sec. Following the rest period, the paste was mixed for an additional 30 sec at the same speed. Once mixing was complete, 19 mL of the paste was immediately transferred to the rheometer measurement system (cup and helical bob geometry) and subjected to a shear rate of 50 s^{-1} at a controlled temperature of 23 ºC for 90 sec, followed by a three-minute rest. This 90 sec period was found to be sufficient to ensure that an equilibrium shear rate was reached. After the rest period, a sweep of shear rate was then conducted on the paste in accordance with ASTM C 1749 (2017). The paste was subjected to a shear rate of 1 s^{-1} for 45 sec before increasing the shear rate to 10 s^{-1} for 45 sec. The shear rate continued to be increased by increments of 10 s^{-1} and held for 45 sec until reaching 50 s^{-1}, then decreased at the same increment and interval until reaching rest. Paste flow curves were then analyzed using the Bingham model to find the viscosity and yield stress of the mixtures (Mechtcherine et al., 2014). These values were used in order to determine the effects that the SCMs have on the workability of the paste. The flow curves are shown in Figure 3.1. The y-intercept of the trendlines corresponds to the yield stress and the slope corresponds to the viscosity. Table 3.3 shows these values for each mixture.
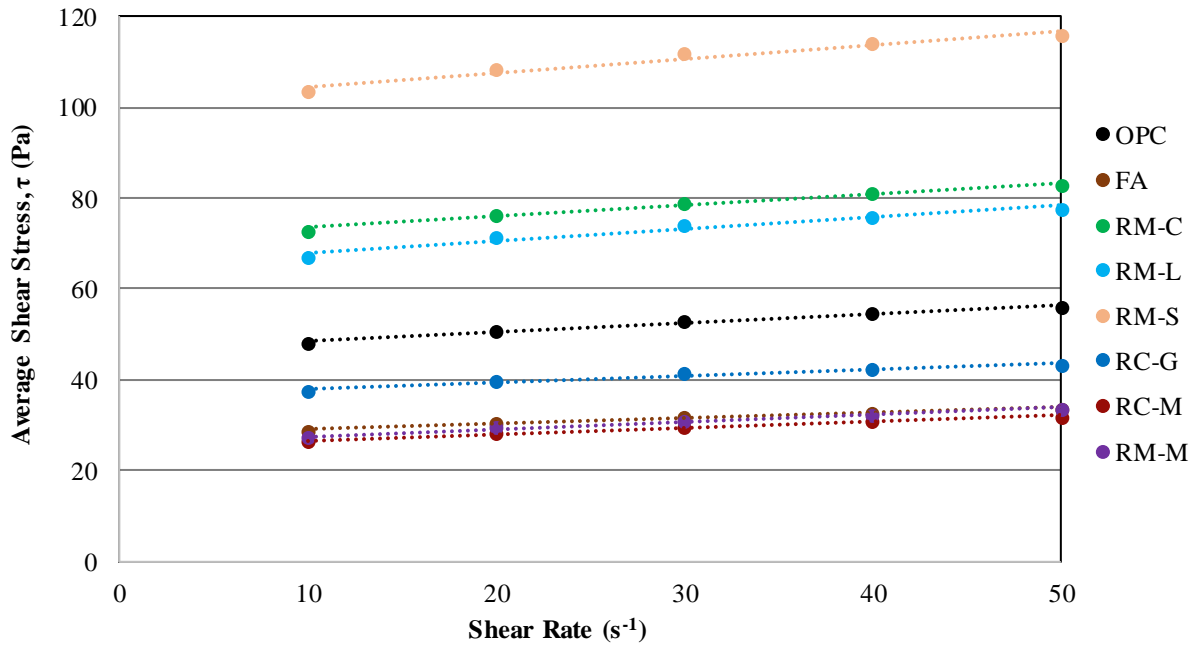

Figure 3.1: Flow curves of cement pastes containing control materials and fly ashes

Table 3.3: Bingham Parameters

Supplier	Material	Yield Stress (Pa)	Viscosity (Pa·s)
Control	OPC	46.73	0.19
	FA	27.90	0.12
B	RM-C	70.92	0.25
	RM-L	65.43	0.26
	RM-S	101.50	0.31
C	RC-G	36.63	0.15
	RC-M	25.34	0.14
	RM-M	26.04	0.16

Lower yield stresses and viscosities in Table 3.3 correspond with SCMs with larger as well as rounder particles (Tables 2.7 and 2.8). Yield stresses were the highest for more angular particles as well as smaller particle sizes.

As mentioned in Chapter 2, zeta potential provides insight about agglomeration mechanisms. As the absolute value of the zeta potential magnitude increase, agglomeration among particles decreases. From Table 2.10, OPC had the lowest absolute zeta potential value, which would suggest that the yield stress of OPC paste would be greater than that of the other pastes. This is consistent with the results seen for the FA, RC-G, RC-M, and RM-M pastes. However, the pastes with materials from Supplier B displayed higher yield stresses than the OPC paste, and this highlights the complex nature of flow behavior as there are other parameters (e.g., packing effects, hydrodynamic interactions, shape, etc.) that impact the rheological behavior.

With respect to viscosity, all pastes containing the alternative SCMs displayed similar viscosities as the FA paste, except for the materials from Supplier B. These materials had similar viscosities that were approximately two times greater than the control. The higher values associated with those pastes as compared to the FA pastes are likely related to the angular shape and textured surface of the particles impacting interparticle friction amongst the particles. However, the higher values associated with RM-C were not expected since the particle shapes of RM-C are predominantly round.

3.2 Admixture Interaction Testing

Admixture interaction testing was also conducted on pastes to determine the compatibility between reclaimed and remediated ashes and admixtures. Compatibility with water reducing agents (WRAs) was examined using rheology testing. Compatibility with air-entraining agents (AEAs) was examined using foam index testing.

Water-reducing agents Sika® ViscoCrete® 1000 and Sika® ViscoCrete® 2110 were used to gain insight about admixture-SCM compatibility. Similar to the paste rheology testing that was discussed in the previous section, an Anton Paar MCR 301 rheometer was used. ASTM C 1738 (2014) was also followed for the mixing procedure; however, WRAs were added to the mixing water prior to the addition of the dry material. Multiple paste mixtures were produced, starting with admixture dosages of 0.1% by weight of cementitious materials (% wt. cm), with incremental

dosage increases of 0.1% until a constant minimum yield stress value was achieved. Following mixing, 19 mL of the paste was immediately transferred to the rheometer measurement system and the same rheometer procedure, as mentioned in the previous section, was utilized. The saturation dosage was determined as the minimum dosage of WRA beyond which negligible changes in yield stress values occurred. The saturation dosage provides insight into the maximum amount of WRA to be used in a concrete mixture. Exceeding the saturation dosage has economic disadvantages for a mixture since dispersion efficiency of the admixture has already been maximized. Exceeding the saturation dosage also has engineering disadvantages since overdosing can increase the risk of bleeding and segregation. Table 3.4 shows the saturation dosages for both WRAs for the control materials as well as RM-C, RM-S, RC-G, and RC-M.

Table 3.4: Saturation WRA Dosages for Cement Pastes

| Supplier | Material | Admixture Dosage (% wt. cm) | |
		ViscoCrete®1000	ViscoCrete®2110
Control	OPC	0.5	0.5
	FA	0.5	0.3
B	RM-C	0.4	0.3
	RM-S	0.5	0.5
C	RC-G	0.5	0.4
	RC-M	0.5	0.4

The results of the saturation WRA dosages indicate that the remediated and reclaimed ashes tested do not have a substantial impact on the saturation dosage amount as compared to the production fly ash. Most of the remediated and reclaimed ashes saturation dosages are within one increment of the saturation dosage needed for the production fly ash, and they achieved their saturation points at similar yield stress values (1- 5 Pa). However, as shown in Figures 3.2 and 3.3 (additional plots included in Appendix D), differences in workability behavior did occur in the presence of the admixtures at dosages below the saturation point (e.g. at 0.2% dosage of Viscocrete® 1000 the yield stress value of the FA, RM-C and RC-G mixtures were 21 Pa, 50 Pa, and 34 Pa, respectively). As such, when selecting an WRA to be used with a remediated or reclaimed ash, testing should be done to assess its workability behavior at different admixture dosages (as well as the stiffening, strength gain, and workability loss over time) to confirm that there are no incompatibility issues. Some mixtures displayed a gradual, continuous decrease in yield stress with increasing admixture dosage (e.g. RM-S in the presence of Viscocrete® 2110), whereas other materials were more sensitive to changes in the admixture dosage (e.g. RM-C in the presence of Viscocrete® 2110). The gradual, continuous response is the preferred response since this tends to lead to a more robust mixture performance.
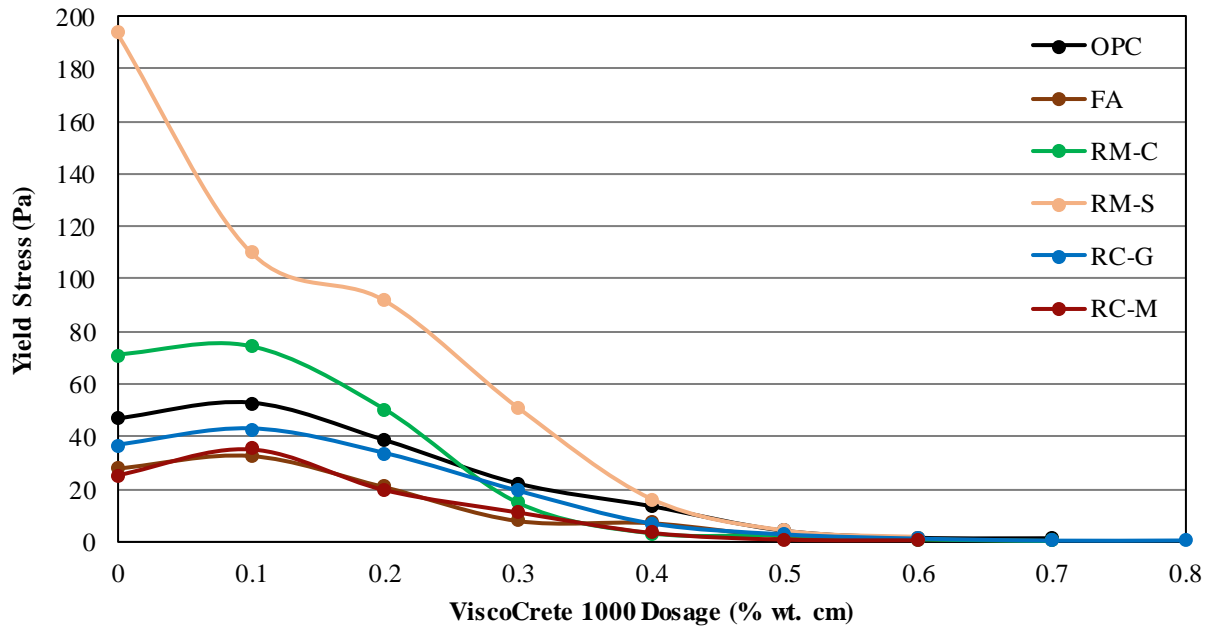
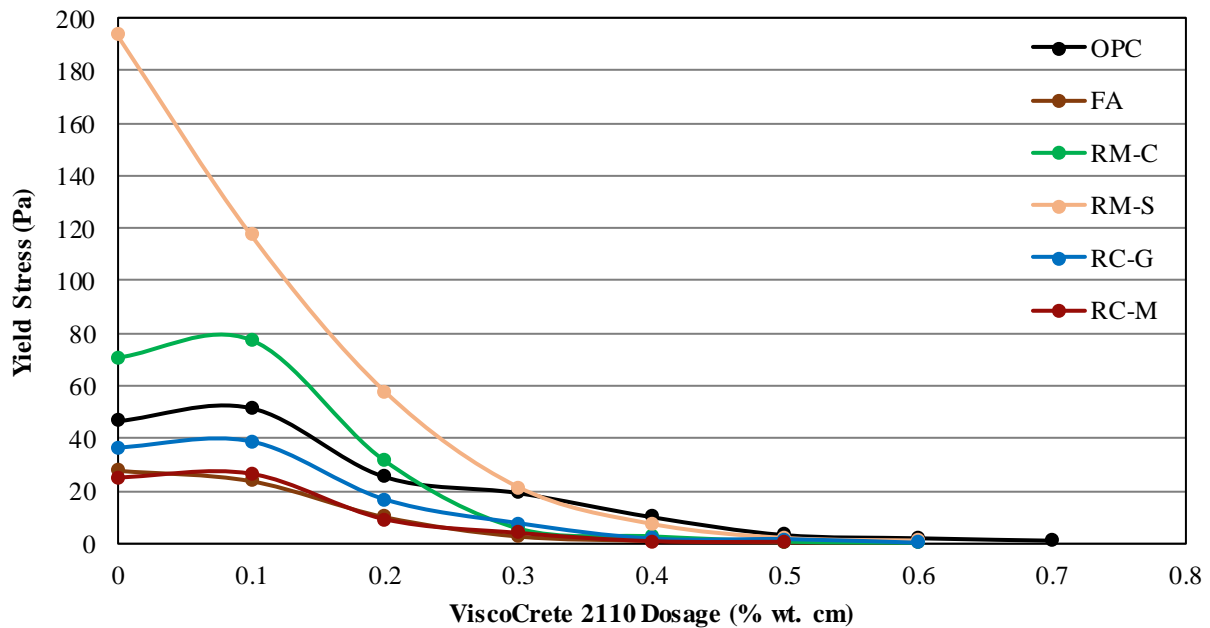*Figure 3.2: Effect of ViscoCrete® 1000 dosage on paste yield stress*

Figure 3.3: Effect of ViscoCrete® 2110 dosage on paste yield stress

Admixture interaction testing was also conducted on an AEA, Sika® AIR, to evaluate how the carbon content of the reclaimed and remediated fly ashes affected the required dosage of AEA in the pastes. In order to make this evaluation, the foam index test was used. The foam index test

is a titration test where a combination of water and cementitious materials is mixed in a closed container and then titrated with AEA until a defined endpoint is reached (Folliard et al., 2009). This can be a good indicator for how different materials affect air entrainment in concrete, with higher values indicating poorer air entrainment of the fly ashes. However, many variations of the foam index test exist, leading to variability in results between different testing parties. In a series of test evaluations of the foam index test, Folliard et al. (2009) developed a test with a precision within plus or minus one incremental dose. This test was adapted for the research presented in this report. The procedure consisted of using a 118 mL (4 oz) plastic vial with a hinged snap-on lid filled with paste mixtures composed of 25 g of cementitious materials, with a w/cm equal to 2.0 and an SCM-to-cementitious materials ratio (SCM/cm) equal to 0.33. Water was first added into the vial, followed by the cement-SCM blend, which was then capped and manually agitated by shaking the vial for a duration of 10 sec at a frequency of 4 ± 0.5 shakes/sec. A "shake cycle" consisted of rapidly lowering the vial by 0.2 to 0.25 m and then returning it to its original position. Following agitation, the vials were uncapped and a 50 μL (0.0017 oz) drop of AEA, diluted to 5% of the as-received concentration from the manufacturer, was added to the paste using a calibrated pipette. The vial was then capped and agitated following the same shaking procedure. At the end of the shake cycle, the vial was immediately uncapped and allowed to rest for 20 sec on a level surface free from disturbances. Once the rest period was complete, if the foam had not reached the defined endpoint, an additional drop of 5% AEA was added and the shaking procedure was repeated until the defined endpoint was reached. The endpoint was defined as when an unbroken foam cover exists on the water surface of the paste. The amount of AEA used to stabilize the foam is shown in Table 3.5 for the control materials as well as the reclaimed and remediated fly ashes.

The amount of air-entraining admixture needed to achieve a stable foam in the foam index test typically increases with increasing LOI (Folliard et al., 2009). Foam index testing showed that pastes containing FA, RC-G and RM-L required the minimum dosage of AEA, based off the dosage size and concentration used in the test, to generate an unbroken cover of foam, indicating that the measured dosage was sufficient to entrain air. This agrees with LOI results shown in Table 2.5; FA, RC-G and RM-L all had low LOI values. RM-C and RM-L pastes required higher dosages of AEA in comparison to the control FA paste. Interestingly, despite having a low LOI, RC-M paste required the highest dosage of AEA to stabilize the foam. This is because the fly ash is activated carbon injected, according to the supplier. Activated carbon is highly absorbent of chemicals, therefore, fly ashes with activated carbon require higher dosages of AEA to account for this absorption. The LOI testing does not distinguish between unburnt carbon and activated carbon, so these results can be misleading. RM-M paste performed better than RC-M paste, requiring half the amount of AEA in order to stabilize the foam. This shows that remediation techniques were effective in reducing the adverse effects of activated carbon.

Table 3.5: Foam Index Values for Cement Pastes

Supplier	Material	Foam Index (mL AEA/100 kg cm)
Control	FA	10
B	RM-C	30
	RM-L	10
	RM-S	40
C	RC-G	10
	RC-M	60
	RM-M	30

One 50 µL drop of AEA diluted to 5% is equivalent to 10 mL of AEA per 100 kg of cm.

3.3 Isothermal Calorimetry

Isothermal calorimetry was performed to measure the heat from cement hydration and examine the effects of SCMs on cement hydration kinetics. The control mixture consisted of 25 g cement and 11.25 g water, giving a w/cm of 0.45. For the SCM and quartz-containing mixtures, 20% of the cement by mass was replaced by each SCM, while the water content was held at the same value. Prior to running the tests, the pastes were mixed for 2 min using an overhead laboratory mixer at 1600 rpm. Following mixing, 15 g of the paste sample was placed into a 20 mL glass ampoule, sealed, and placed in a Thermometric TAM Air Isothermal Calorimeter at 23 ºC. The rate of hydration was then measured for 72 h. The rates of heat evolution and the cumulative heats for the mixtures are shown in Figures 3.4-3.6 and 3.7-3.9, respectively.

In Figure 3.4, it is clear that the natural minerals from Supplier A exhibit filler effects, similar to the quartz. The filler effects consist of increasing the peak rate of heat evolution by providing surfaces for nucleation and growth of calcium silicate hydrate (C-S-H) and CH (Lothenbach, et al., 2011). This also resulted in a slightly higher cumulative 3-day heat, Figure 3.7, suggesting a higher degree of hydration of the cement, caused by the enhancement of cement hydration from the filler effect.

In Figure 3.5, most of the SCMs from Supplier B also acted as fillers in the first 24 h. The exception to this is RM-C, which caused a delay in the hydration of portland cement. It is common for fly ash to delay cement hydration and setting (Nocun-Wczelik, 2001; Fajun, et al., 1985), so this response is not unusual and is likely not due to the remediation of the fly ash. As with the natural minerals from Supplier A, the filler effect caused a slight increase in the 3-day cumulative heat, Figure 3.8.

Interestingly, the SCMs from Supplier C did not exhibit filler effects, Figure 3.6. This is likely due to their larger particle size. For instance, the control fly ash (FA) has a median particle diameter of 27 µm, which is larger than that of the cement (OPC) at 14 µm. Reclaimed fly ashes RC-G and RC-M in Figures 3.6 and 3.9 have median particle diameters of 22 and 13 µm, respectively, which are larger than the fly ashes from Supplier B, which have median particle diameters of 6-9 µm. These larger particle sizes reduce filler effects; however, the presence of these particles still enhances growth of hydration products, resulting in a higher 3-day cumulative heat for these pastes in comparison to the OPC paste.

It should be noted that all of the data plotted in Figures 3.4-3.9 are normalized per gram of cement, not per gram of paste or cementitious material. This was done in order to examine the impact of the SCMs on cement hydration kinetics. All of the SCMs tested dilute the cement content of the paste, thus reducing heat of hydration from the paste, and can be effectively used for temperature control plans for concrete.
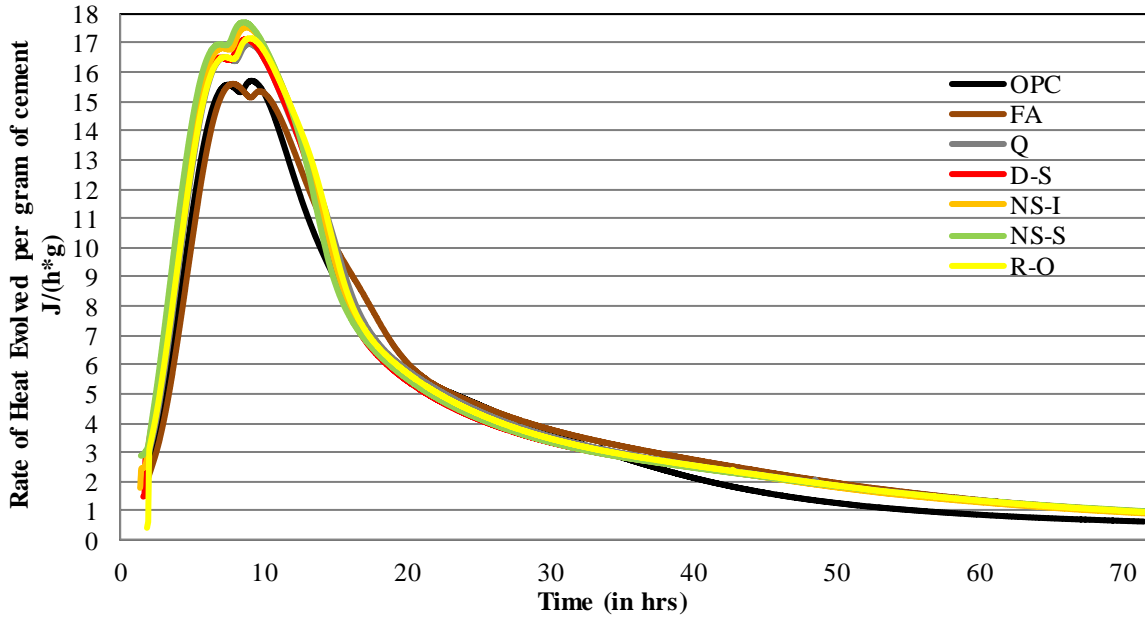

Figure 3.4: Rate of heat evolution of cement pastes containing control materials and Supplier A materials
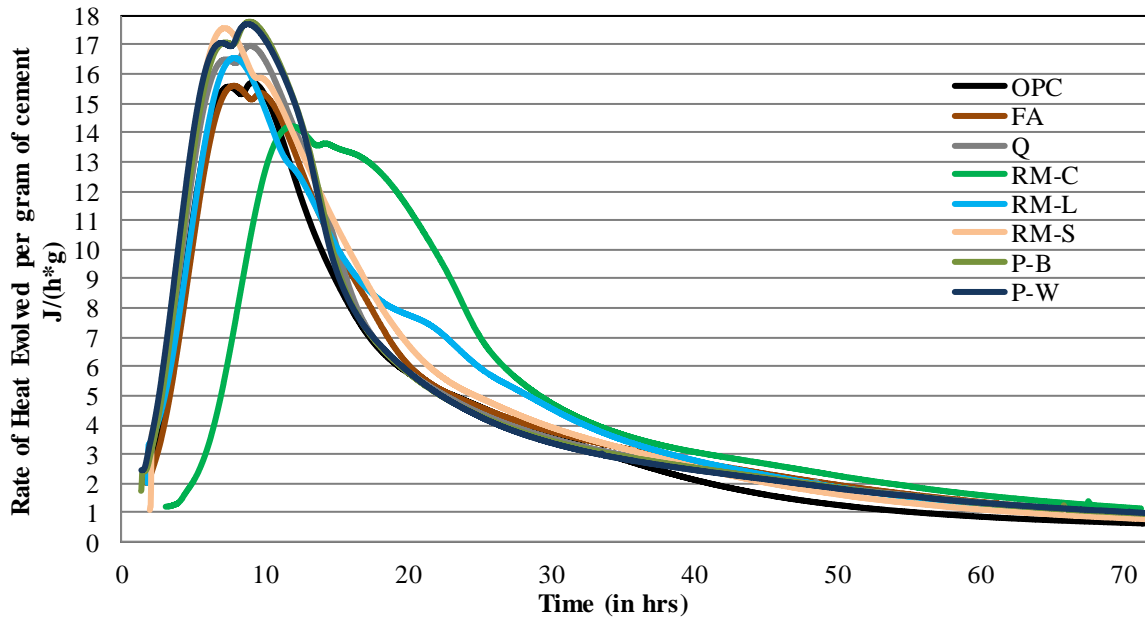
Figure 3.5: Rate of heat evolution of cement pastes containing control materials and Supplier B materials
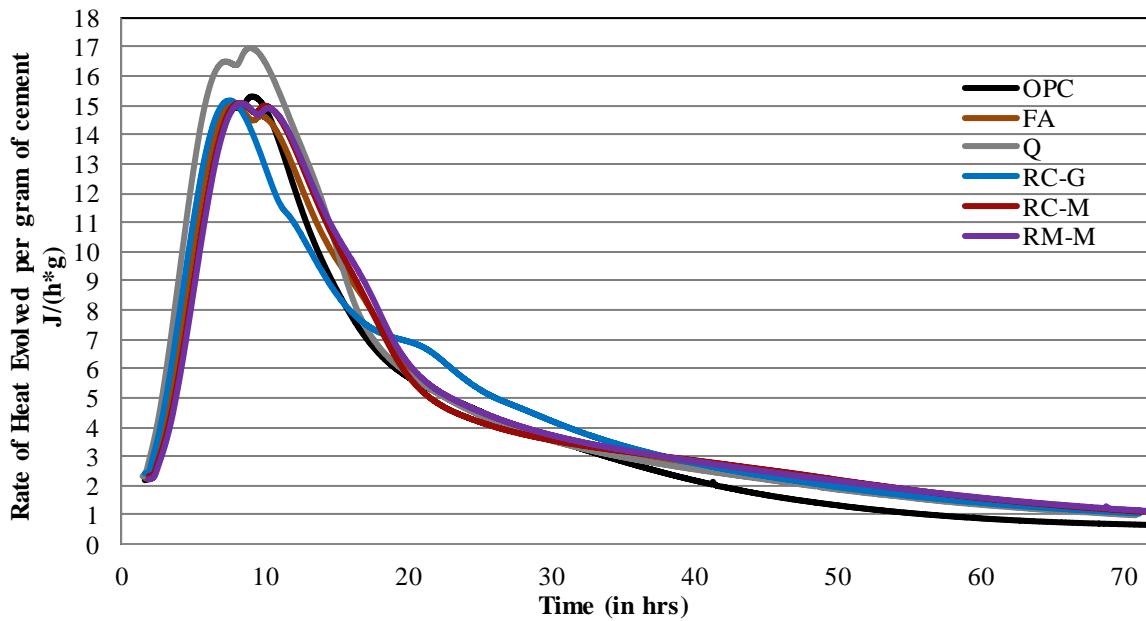
Figure 3.6: Rate of heat evolution of cement pastes containing control materials and Supplier C materials
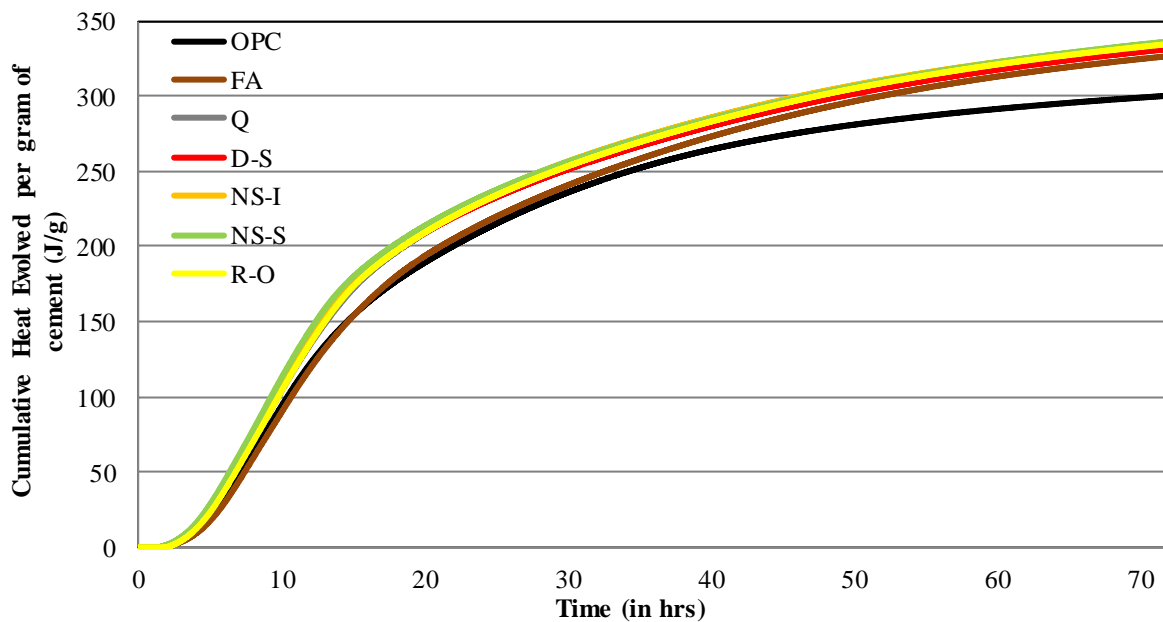
Figure 3.7: Cumulative heat evolved of cement pastes containing control materials and Supplier A materials
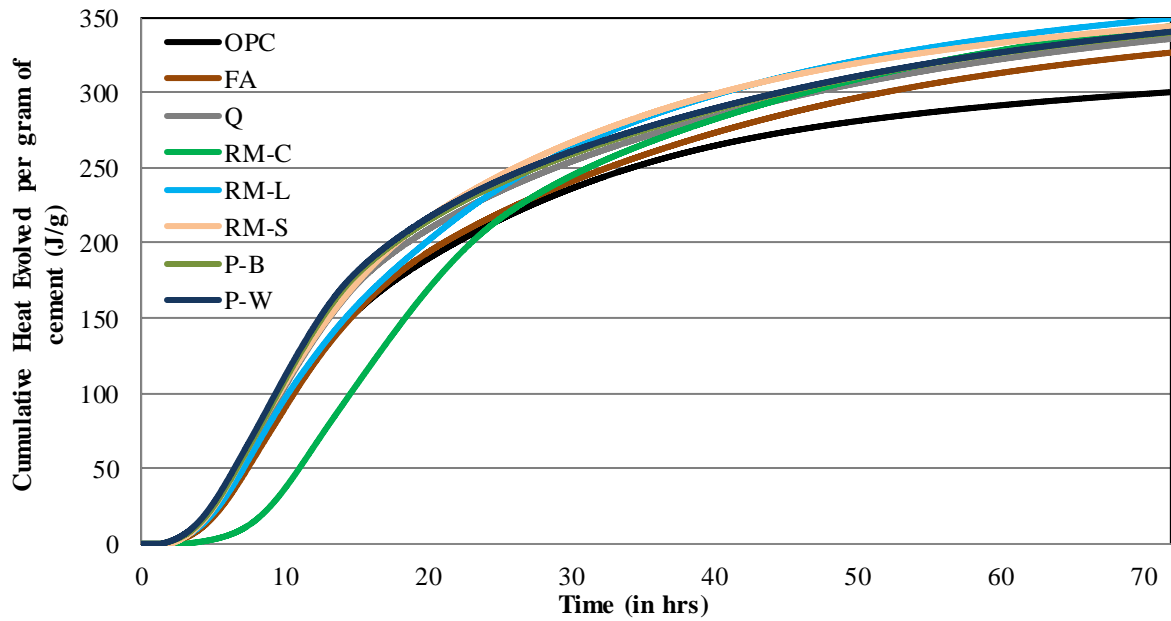
Figure 3.8: Cumulative heat evolved of cement pastes containing control materials and Supplier B materials
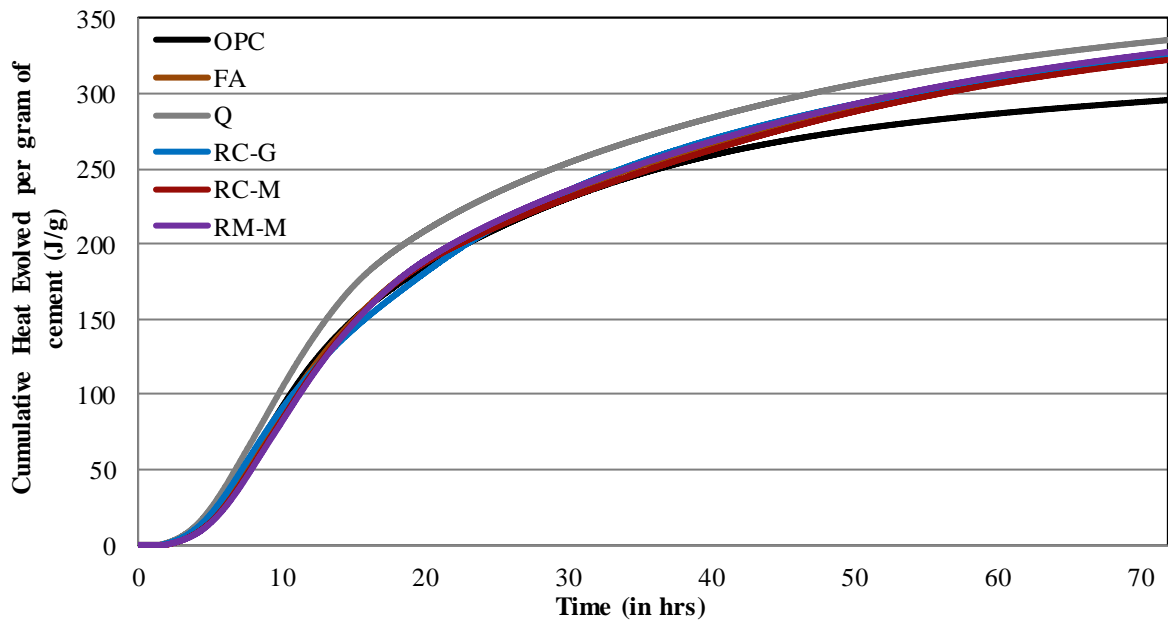
Figure 3.9: Cumulative heat evolved of cement pastes containing control materials and Supplier C materials

3.4 Differential Scanning Calorimetry/Thermal Gravimetric Analysis (DSC/TGA) for Pozzolanicity

Differential scanning calorimetry (DSC) and thermal gravimetric analysis (TGA) were used to quantify the CH content in pastes. The pastes contained a 20% cement replacement by mass with SCMs and had a w/cm of 0.45. The same mixing procedure was used as for isothermal calorimetry. Sample mixtures were separated into four individual containers and cured at 23 ºC and 100% relative humidity (RH) to be tested at 1, 7, 28 and 90 days. Upon reaching the target age, the samples were removed and hydration was stopped using vacuum desiccation. First, the edges of the sample were removed and discarded in order to remove calcium hydroxide crystals that orient along the edges of the sample and walls of the container. Next, the sample was crushed to pass the No. 100 sieve (150 μm) and then placed in a vacuum desiccator for a minimum of two weeks to cease hydration. The samples were then ground to pass the No. 325 sieve (45 μm) and placed back under vacuum prior to DSC/TGA testing to prevent carbonation of the materials.

The DSC/TGA testing was performed utilizing a Mettler Thermogravimetric Analyzer, Model TGA/DSC 1. The heat flow and mass loss of 10 mg of each material in a 70 μL crucible were recorded as the materials were heated from 40–1000 ºC at a rate of 20 ºC/min within a chamber with N_2 gas flowing at 50 mL/s to prevent carbonation of the material while the test was underway. The objective of the DSC/TGA testing is to determine the mass loss of water during the degradation of CH, which typically occurs between approximately 350-550 ºC (Kim and Olek, 2012). The DSC curve was used to pinpoint the exact start and end temperatures when the mass loss occurred. The mass loss within this region is then used to calculate the amount of CH present in the tested sample, which was converted to the amount of CH per gram of cement by normalizing by ignited weight and accounting for the mass percent of SCM. The CH contents of the SCM blend and control pastes are shown in Figures 3.10-3.12.

In Figure 3.10 it is clear that the natural minerals increase early CH content. This has been observed before and is a result of the filler effect causing increased formation of CH and C-S-H due to the increased sites for nucleation and growth (Lothenbach et al., 2011; Antoni et al., 2012). When the CH content of a paste is lower than the control, this indicates that a pozzolanic reaction has occurred. This happens as early as 7 days for some of the materials in Figures 3.11 and 3.12. It is clear from Figure 3.10 that most of the natural minerals from Supplier A are not pozzolanic because they do not reduce CH content of the pastes and have similar CH contents as the inert quartz-containing paste. NS-I appears pozzolanic at 90 days, but this is likely the result of a testing error because it does not match the expected trend based on the earlier ages and other natural minerals from Supplier A. Most of the remediated and reclaimed fly ashes are pozzolanic, with only RC-G showing questionable pozzolanicity. Additionally, P-B shows less pozzolanicity than P-W.
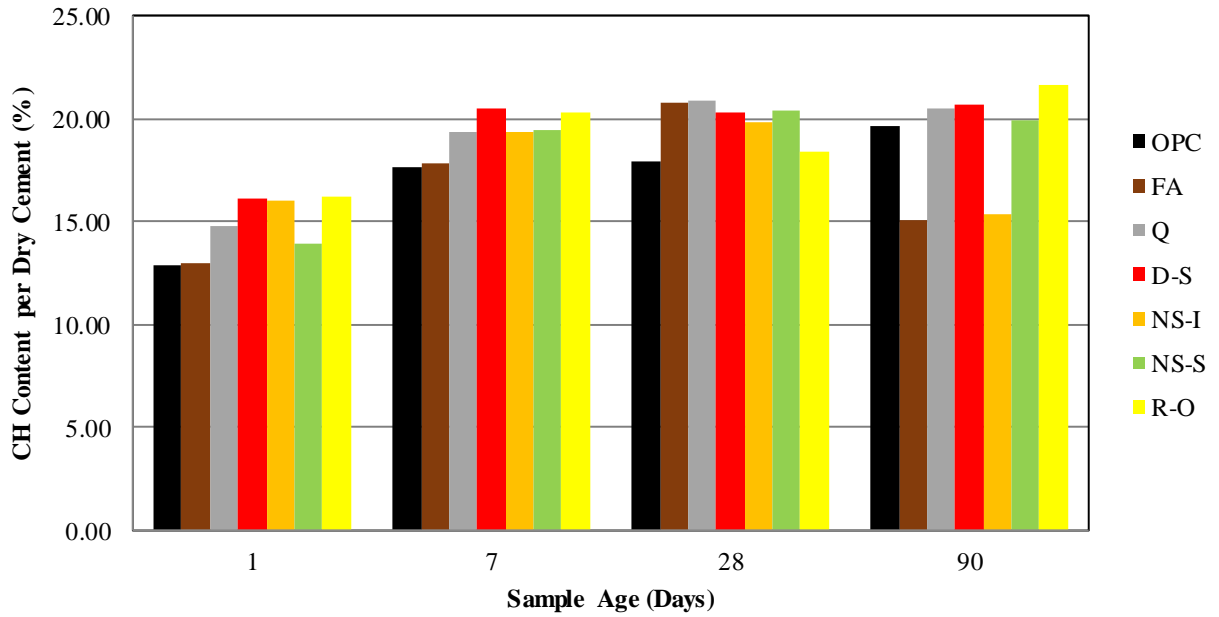
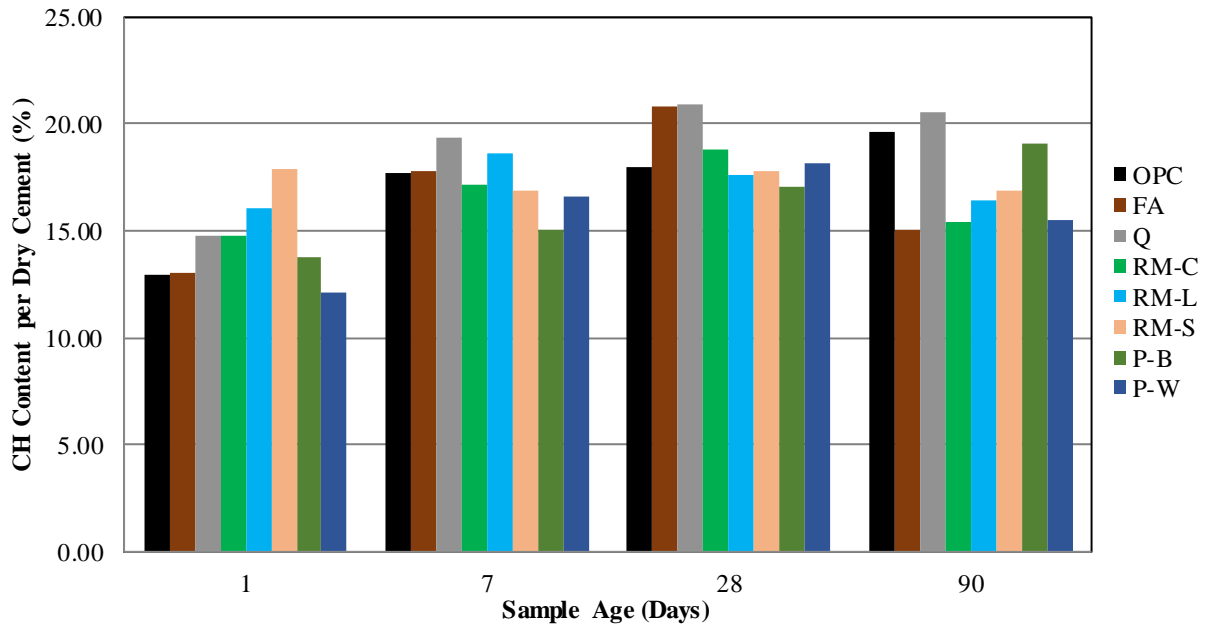*Figure 3.10: Calcium hydroxide content of control pastes and pastes containing materials from Supplier A*

Figure 3.11: Calcium hydroxide content of control pastes and pastes containing materials from Supplier B
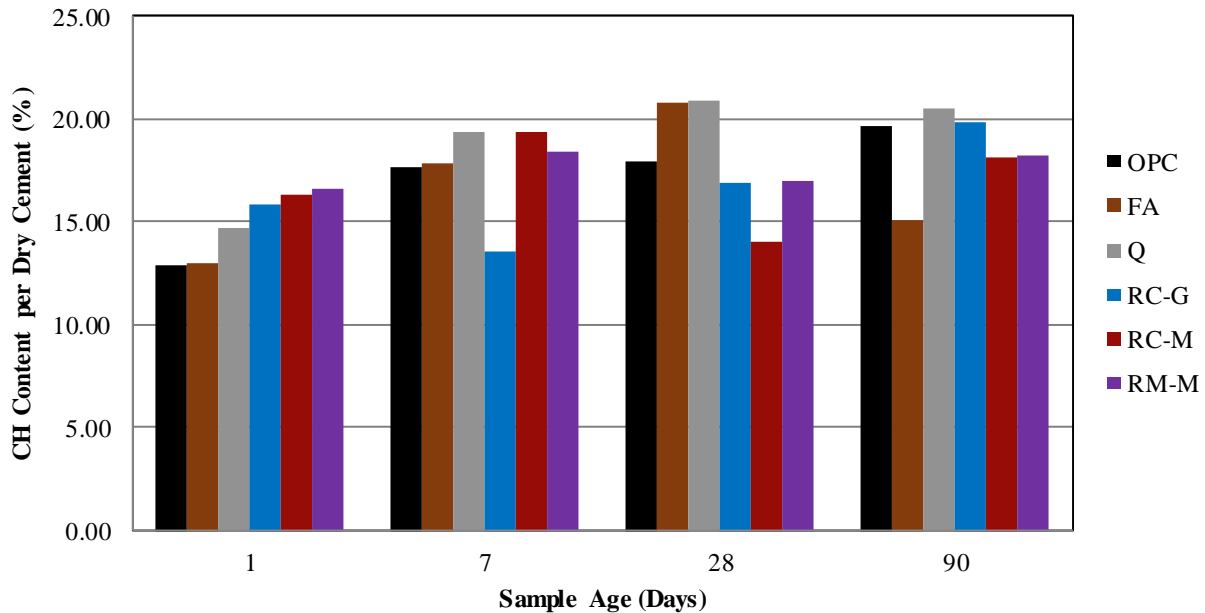
Figure 3.12: Calcium hydroxide content of control pastes and pastes containing materials from Supplier C

3.5 Conclusions from Paste Testing

Rheology testing on pastes showed the impact of reclaimed and remediated fly ashes on viscosity and yield stress; rheological behavior depended on the nature of the ash. Ashes obtained from Supplier C exhibited rheological behavior similar to that of pastes containing the production ash, FA. A significant increase in yield stress was seen in pastes containing fly ash from Supplier B. This was attributed to differences in size and shape of these ashes as compared to the other fly ashes. It was seen that lower yield stresses correspond with SCMs with larger as well as rounder particles.

The results of testing saturation WRA dosages indicate that the remediated and reclaimed fly ashes tested do not have an adverse effect on the saturation dosage in comparison to the control materials. However, admixture demand is likely to differ between the mixtures since the yield stress values of the mixtures are not similar at dosages below saturation. When selecting a WRA for a fly ash, testing should be performed using the ash to ascertain the saturation dosage as well as the potential for workability loss and strength gain in the presence of the WRA.

Foam index testing showed that minimum dosage of AEA tested should be sufficient to entrain air in pastes containing FA, RC-G, and RM-L. This was expected, since these fly ashes had low LOI values. However, despite having the lowest LOI of the reclaimed and remediated fly ashes, RC-M paste required the highest dosage of AEA to stabilize the foam. This is because the fly ash is activated carbon injected, according to the supplier. When RC-M was remediated, resulting in RM-M, the dosage of AEA needed to stabilize the foam was reduced by half, indicating successful remediation.

Isothermal calorimetry is useful for detecting filler effects in cement hydration and for determining heat of hydration of cementitious systems. It is clear in the plots of heat evolution and cumulative heats in Figures 3.4-3.9 that Q and the natural minerals provided by Supplier A exhibit

filler effects. The production fly ash, FA, RC-G, and RC-M pastes did not exhibit filler effects, likely due to their larger particle size. However, the presence of these particles still enhances growth of hydration products, resulting in a higher 3-day cumulative heat for these pastes in comparison to the OPC paste. RM-C had a delayed heat of hydration peak in Figure 3.5, which is not uncommon because the use of a Class F fly ash can delay cement hydration and setting time of concrete (ACI 232, 2003). All of the SCMs tested dilute the heat from cement in concrete mixtures and can be used in temperature control plans.

It is clear that all of the materials increased early CH content (Figures 3.10-3.12) because of filler effects and enhanced hydration. When the CH content of a paste is lower than the control, this indicates that a pozzolanic reaction has occurred. This happens as early as 7 days for some of the materials, including RM-C, RM-S, P-B, P-W, and RC-G. At 90 days, P-B, P-W, and most of the remediated and reclaimed fly ashes indicate pozzolanic behavior, with only RC-G showing questionable pozzolanicity. The natural minerals from Supplier A are not pozzolanic, with CH contents of pastes similar to that of the inert quart filler, Q.

In summary, the paste testing results indicate that the natural minerals provided by Supplier A are inert. All of the materials provided by Suppliers B and C exhibited pozzolanic activity, with the possible exception of RC-G. The high yield stresses of the remediated fly ash pastes can be attributed to the small size and angular shape of their particles. This can be altered with water-reducing agents (WRAs), which can lower the yield stress and viscosity of the paste at certain dosages. The foam index test gives a good indication that RM-C, RM-S, and RC-M will require more AEA than the other fly ashes to produce air-entrained concrete.

Chapter 4. Mortar Testing

Mortar samples were tested for workability, strength-activity index, compressive strength, alkali-silica reaction, and sulfate resistance by means of ASTM C1437, ASTM C618/C311, ASTM C109, ASTM C1567, and ASTM C1012, respectively, as outlined in Table 4.1. The procedures and results of these tests are described in this chapter. Mortar samples for testing were mixed in accordance with ASTM C305 (2014).

Table 4.1: Mortar Tests

Property	Test Method
Workability	ASTM C1437
Strength-Activity Index	ASTM C618/C311
Compressive Strength	ASTM C109
Alkali-Silica Reaction	ASTM C1567
Sulfate Resistance	ASTM C1012

4.1 Mortar Flow

Mortar flow of the materials was determined by the sum of four measurements of the diameter of the mortar after 25 drops of a flow table as outlined in ASTM C1437 (2015). The flow table, as well as the calipers used for measurements, both conform to ASTM C230 (2014). Testing was performed in order to determine how each SCM alters workability in comparison to the control portland cement mixture. The results of the mortar flow testing are presented in Table 4.2.

Since the w/cm of each mixture was fixed, mortar flows that are greater than the OPC mortar indicate that the material is more fluid, whereas mortar flows that are less than the OPC indicate that the material is less fluid. Six of the materials have mortar flows of at least 120, with the largest mortar flow at 143 from RM-M. Of these six materials, five of them are fly ashes: FA, RM-C, RC-G, RC-M, and RM-M. Fly ashes typically increase flow in cementitious mixtures compared to straight cement mixtures due to the round shape of the fly ash particles (Ramachandran, 1995), which allows the particles to move past one another easier in comparison to the angular shape of cement particles. The ESEM images of these five fly ashes shown in Appendix A confirmed that the particles are round.

The remaining two fly ashes, RM-L and RM-S, have mortar flows lower than the OPC. The ESEM images of these two fly ashes, shown in Appendix A indicate that the particles are primarily angular in shape and/or textured, which would likely increase interparticle friction amongst particles and hinder the particles from moving past one another. The remaining materials that had mortar flows similar to, or greater than, OPC are Q, D-S, NS-I, R-O, P-B, and P-W. The particle shapes and sizes of these materials are similar to the OPC. The material with the lowest mortar flow is NS-S, with 95. Similar to RM-L and RM-S, the particles are primarily angular in shape and textured, hindering the particles from moving past one another. Additionally, the NS-S particles appear to be porous from the ESEM images in Appendix A, which could contribute to a lesser flow rate due to the absorption of water.

Table 4.2: Mortar Mixture Flow Results

Supplier	Material	Mortar Flow
Control	OPC	110
	FA	126
	Q	112
A	D-S	115
	NS-I	115
	NS-S	95
	R-O	120
B	RM-C	124
	RM-L	104
	RM-S	103
	P-B	113
	P-W	107
C	RC-G	121
	RC-M	131
	RM-M	143

4.2 Compressive Strength

The SCMs and control materials were tested for compressive strength based on ASTM C109 and were tested at 1, 3, 7, 28, 56, and 90 days. The mixture designs consisted of a 20% by mass replacement of the SCMs, a ratio of fine aggregate-to-cementitious materials of 2.75, and a fixed w/cm of 0.485. The average compressive strengths of three mortar cubes were evaluated at each specified age. ASTM C109 gives a maximum permissible range between three specimens at 8.7% of the average. If the range of the materials exceeded the maximum, the specimen that differed most from the average was discarded, and a maximum permissible range between the remaining two specimens was set at 7.6% of the average. A new mixture was made and tested if the remaining two specimens did not meet the 7.6% requirement. Compressive strength results are shown in Figures 4.1-4.3. Compressive strengths of the materials normalized to the OPC control are shown in Figures 4.4-4.6. Error bars represent the range of measured values.

In Figure 4.1, the compressive strengths of the mortars containing natural pozzolans from Supplier A did not increase significantly beyond 28 days. At 90 days, the strengths of the mortars were slightly greater than the mortar containing Q, with the exception of the mortar containing D-S. It should be noted from Figure 4.4 that all of the SCMs, including the quartz control material, resulted in compressive strengths within 75% of the OPC control mortar at all ages, in spite of the fact that it is highly likely that none of these materials are pozzolanic. This point will be discussed further in the next section with respect to SAI testing.

In Figure 4.2, the compressive strengths of the mortars containing remediated fly ashes from Supplier B continuously increased and surpassed the magnitude of the OPC control mortar

at 28 days. It is quite clear from Figure 4.5 that all of the SCMs increased the strength of the mortars compared to the OPC control by 28 days. The compressive strengths of mortars containing P-W were the highest at 90 days, similar to the mortar containing FA.

In Figures 4.3 and 4.6, the compressive strengths of the mortars containing fly ashes from Supplier C continuously increased up to 90 days, with the magnitudes being greater than the OPC mortar, and less than the FA mortar, at 90 days. The strengths of all of the fly ashes from Supplier C were similar to FA at later ages.
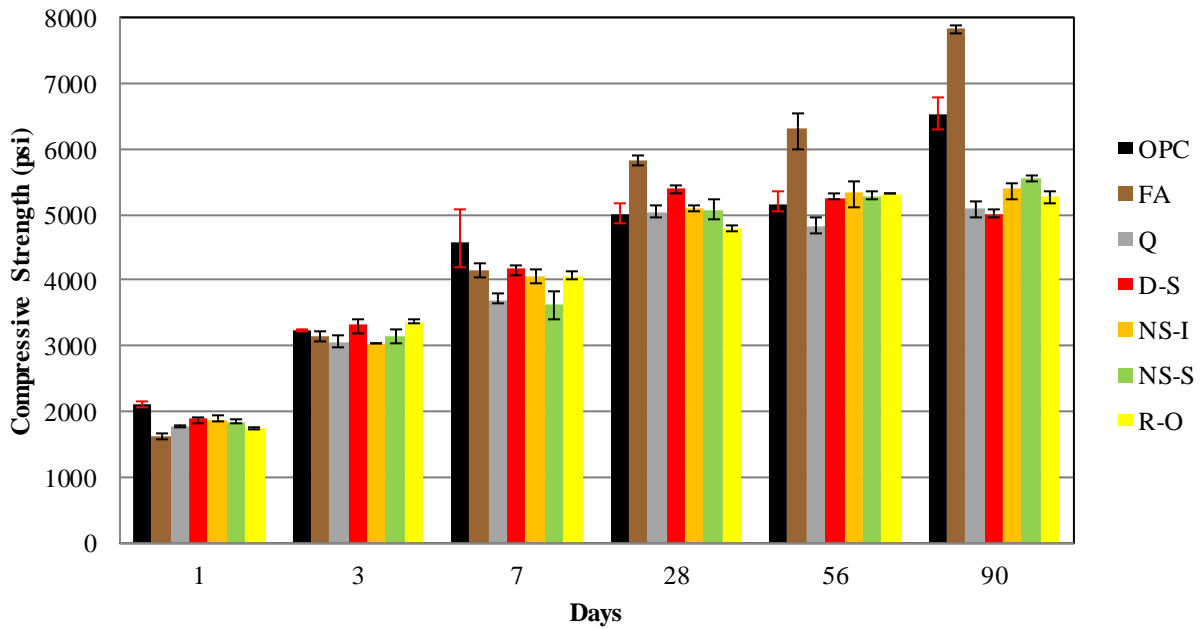
Figure 4.1: Compressive strengths of mortar samples containing controls and SCMs from Supplier A
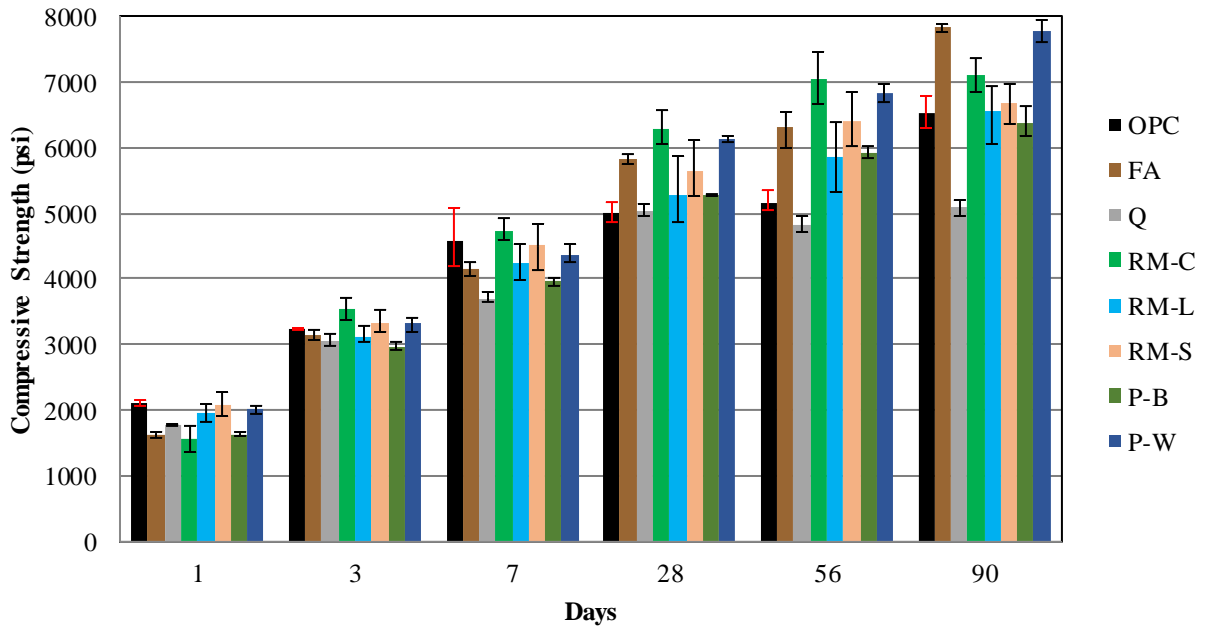
Figure 4.2: Compressive strengths of mortar samples containing controls and SCMs from Supplier B
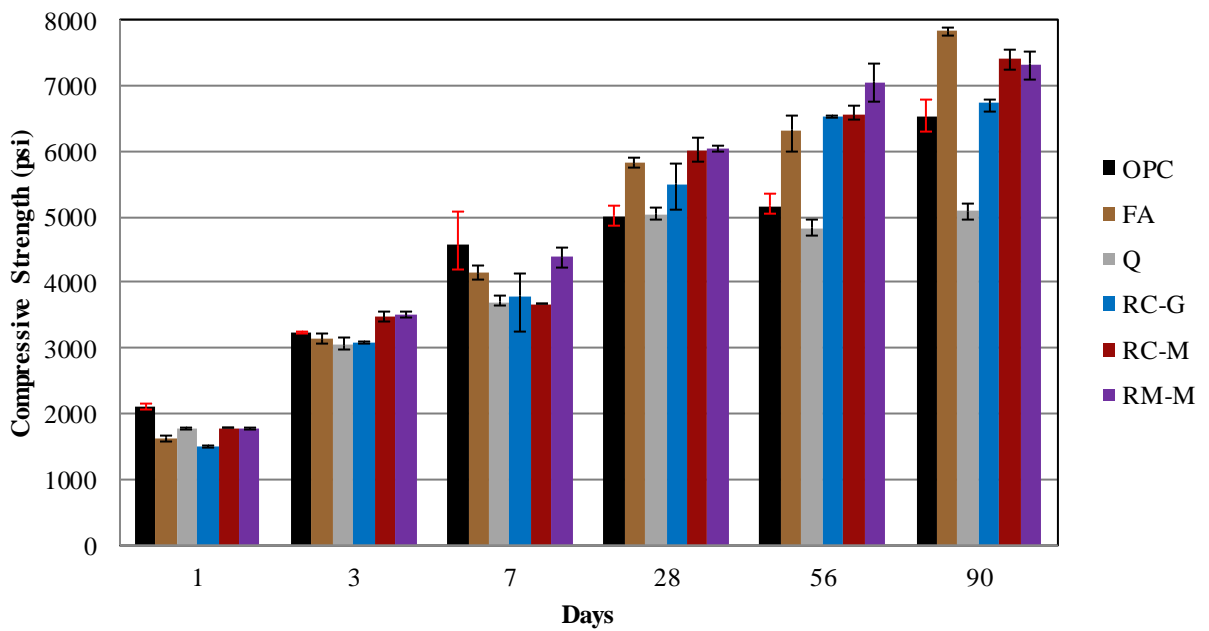
Figure 4.3: Compressive strengths of mortar samples containing controls and SCMs from Supplier C
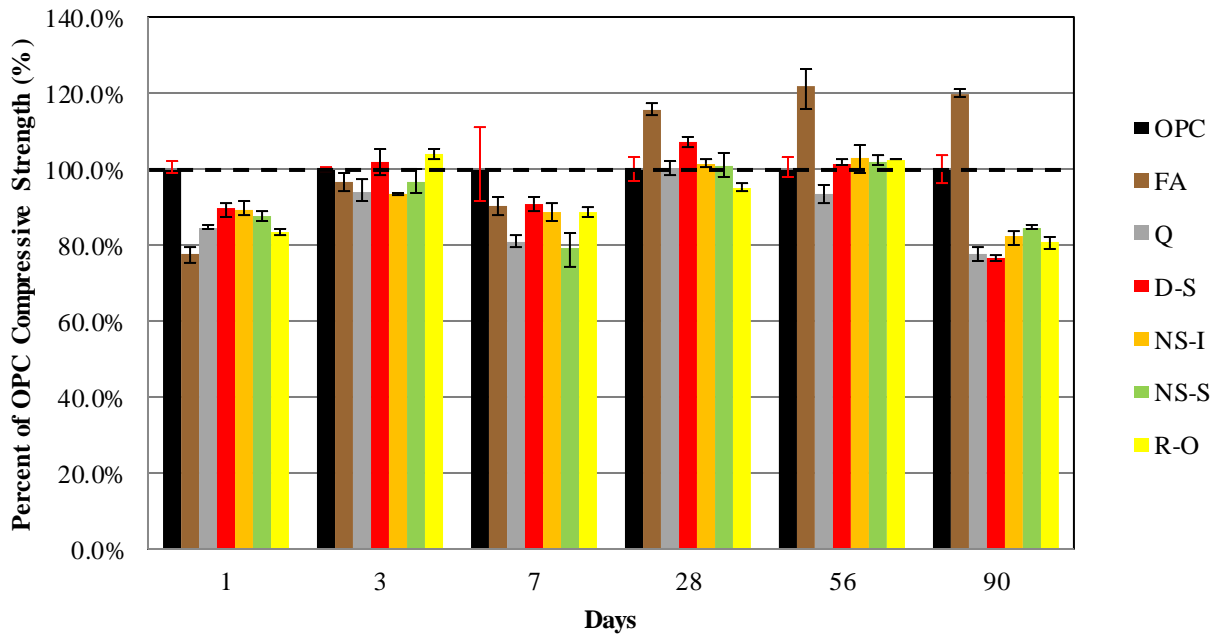
Figure 4.4: Normalized compressive strengths of mortar samples containing controls and SCMs from Supplier A
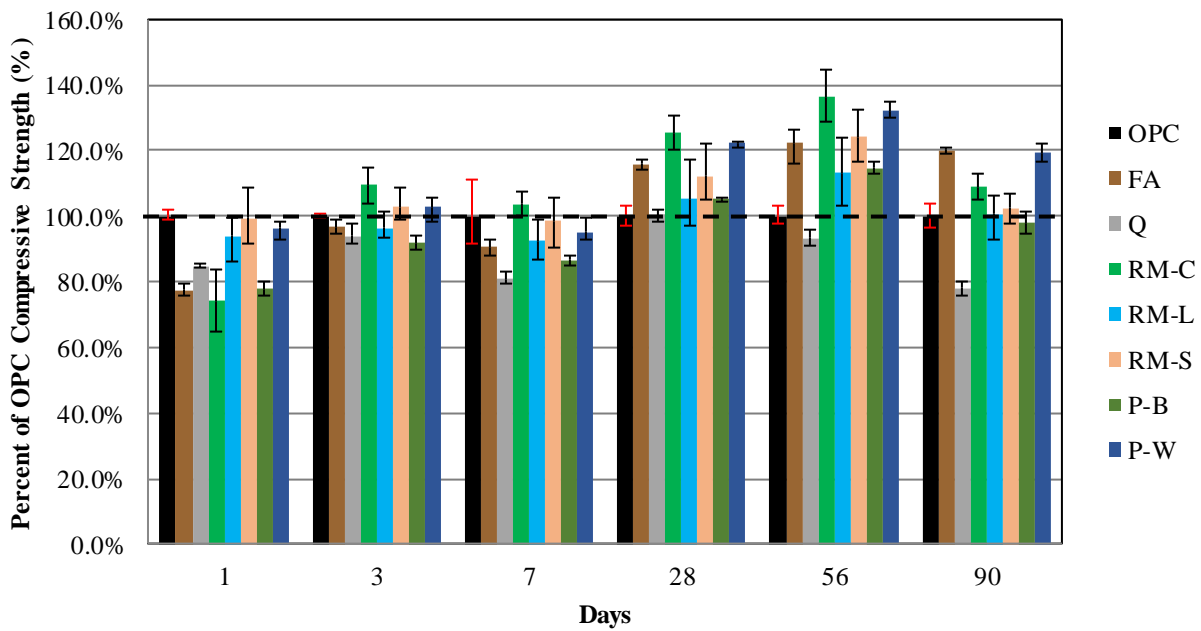
Figure 4.5: Normalized compressive strengths of mortar samples containing controls and SCMs from Supplier B
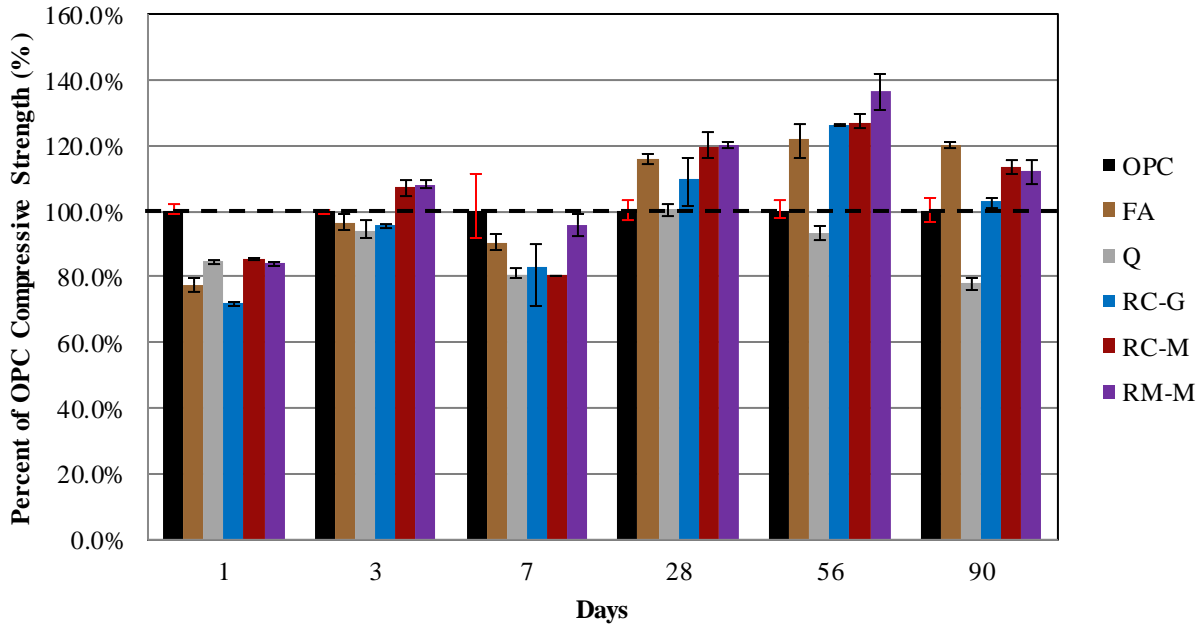
Figure 4.6: Normalized compressive strengths of mortar samples containing controls and SCMs from Supplier C

4.2.2 Strength-Activity Index

The strength-activity index (SAI) of the materials was determined by measuring the compressive strength of mixtures as outlined in ASTM C311 (2013) and performed in accordance with ASTM C109 (2013). In the SAI test, the w/cm is varied to achieve a constant flow, and the water requirement to achieve this flow is reported. ASTM C618 (2012) specifies that in order for a material to be considered a Class F fly ash, Class C fly ash, or Class N pozzolan, the SAI must be, at a minimum, 75% of the control at 7 or 28 days. The results of SAI testing are presented in Table 4.3. The SAI testing results were provided by the material suppliers, with the exception of the samples indicated with an asterisk, which were performed at UT. No data are provided for FA, Q, RC-M, and RM-M mortars since these were not tested. The test has been criticized for not effectively evaluating pozzolanic and cementitious properties of fly ash due to the varying water content (Sutter and Bentz, 2017). However, even with a fixed water content (Figures 4.4-4.6), all of the materials pass the 75% criterion at 7 and 28 days, including quartz, which is a known inert material. Therefore, the SAI criteria are not effective at gauging pozzolanicity. They are only effective for determining if an SCM is harmful to strength development, which does not apply to any of the tested materials.

Table 4.3: SAI and Water Requirement for Mortars Prepared with SCMs

Supplier	Material	SAI (%)		Water Requirement (%)
		7 Days	28 Days	
A	D-S	--	79	--
	D-S	86	81	112
	NS-I	--	81	--
	NS-I	70	75	112
	NS-S	--	79	--
	NS-S	75	69	110
	R-O	--	82	--
	R-O	89	92	103
	R-O	91	93	103
B	RM-C	90	113	101
	RM-L	89	93	102
	RM-S	110	125	102
	P-B	89	92	95
	P-W*	95	122	100
C	RC-G	79	93	100

4.3 Alkali-Silica Reaction

Durability of the mortars was tested using ASTM C1567 (2013) to evaluate the ability of the materials to control deleterious internal expansion due to alkali-silica reaction (ASR). Mixture proportions consisted of 1 part of cementitious materials to 2.25 parts of graded reactive fine aggregate by weight with a w/cm of 0.47 as prescribed by ASTM C1567. A replacement of 20% by mass was used for all SCMs initially. Expansion of the mortar bars was evaluated at 3, 7, and 14 days. If the expansion in the bars at 14 days was less than 0.1%, the materials were deemed effective in preventing ASR. If expansions of the bars were near or exceeded 0.1% at 14 days, the replacement of cement in the system was increased. The ASR plots for the materials can be seen in Figures 4.7-4.9.

The materials that did not expand above the given threshold of 0.1% at 14 days include all of the materials from Suppliers B and C, with the exception of RM-M (20), which had an expansion of 0.11 at 14 days. The replacement percentage of RM-M was increased to 25%, and expansion was controlled at this dosage (Figure 4.10). The replacement percentage of RC-M was also increased to 25% as an extra precaution due to RC-M (20) having an expansion of 0.07 at 14 days, which lies close to the threshold.

All of the natural minerals from Supplier A caused expansions beyond the threshold, Figure 4.7. These materials have higher alkali contents in comparison to the other materials, which contribute to the ASR. Replacement percentages were increased to 30% for all of the Supplier A natural minerals to assess their ability to mitigate ASR at a higher dosage. Although there was a decrease in expansion, the natural minerals still expanded beyond the threshold, Figure 4.7. This

decrease could be due to the dilution of available alkalis from the cement because it also occurs with quartz, Q. Based on the data in the previous section on CH content and compressive strength, the materials from Supplier A are not pozzolanic, which agrees with the data on ASR mitigation.
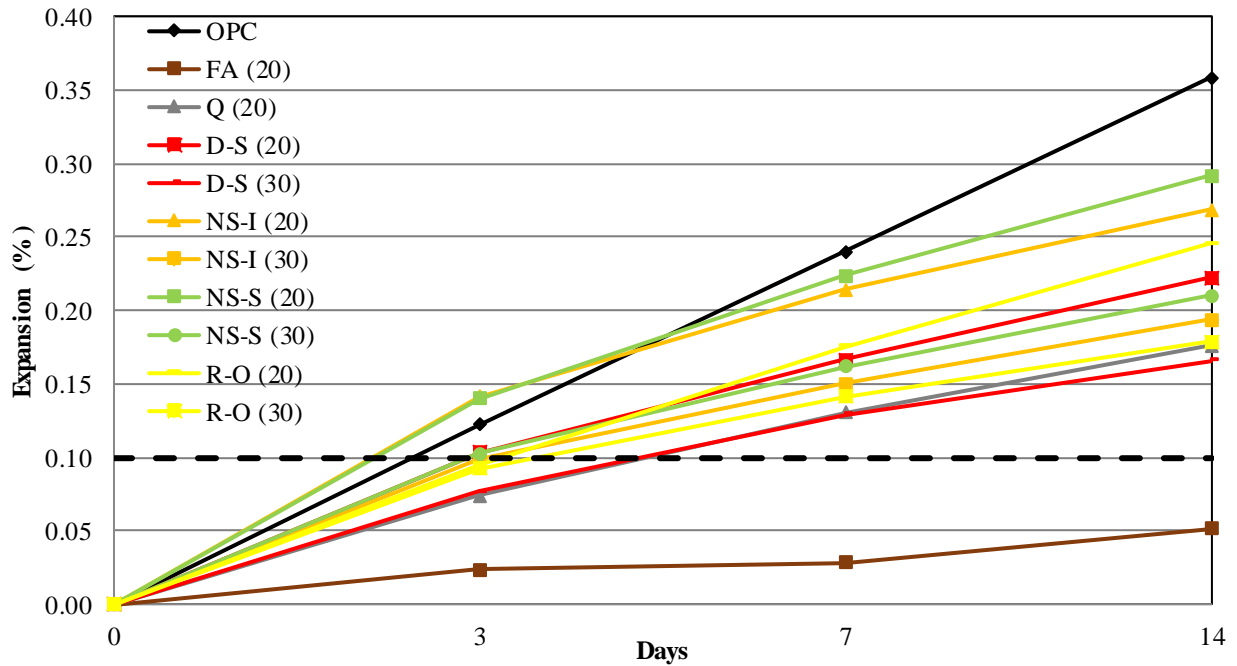
Figure 4.7: Alkali-silica reactivity of mortar samples containing controls and SCMs from Supplier A. Dashed line denotes ASTM C1567 maximum limit for ASR
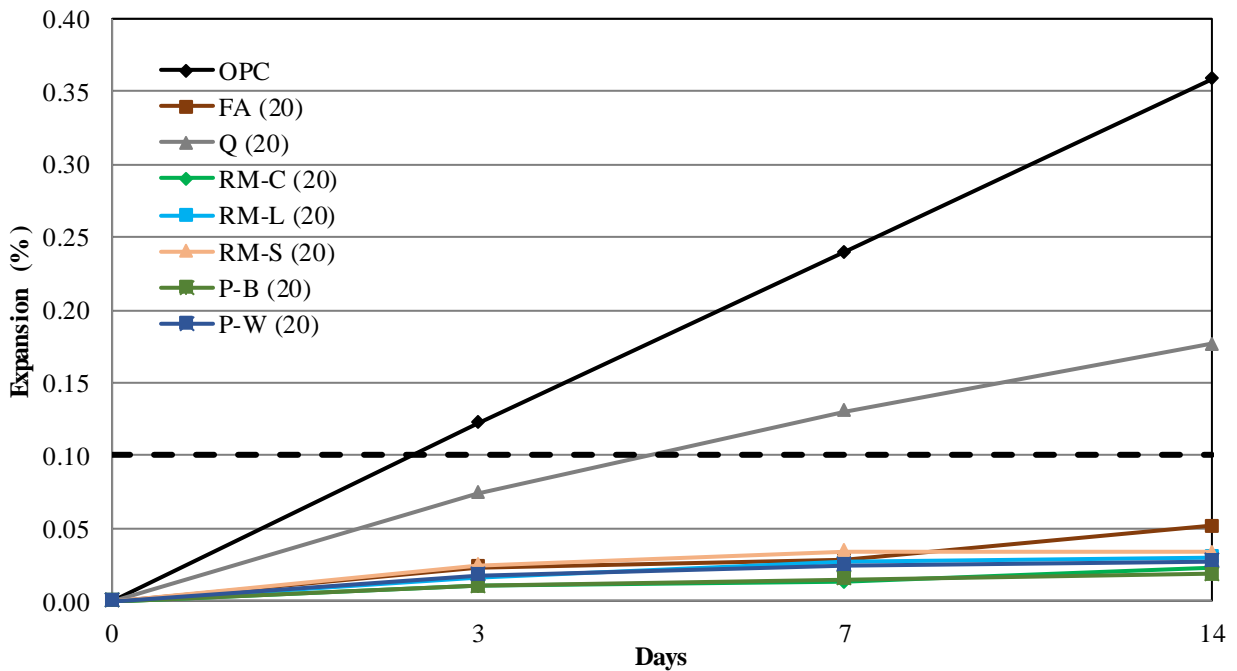
Figure 4.8: Alkali-silica reactivity of mortar samples containing controls and SCMs from Supplier B Dashed line denotes ASTM C1567 maximum limit for ASR

44
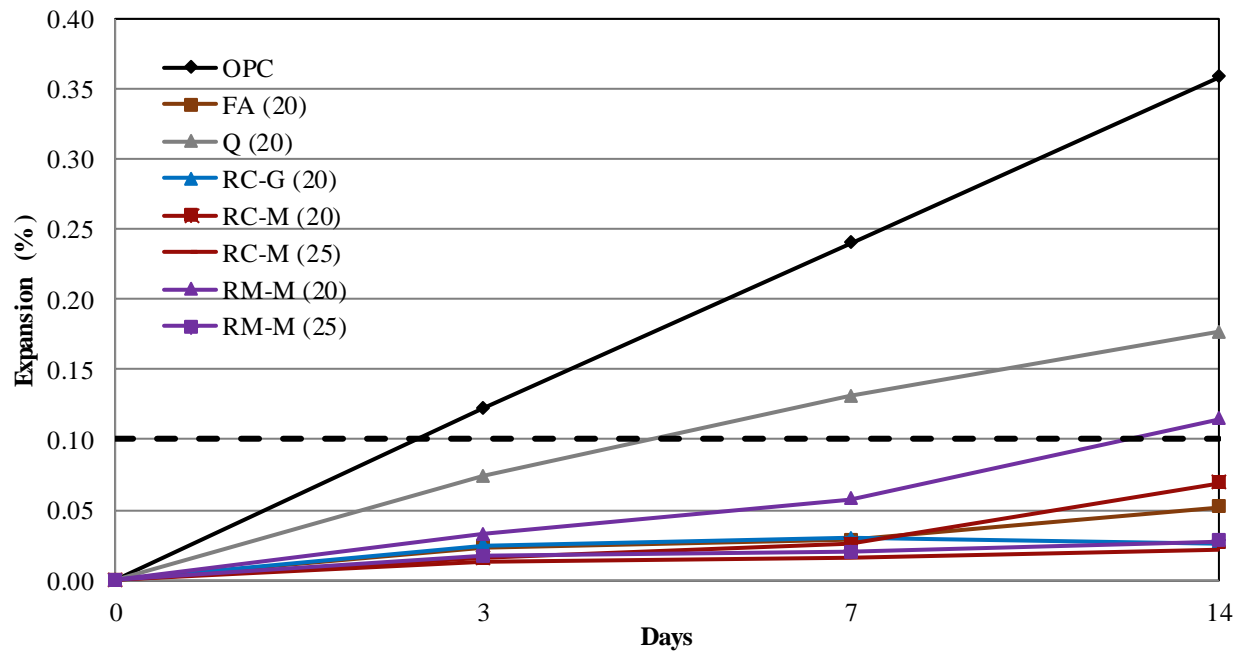
Figure 4.9: Alkali-silica reactivity of mortar samples containing controls and SCMs from Supplier C Dashed line denotes ASTM C1567 maximum limit for ASR

4.4 Sulfate Resistance

Durability of the mortars was also tested using ASTM C1012 (2015) to assess the ability of the materials to resist sulfate attack. Mixture proportioning complied with ASTM C109, where mixture designs consisted of a ratio of fine aggregate-to-cementitious materials of 2.75, and a w/cm of 0.485. Replacement dosages of 20% by mass were used for all SCMs with the exception of RC-M and RM-M, which were replaced at 25% to match the proportions for ASR.

Expansion of the mortar bars was evaluated in accordance with ASTM C1012 for up to 12 months. As per ACI 201 (2016), if the expansion in the bars before or at 6 months exceeded 0.05%, the materials were deemed ineffective at sulfate resistance. If expansion in the bars after 6 months and before or at 12 months exceeded 0.1%, the materials were also deemed ineffective in sulfate resistance (ACI 201, 2016). The sulfate expansion plots for the materials can be seen in Figures 4.10-4.12. Measurements that do not continue to 12 months are due to complete failure of the bars preventing any further expansion evaluation.

Expansion testing revealed that the materials with expansions less than 0.1% include RM-C, RM-L, RM-S, and P-W. Materials that failed included OPC, FA, D-S, NS-I, NS-S, R-O, P-B, RC-G, RC-M, and RM-M.
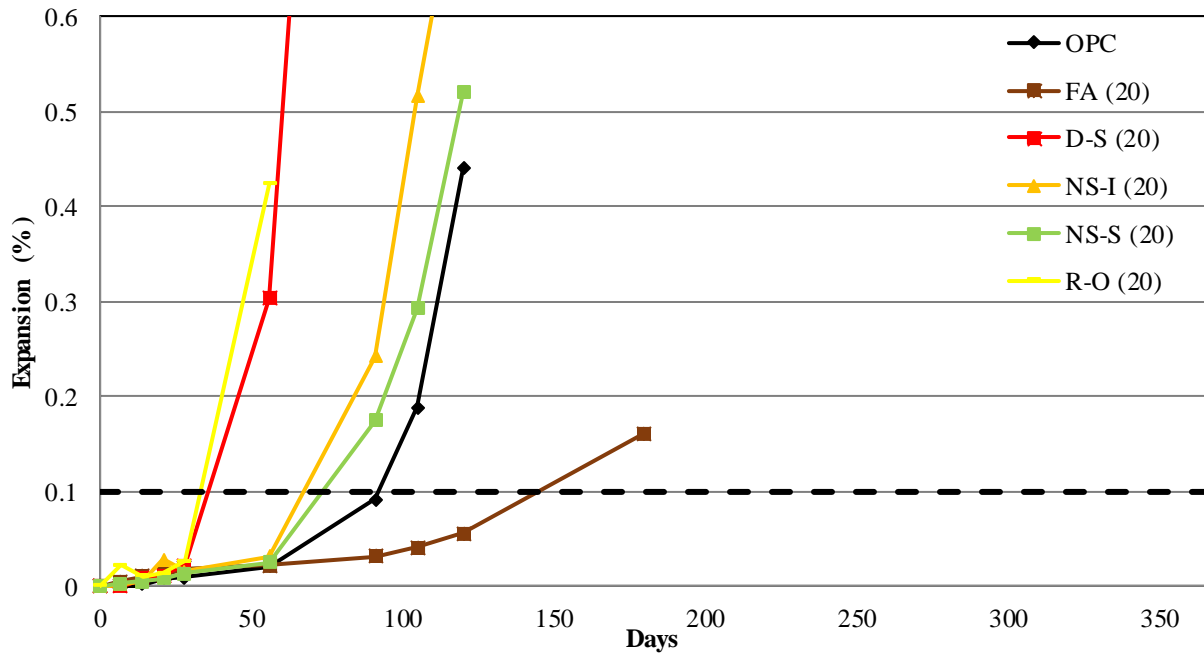
Figure 4.10: Sulfate resistance of mortar samples containing controls and SCMs from Supplier A. Dashed line denotes ACI 0.1% limit for expansion
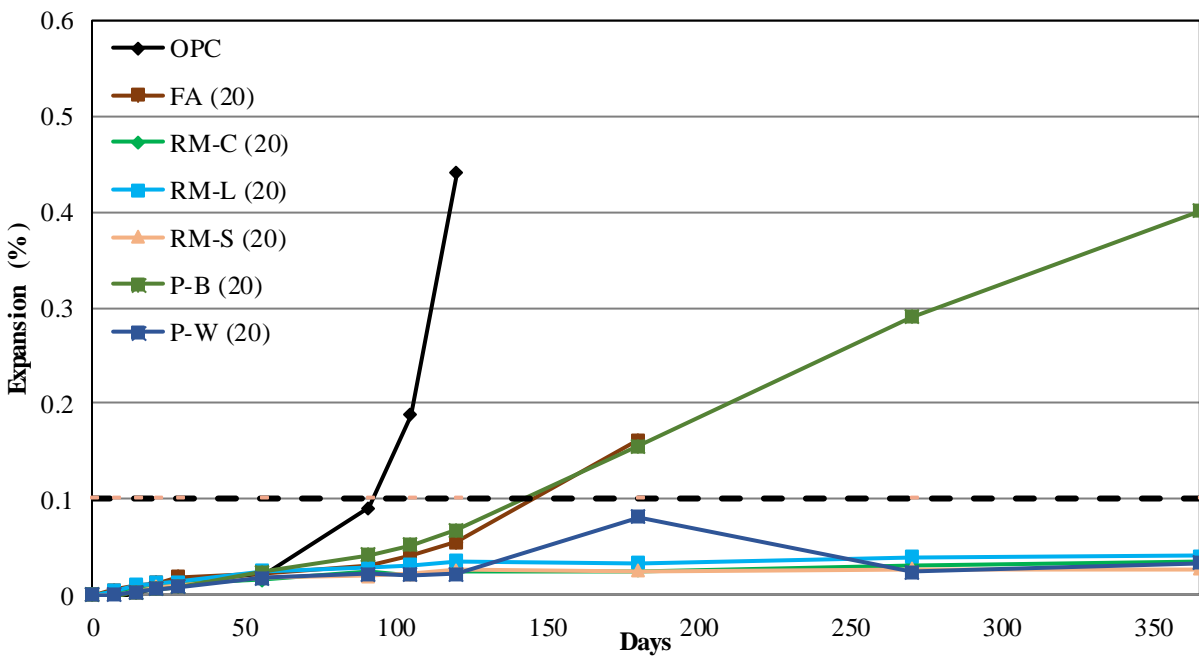
Figure 4.11: Sulfate resistance of mortar samples containing controls and SCMs from Supplier B. Dashed line denotes ACI 0.1% limit for expansion
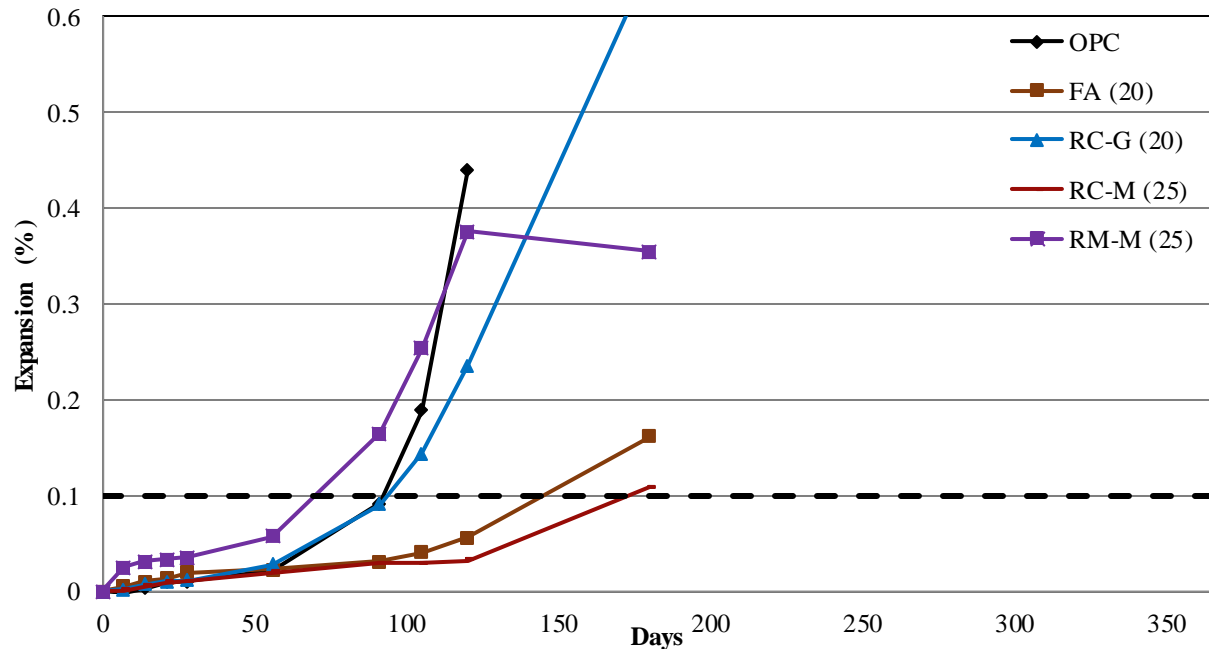
Figure 4.12: Sulfate resistance of mortar samples containing controls and SCMs from Supplier C. Dashed line denotes ACI 0.1% limit for expansion

4.5 Conclusions from Mortar Testing

Mortar flow was used to examine the effects of SCMs on workability. FA, R-O, RM-C, RC-G, RC-M, and RM-M mortars all had flows larger than the OPC mortar, indicating that the mixtures were more fluid. Fly ashes typically increase flow compared to straight cement mixtures due to the round shape of the fly ash particles, which allows the particles to move past one another easier in comparison to the angular shape of cement particles (ACI 232, 2003). Materials with mortar flows similar to OPC mortar include Q, D-S, NS-I, P-B, and P-W. The particle shapes and sizes of these materials are similar to OPC. RM-L and RM-S mortars had flows lower than the OPC mortar. The particles of these two materials are primarily angular in shape and/or textured, which would likely increase interparticle friction amongst particles, hindering movement past one another. NS-S mortar had the lowest flow at 95. In addition to having particles that are primarily angular in shape and textured, the NS-S particles appear to be porous, which could contribute to a lesser flow rate due to the absorption of water.

Compressive strength testing of mortars was performed to determine the effects of the SCMs on strength and to evaluate conformance with SAI criteria. Mortars containing the reclaimed and remediated fly ashes as well as the natural minerals provided by Supplier B continuously increased up to 90 days and surpassed, or were equal to, the magnitude of the OPC control mortar at 28 days. The compressive strengths of mortars containing the natural minerals provided by Supplier A did not increase significantly beyond 28 days and have similar strengths to Q mortars at 90 days, indicating that the materials are inert. In spite of this, all SCMs that were tested for SAI, including quartz, passed the SAI criteria.

All of the SCMs provided by Suppliers B and C controlled ASR expansion below the threshold of 0.1% at 14 days, with the exception of RM-M (20), which had a 14-day expansion of 0.11%. RC-M (20) approached the 0.1% threshold with an expansion of 0.07% at 14 days. Due to

the performance of RM-M and RC-M, the replacement percentage of RM-M and RC-M was increased to 25%, which reduced the 14-day expansions well below the control FA (20) to 0.03% and 0.02%, respectively. All of the natural minerals from Supplier A caused expansions beyond the threshold for ASR testing, at replacement percentages of 20% and 30%.

Sulfate resistance testing revealed that the mixtures with expansions less than 0.1% at 12 months include the mortars containing RM-C, RM-L, RM-S, and P-W. Mortars containing the other materials expanded beyond 0.1% before 12 months at various times, with P-B and RC-M taking the longest to fail, between 4 and 6 months. RC-G expanded beyond 0.1% prior to 15 weeks. RM-M and all of the natural minerals provided by Supplier A expanded beyond 0.1% prior to 13 weeks. It is possible that increasing the dosage of these SCMs would improve their performance.

Similar to results from paste testing, mortar testing revealed through compressive strength testing that all of the materials provided by Suppliers B and C exhibited pozzolanic activity. The materials provided by Suppliers B and C were also successful in minimizing expansion due to ASR below the threshold set forth by the standard; however, only the remediated fly ashes and P-W were able to prevent expansion due to sulfate attack past the reference threshold. Also similar to results from paste testing, the compressive strength testing revealed that the materials provided by Supplier A are inert. The materials provided by Supplier A were also unable to suppress expansion beyond the specified thresholds for ASR and sulfate attack. Mortar flow results indicated that RM-L, RM-S, and P-W have the potential to reduce the flowability of concrete (i.e., increase water demand), but this is not of great significance since the low flowability can be remediated with the use of water-reducing agents.

Chapter 5. Concrete Testing

Concrete testing was conducted on mixtures containing the same SCMs as those evaluated during the paste and mortar studies. All concrete tests were standardized ASTM tests (Table 5.1). The concrete was made using the same cement as used in paste and mortar studies (OPC), along with Colorado River sand and a Colorado River gravel for the fine and coarse aggregate, respectively. Both of these aggregates were sourced from Webberville, Texas. Control materials were also tested for comparison with the SCMs.

The mixture design generally followed ACI 211 Proportioning Concrete Mixtures (ACI 211, 1991) for structural concrete. The desired design had a target strength of 4500 psi and a target slump of 4 in. A 20% replacement of cement by mass was used for each SCM because this amount was determined in Task 3 to be sufficient to control expansion due to ASR for most of the SCMs. Additionally, a w/cm of 0.485 was used for all mixtures to provide for adequate workability. An example of a concrete mixture proportion is shown in Table 5.2 for a straight cement mixture. All other mixture proportions are shown in Appendix E. The Colorado River gravel was air-dried prior to batching due to a high moisture content affecting the water demand of the concrete. Concrete mixing was performed in accordance with ASTM C192 (2016) for machine mixing. Concrete samples were tested for workability, air content, setting time, compressive strength, and chloride ion penetrability by means of ASTM C143, ASTM C231, ASTM C403, ASTM C39, and ASTM C1202, respectively, as outlined in Table 5.1.

Table 5.1: Tests for Concrete Properties

Property	Test Method
Slump	ASTM C143 (Tex 415-A)
Air Content	ASTM C231
Setting Time	ASTM C403
Compressive Strength	ASTM C39 (7, 28, 56, & 90 days)
Rapid Chloride Penetrability	ASTM C1202 (after 56 days)

Table 5.2: OPC Concrete Mixture Design

Component	Amount (lb/yd^3)
OPC	564
Water	265
Coarse Aggregate	1807
Fine Aggregate	1342
Air	2 vol. %

5.1 Slump

Slump testing is the most common way to gauge concrete workability in the field and in the lab. To examine the effects that the SCMs have on concrete workability, slump tests were performed on the concrete mixtures. Immediately following concrete mixing, slump testing was performed in accordance with ASTM C143 (2015). One slump test was performed for each mixture (Table 5.3). After measuring the slump, the used material was placed back into the rotary drum mixer for 30 sec to reintegrate the sample with the rest of the mixture before proceeding with additional testing.

Although the targeted slump of the control OPC mixture was 4 in., the OPC mixture had a slump of 6 in. Concrete mixtures with similar slumps contained Q, NS-I, P-B, RC-G, and RM-C. All of these materials, including OPC, had small-to-medium sized particles based on the particle size distribution analysis (Table 2.7), and angular particles, as shown in the ESEM images in Appendix A, with the exception of RC-G. Since cement has medium particles that are angular, it is expected that SCMs with similar size and angularity do not change slump. RC-G had large particles that were typically spherical with some irregularly-shaped and agglomerated particles, so the impact of RC-G on slump is likely not related to particle size and shape.

Concretes with RC-M, RM-M and FA had significantly higher slumps than OPC concrete; all three of these SCMs increased slump by approximately 50%. All of these SCMs had medium-to-large particles that were spherical, which is expected to increase slump by reducing water demand. Removing water from these mixtures would help achieve the desired slump as well as increase the compressive strength of the concrete. However, changing the w/cm to achieve a target slump was not within the scope of work.

Concretes with D-S, R-O, RM-L, and P-W had lower slumps than OPC concrete. These SCMs had small-to-medium particles that were angular, with the exception of RM-L, which contained some larger particles that appeared to be porous. Small, angular, porous particles increase water demand, thus decreasing slump. Concretes with NS-S and RM-S were had the lowest slumps, with NS-S concrete having a third of the slump of OPC concrete and RM-S concrete having less than half the slump of OPC concrete. The NS-S particles had medium size, were angular, and appeared to be porous. RM-S particles had small and large particles, and exhibited the most angularity. The slump behavior of the concretes with remediated and reclaimed ashes is consistent with the rheological properties of these materials.

5.2 Air Content

Air content testing was performed in accordance with ASTM C231 (2017). Concrete was leveled using a flat strike-off plate compliant with ASTM C138 (2017), allowing unit weight to be calculated. Air content testing was performed once for each of the mixtures. Table 5.4 shows the air contents and unit weights of all of the concrete mixtures.

Entrapped air accounted for 2% of the volume of the concrete mixture in the design process. Air content testing revealed values slightly greater than 2%, with the exception of RC-M concrete, which had an air content of 1.70%. This slight variation does not pose a concern to the concrete mixtures as these mixtures did not contain air entraining admixtures, so the volume of air is only important for determining yield, and will not impact freeze-thaw resistance or strength. The unit weights of the concretes were all similar.

Table 5.3: Measured Slumps of Concrete Mixtures

Supplier	Material	Slump (in.)
Control	OPC	6.00
	FA	8.25
	Q	6.25
A	D-S	3.50
	NS-I	5.00
	NS-S	2.00
	R-O	4.75
B	RM-C	5.50
	RM-L	4.75
	RM-S	2.75
	P-B	5.50
	P-W	4.38
C	RC-G	6.50
	RC-M	9.00
	RM-M	8.25

Table 5.4: Concrete Mixture Air Contents and Unit Weights

Supplier	Material	Air Content (%)	Unit Weight (lb/ft^3)
Control	OPC	3.20	144.0
	FA	2.25	145.2
	Q	3.40	143.6
A	D-S	2.70	145.2
	NS-I	3.15	144.8
	NS-S	2.30	146.0
	R-O	3.40	144.4
B	RM-C	2.35	145.6
	RM-L	3.05	145.2
	RM-S	2.10	145.6
	P-B	2.90	144.4
	P-W	3.00	144.4
C	RC-G	3.10	144.0
	RC-M	1.70	146.4
	RM-M	2.10	146.8

5.3 Setting Time

Time of set of all of the mixtures was determined using ASTM C403 (2016). A delay in setting time can cause problems in the field for concrete laborers and put construction behind schedule. In order to prepare samples for the test, fresh concrete was sieved using a vibrating plate to separate the mortar from the coarse aggregate. After sieving, an adequate amount of mortar was placed into a cylindrical container and consolidated using the vibrating plate. A loading apparatus was used with needles of varying bearing areas to measure the force required to cause the penetration of the needles into the mortar. Samples were initially tested 3 to 4 hours after concrete mixing, and subsequent tests were performed at 30 min to 1 hour intervals until a penetration reading equal to or exceeding 4000 psi was obtained. Plots of the penetration resistance versus time are shown in Figures 5.1-5.3. The initial time of set is deemed to be at 500 psi by the standard, whereas, final set corresponds to a penetration resistance of 4000 psi. Setting time was measured once for each of the concrete mixtures.

It is known that the use of some SCMs can delay the setting time of concrete (Fajun et al., 1985; ACI 232, 2000). Additionally, the dilution of cement in the mixture by SCMs or fillers can also delay the setting time of the concrete, yet the addition of nucleation sites provided by fine SCMs can sometimes counteract these effects (Bentz et al., 2017). As expected, the initial and final times of set for all of the SCM concretes was longer than that of OPC concrete. The control fly ash, FA, and RC-G resulted in similar initial and final times of set, both reaching final set at approximately 300 minutes after mixing. D-S, NS-I, NS-S, and R-O all displayed final set times falling between the final setting of OPC concrete and FA concrete. RM-L, RM-S, RM-M, and RC-M concretes all had longer final set times, occurring between approximately 330 and 345 minutes after mixing. P-W concrete had a final set time near that of OPC concrete, while P-B concrete reached final set nearly one hour later. RM-C concrete had a delayed final set time at approximately 500 minutes after mixing with an initial set time after 360 minutes. This can lead to issues in the field when concrete finishing in a timely manner is necessary to proceed in the construction process. It is not known why RM-C delayed setting more than the other SCMs.

5.4 Compressive Strength

Following concrete mixing and slump testing, concrete was cast into fourteen 4 in. by 8 in. plastic molds in accordance with ASTM C192 (2016). Once all cylinders were cast, they were then stored in a temperature-controlled room at 73 ºF for 24 hours before the specimens were removed from their molds. All specimens were then cured at 73 ºF and 100% relative humidity until they reached the desired age. The SCMs and control materials were tested for compressive strength based on ASTM C39 (2017) at 7, 28, 56 and 90 days. Similar to mortar strength tests, the compressive strengths of the concrete cylinders were evaluated over time to determine if the SCMs are pozzolanic, thus increasing strength over time. Compressive strength results are shown in Figures 5.4-5.6.
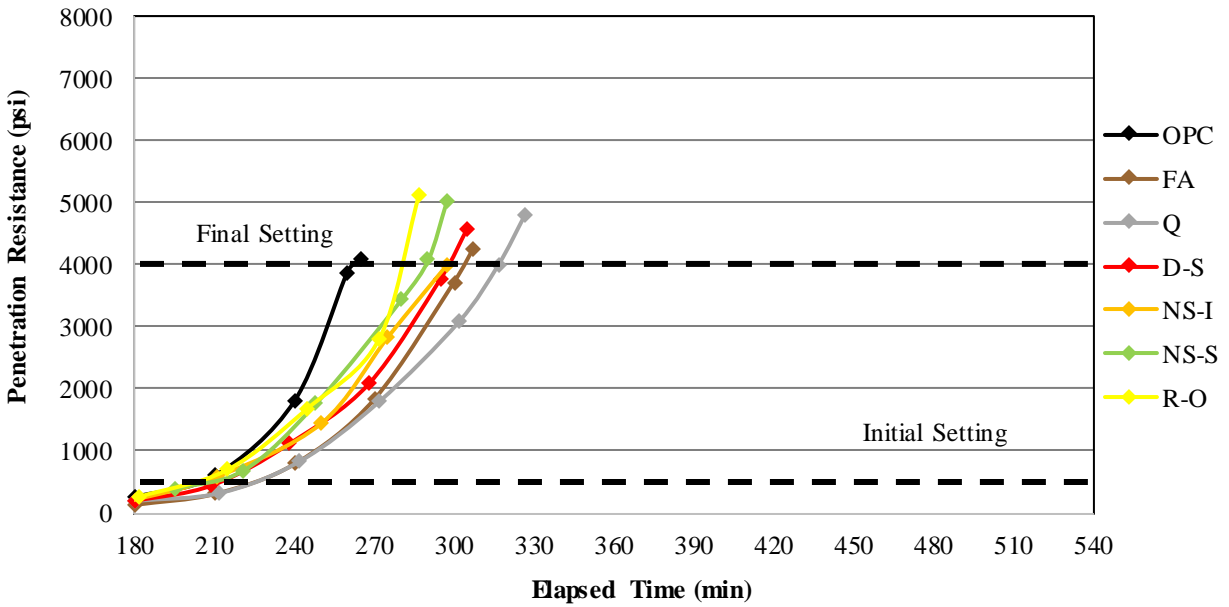
Figure 5.1: Time of set concrete mixtures containing controls and SCMs from Supplier A
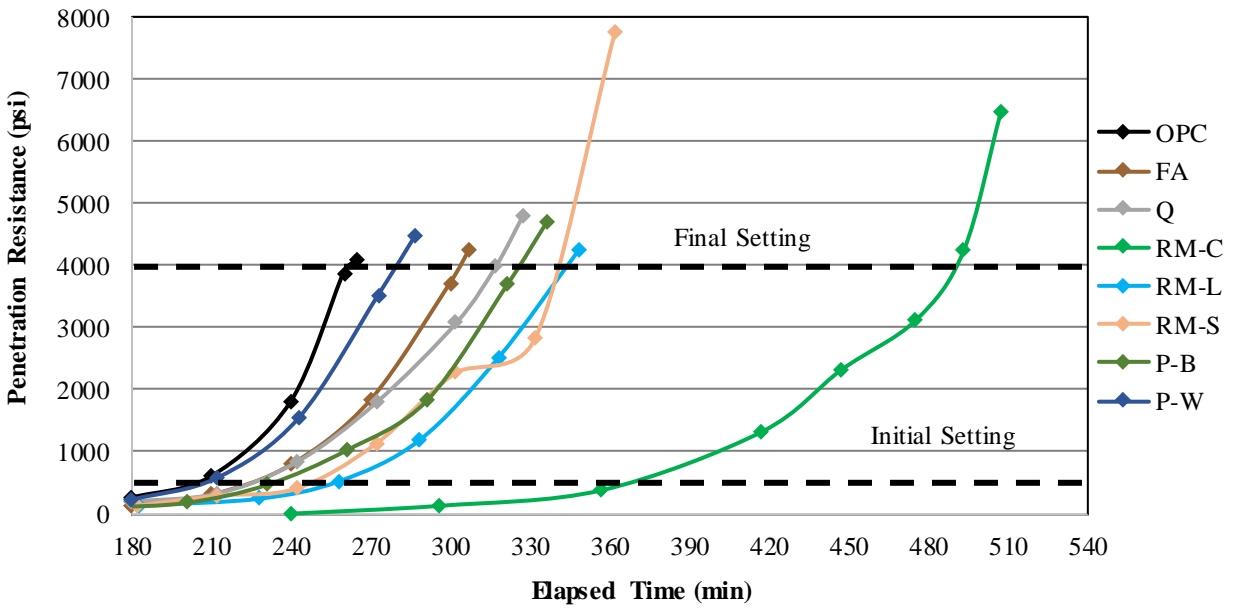
Figure 5.2: Time of set concrete mixtures containing controls and SCMs from Supplier B
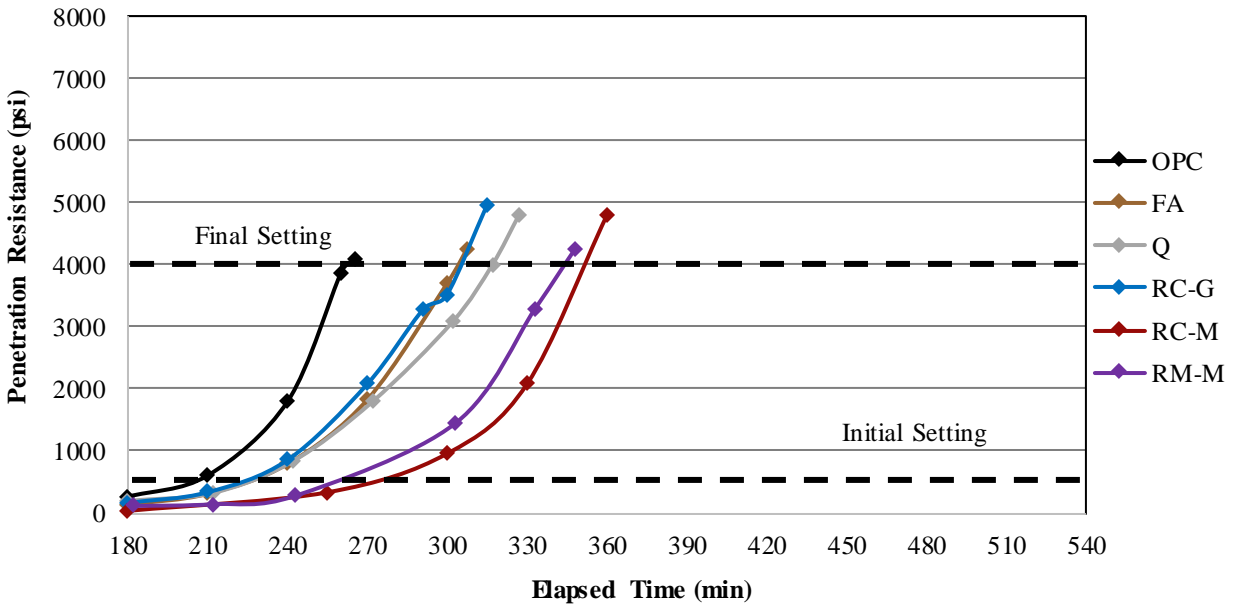
Figure 5.3: Time of set concrete mixtures containing controls and SCMs from Supplier C
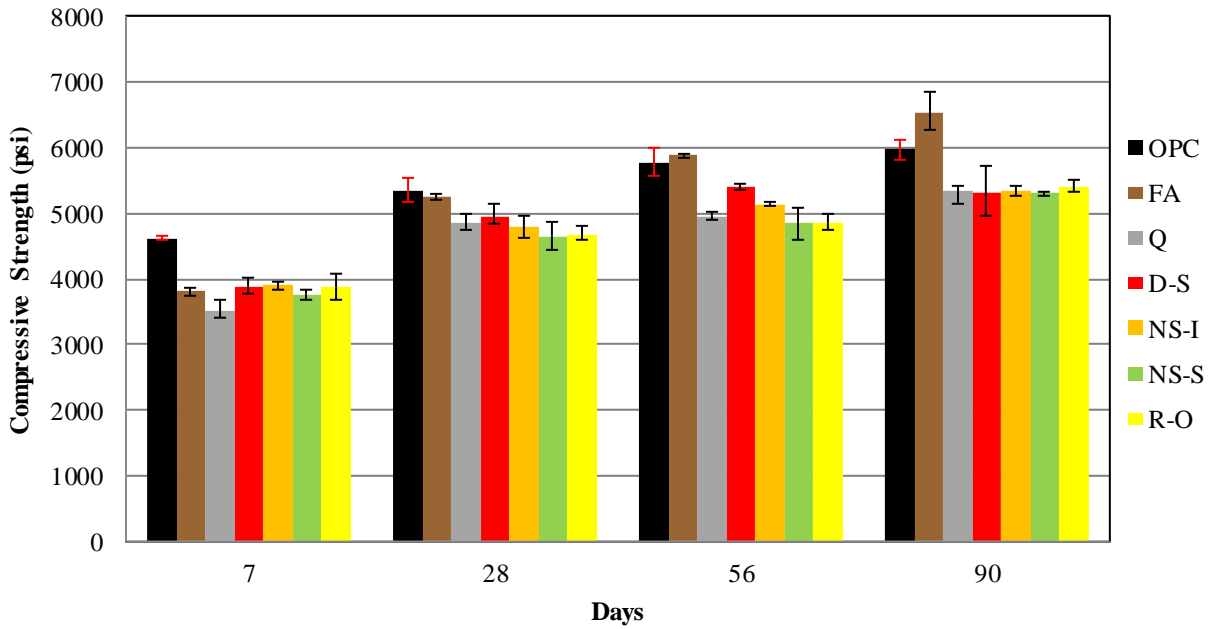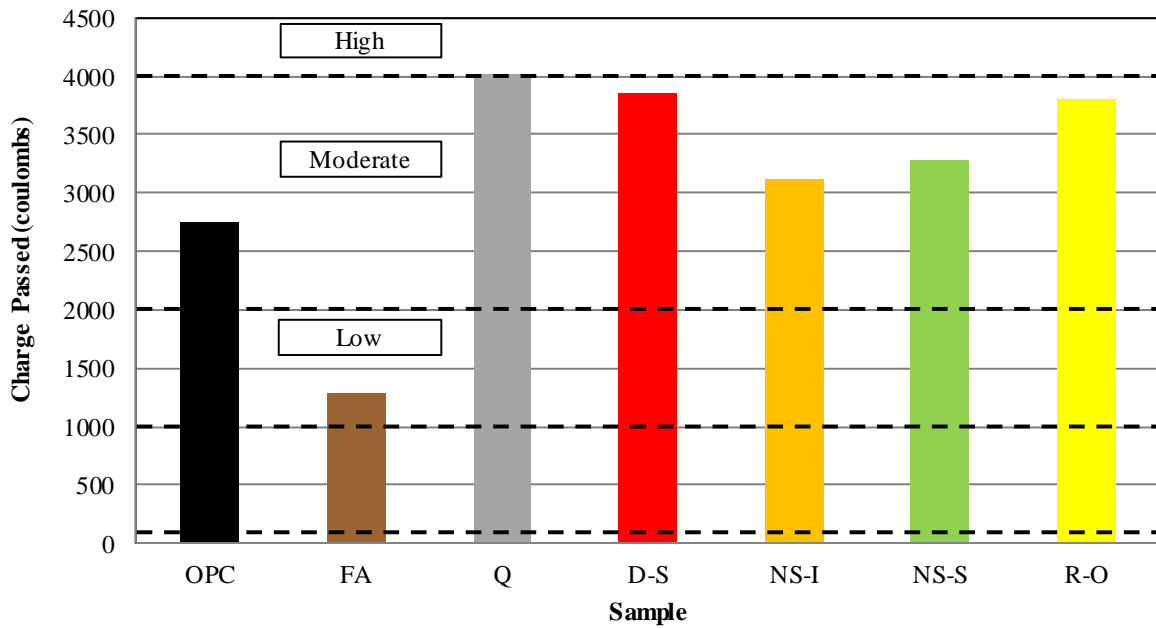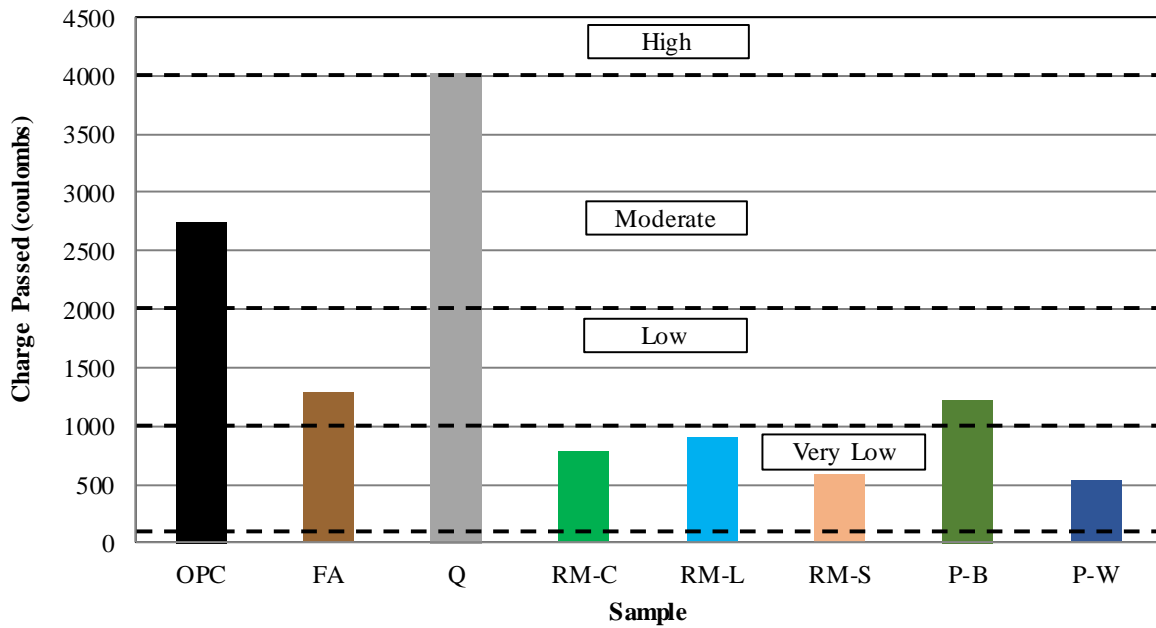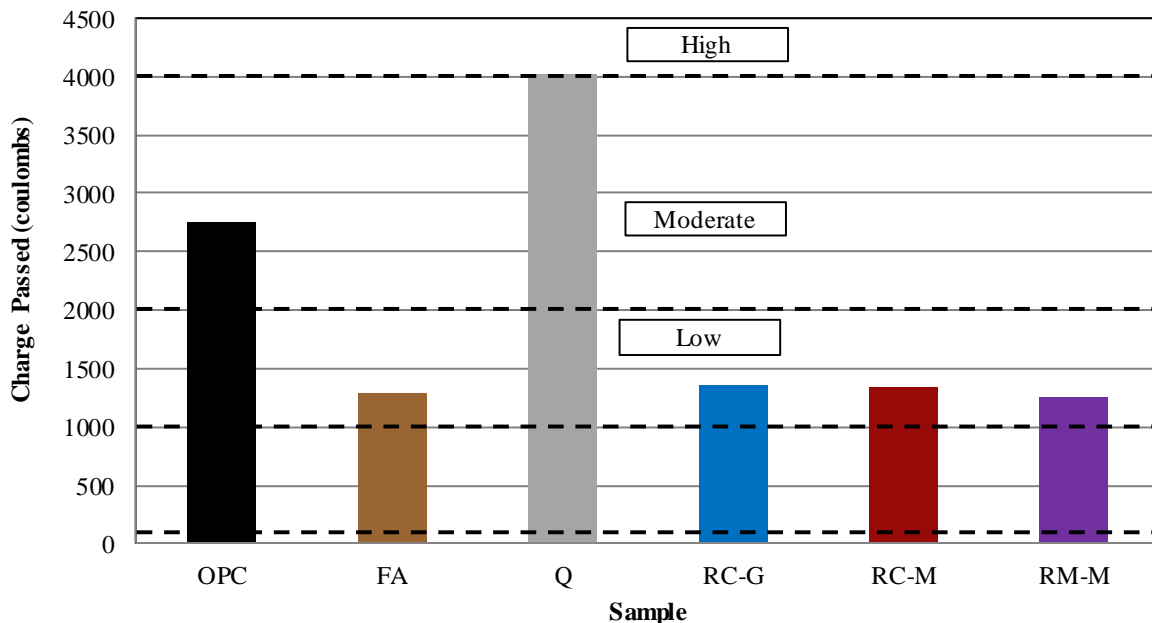

Figure 5.4: Compressive strength results of concrete mixtures containing controls and SCMs from Supplier A
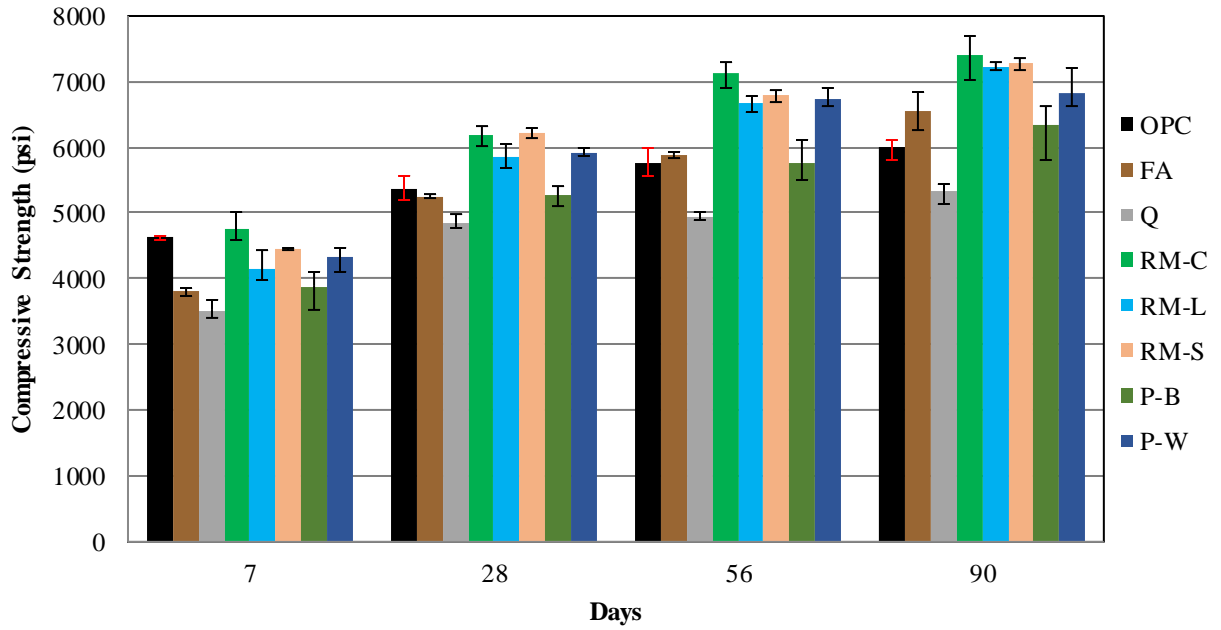
Figure 5.5: Compressive strength results of concrete mixtures containing controls and SCMs from Supplier B
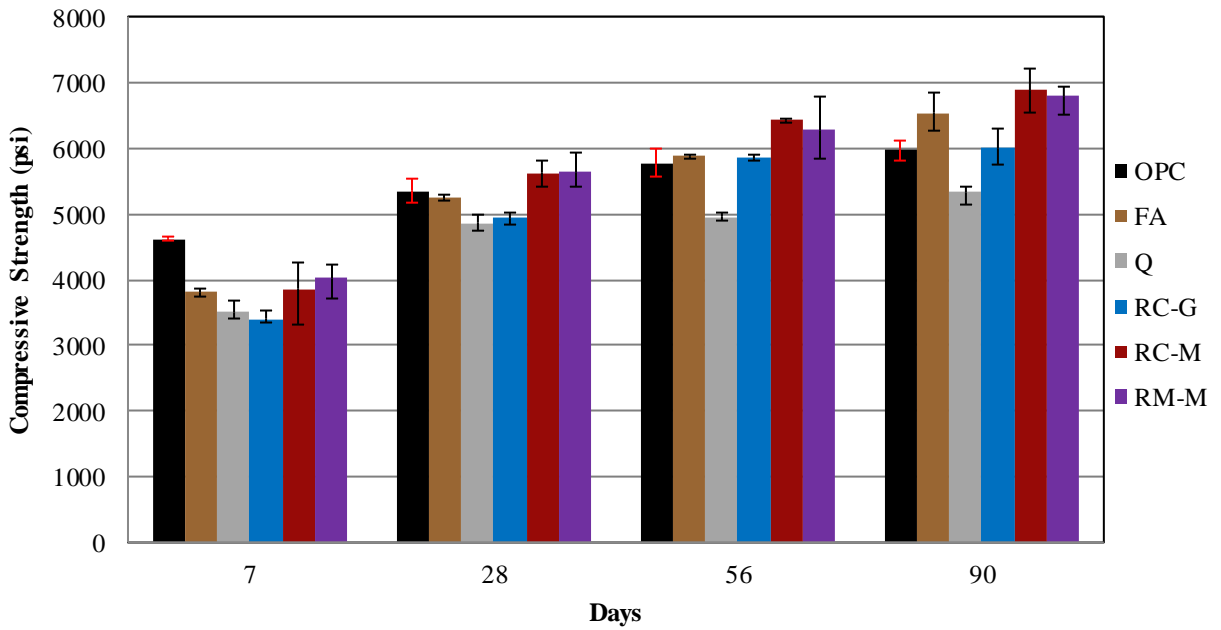
Figure 5.6: Compressive strength results of concrete mixtures containing controls and SCMs from Supplier C

In Figure 5.4, the compressive strengths of the concretes containing natural minerals from Supplier A did not increase significantly beyond 28 days. At 90 days, the compressive strengths were equivalent to that of the Q concrete. In Figure 5.5, the compressive strengths of the concretes the materials provided by Supplier B continuously increased and surpassed the magnitude of the OPC control concrete at 28 days, with the exception of P-B concrete, which had similar results to OPC concrete. In Figure 5.6, the compressive strengths of the concretes containing fly ashes from Supplier C continuously increased up to 90 days, with the magnitudes being equal to or greater than the OPC concrete by 56 days. The strengths of all of the concrete samples containing fly ashes from Supplier C were similar to the concrete with FA at later ages.

5.5 Rapid Chloride Penetrability

Rapid chloride penetrability testing (RCPT) was conducted in accordance with ASTM C1202 (2012). Sample preparation began once concrete cylinders reached 56 days of curing. The concrete cylinders were cut using an oil-lubricated concrete saw, first removing less than 0.25 in. from the top finished surface, then cutting a 2 in. thick sample from the top of the cylinder, parallel to the top of the cylinder. Once the cylinders were cut, the 2 in. samples were soaked in soapy water overnight to remove oil left from the saw, which has potential to skew the results. After soaking, the concrete samples were rinsed, and sample preparation and testing procedures were followed per ASTM C1202. Samples were subjected to 60 V of electricity for 6 hours, with readings taken every 30 minutes. RCPT was conducted once for each concrete mixture and the results are shown in Figures 5.7-5.9, which also shows the designations for penetrability resistance as outlined by ASTM C1202.

RCPT provides a good indication of permeability of the concrete, which can be correlated with porosity. The pozzolanic reaction densifies the concrete matrix, reducing porosity, which in turn reduces the ability for ions to penetrate (ACI 201, 2016). Figure 5.7 shows that the concretes made with natural minerals from Supplier A have more charge passed than OPC concrete, with D-S and R-O concretes nearly reaching high levels of charge passed of Q concrete. Figures 5.8 and 5.9 show that all of the materials from Suppliers B and C are effective in reducing chloride ion penetrability of concrete, with P-W concrete having the lowest amount of charge passed. It is interesting to note that P-B and RC-G concretes, which had similar results to OPC concrete in compressive strength, had the largest magnitude of charge passed through the concrete for the materials provided by Suppliers B and C; however, the magnitude of the charge passed was still significantly lower than that of OPC concrete.

Figure 5.7: RCPT results of concrete mixtures containing controls and SCMs from Supplier A

Figure 5.8: RCPT results of concrete mixtures containing controls and SCMs from Supplier B

Figure 5.9: RCPT results of concrete mixtures containing controls and SCMs from Supplier C

5.6 Conclusions from Concrete Testing

Concrete testing was performed to determine the suitability of the SCMs as Class F fly ash substitutes in concrete. Concrete mixtures containing NS-I, P-B, RM-C, and RC-G had little effect on the workability of concrete, having comparable slumps to the OPC mixture. RC-M, RM-M, and FA concretes had significantly higher slumps than the OPC concrete, increasing slump approximately 50%. D-S, NS-S, RM-L, RM-S, and P-W decreased concrete slump, with NS-S and RM-S concrete having less than half the slump of OPC concrete. These lower slumps indicate that problems with workability could arise in the field unless WRAs are used.

The times of set for all the concrete mixtures with SCMs were somewhat longer than that of OPC concrete. RM-C concrete had the longest final setting time at 230 minutes after that of OPC concrete, with an initial time of set at 360 minutes, which can lead to complications in the field when concrete finishing in a timely manner is necessary to proceed in the construction process.

All materials from Suppliers B and C displayed pozzolanic behavior based on the compressive strength testing, with higher long-term strengths than the OPC concrete. P-B and RC-G concretes showed the lowest level of pozzolanicity, having similar strength as OPC concrete at 56 and 90 days. This is consistent with expectations based on paste and mortar testing. Although RM-C concrete had an issue with delaying time of set, it exceeded or matched all concrete mixtures in compressive strength at each testing day. At early ages, it is expected for SCMs to decrease the compressive strength of concrete, which can be seen at 7 days for all the materials, with the exception of RM-C concrete. All of the natural minerals provided by Supplier A appear to be inert, as suggested by no or minimal concrete compressive strength gain beyond 28 days, as well as having similar results to Q concrete at 90 days. Again, this is consistent with paste and mortar studies with these materials.

RCPT provides a good indication of permeability of the concrete. The results of RCPT for the materials provided by Suppliers B and C indicated low permeability of the concretes, agreeing with the pozzolanic behavior observed for these materials, which causes a densification of the concrete matrix, reducing permeability. The results of RCPT also correlate well with the compressive strength results, with concrete containing remediated ashes and P-W having the least amount of charge passed through the samples and also the highest strengths. The results of RCPT for the natural minerals provided by Supplier A also correlate well with the compressive strength results in that the charge passed for concrete containing these materials and the compressive strengths were similar to Q concrete.

From these results, it is apparent that the materials from Supplier B and Suppler C should be suitable for use in concrete as-is, and they provide enough pozzolanic activity to increase long-term compressive strength, with the exception of P-B and RC-G; however, P-B and RC-G should still be suitable as a replacement for concrete due to the similar compressive strengths and slumps to OPC concrete, times of set within one hour of OPC concrete, and the significantly lower amounts of charged passed through the samples in comparison to OPC concrete. Potential issues unrelated to strength are setting time for RM-C and workability for RM-S.

Despite the natural minerals provided by Supplier A not being pozzolanic, their use in concrete does not appear to be detrimental in terms of compressive strength, time of set, air content, and unit weight. However, since the charge passed through the samples in RCPT was greater than that of OPC concrete, particularly for D-S and R-O, the concrete may be susceptible to chloride ingress.

Chapter 6. Conclusions and Recommendations

6.1 Summary and Conclusions

To prepare for the upcoming shortage in fly ash supply due to competing fuel sources and emission standards, potential alternatives were tested following protocols recommended by TxDOT Project 0-6717. The alternative materials that were tested in this implementation project included natural minerals, reclaimed fly ashes, and remediated fly ashes.

All of the natural minerals provided by Supplier A were determined to be inert fillers, with performance in most tests equivalent to the inert ground quartz, Q. The minerals show no pozzolanic activity, no ability to reduce expansion from ASR or sulfate attack, and no ability to increase long-term compressive strength; in fact, they actually increase the charge passed in RCPT testing compared to a straight cement mixture. Therefore, these materials are not recommended for use as a Class F fly ash replacement.

The natural minerals provided by Supplier B, on the other hand, were shown to be pozzolanic and improve concrete performance. They pass ASTM C 618 requirements for natural pozzolans, and performed well in most tests. The only concern is the failure of P-B in preventing expansions from sulfate attack. However, it is likely that increasing the replacement percentage could improve performance in this test.

All of the reclaimed and remediated fly ashes selected for testing exhibited pozzolanic behavior and are able to perform similarly to a production Class F fly ash in certain applications and environments. Material characterization showed that all of the fly ashes selected for further testing passed ASTM C 618 requirements for a Class F fly ash, with the exception of RC-G, which slightly exceeded the moisture content criterion. However, as previously discussed, the supplier should be able to easily remedy this condition.

The remediated fly ashes from Supplier B were more angular in shape in comparison to the round particles of FA. Flowability of pastes, mortar, and concrete was significantly impacted by the particle shapes of the materials with rheological testing showing that the more angular, remediated fly ash pastes had higher yield stresses and viscosities in comparison to the OPC and FA pastes. The reclaimed fly ashes from Supplier C had round particles, so pastes containing these materials performed similarly to FA pastes in rheology testing. The rheology results generally correlated well with mortar flow and concrete mixture slumps.

The results of testing for saturation WRA dosages indicate that the remediated and reclaimed ashes tested do not have an adverse effect on the admixture saturation point in comparison to the production ash. Since compatibility depends on the powder-cement combination, prior to using a WRA with a reclaimed or remediated fly ash, testing should be performed to determine the appropriate admixture type and dosage in which no problems occur with mixture stiffening and strength gain.

Foam index testing indicated that RC-M paste required a higher dosage of AEA despite having a low LOI, likely caused by the presence of activated carbon. RM-C and RM-S, both having higher LOIs than FA, required higher dosages of AEA in foam index testing.

Despite delaying the time of set of concrete mixtures, none of the SCMs had a significant impact on the hydration kinetics of the cement, with the exception of RM-C, which delayed the heat of hydration peak. This correlates to a significantly delayed time of set exhibited by RM-C concrete. Though the use of a Class F fly ash can delay the setting time of concrete, RM-C concrete took over three hours longer than FA concrete to reach final set, which is a more substantial delay

than is usually expected with fly ash (ACI 232, 2003). The delayed hydration and setting did not reduce early strength of RM-C-containing mortars and concrete, however.

CH content and compressive strength testing suggested that RC-G is the least pozzolanic of the fly ashes tested. However, given the successful performance in ASR and RCPT testing, this fly ash is at least minimally pozzolanic.

In terms of durability, all of the fly ashes performed well in ASR and RCPT testing, indicating that a 20–25% replacement of cement by mass is effective in suppressing ASR and reducing the amount of charge passed through the concrete matrix. Only the remediated fly ash mortars were able to withstand sulfate attack, while the reclaimed fly ash and FA mortars failed before six months.

The results of testing are qualitatively summarized in Table 6.1. A green check mark indicates that the SCM performed favorably in a test, a red x suggests that the material did not perform well, a black dash means that the material impact is neutral, and an asterisk indicates that the test was not performed for that material. The desired workability is dependent on the application in the field, so for the purposes of this table having a positive or negative effect on workability was defined as positive being an increase in flowability as compared to the OPC paste and negative as a decrease in flowability as compared to the OPC paste.

Table 6.1: Summary of Effects of SCMs on Cementitious Mixture Performance

Test	Supplier A				Supplier B					Supplier C		
	D-S	NS-I	NS-S	R-O	RM-C	RM-L	RM-S	P-B	P-W	RC-G	RC-M	RM-M
Yield Stress	*	*	*	*	X	X	X	*	*	✓	✓	✓
Viscosity	*	*	*	*	X	X	X	*	*	✓	✓	✓
WRA Interact	*	*	*	*	--	*	--	*	*	--	--	*
AEA Interact	*	*	*	*	--	✓	--	*	*	✓	X	*
CH Content	X	✓	X	X	✓	✓	✓	--	✓	--	--	--
Mortar Flow	--	--	X	✓	✓	X	X	--	--	✓	✓	✓
ASTM C109	X	X	X	X	✓	--	--	--	✓	--	✓	✓
ASR	X	X	X	X	✓	✓	✓	✓	✓	✓	✓	✓
Sulfate	X	X	X	X	✓	✓	✓	X	✓	X	X	X
Slump	X	--	X	X	--	X	X	--	X	--	✓	✓
Setting Time	--	--	--	--	X	--	--	--	--	--	--	--
ASTM C39	X	X	X	X	✓	✓	✓	--	✓	--	✓	✓
RCPT	X	X	X	X	✓	✓	✓	✓	✓	✓	✓	✓

Materials that were not tested in the specified category are denoted with an asterisk (*).

6.2 Recommendations and Suggestions for Future Work

Based on the results of testing and the summary of those results in Table 6.1, the natural minerals from Supplier A should not be used as a replacement for Class F fly ash in concrete. The

minerals are not pozzolanic and cannot improve strength or resistance to ASR, sulfate attack, or chloride ingress. The natural minerals from Supplier B, on the other hand, are appropriate for use as SCMs in concrete, but if P-B is considered in applications requiring sulfate resistance, more testing would need to be performed at a higher cement replacement amount. All of the reclaimed and remediated fly ashes can potentially be used as a production Class F fly ash substitute in concrete. However, the following should be noted:

- The use of both reclaimed fly ashes, RC-G and RC-M, and RM-M should be avoided when sulfate-resistant concrete is required, unless tests with higher cement replacement levels show improved results.
- For use of RM-L and RM-S, a WRA is necessary to increase the flow of the concrete in applications where high flowability is desired.
- RM-C requires the use of an accelerating admixture in order to reduce the time of set. This is necessary in order to avoid complications in the field when concrete finishing in a timely manner is necessary to proceed in the construction process. Additionally, a WRA is required if a flow comparable to FA concrete is desired.
- RC-M, despite a low LOI value, needs more AEA to adequately entrain air in concrete, as suggested by the foam index test results. RM-M, the remediated version of RC-M, required half the dosage of AEA in the foam index paste test proving that the remediation technique was effective. However, RM-M performed worse in ASR and sulfate testing, which could be a result of remediation.

Before the natural minerals and reclaimed and remediated fly ashes can be used in Texas concrete, thought should be given to how the materials will be specified. As mentioned in Chapter 1, currently the only natural pozzolan explicitly allowed for use in Texas concrete is metakaolin. Since the P-B and P-W meet ASTM C618 for Class N pozzolans and could meet the TxDOT durability criteria (TxDOT, 2004) depending on dosage amount, these specifications can be used to approve their use in concrete. With respect to fly ashes, ASTM C618 does not specify that the fly ashes that fall under the specification be production ashes, leaving open the possibility that the standard applies also to reclaimed or remediated ashes. Therefore, using the successful reclaimed and remediated fly ashes in Texas concrete should not be problematic if they meet ASTM C618 and TxDOT (2004) specifications. It is important to note, however, that fly ashes that are remediated through blending with other SCMs or fillers do not fall under ASTM C618 Class C and Class F since they are not 100% fly ash. These materials could be specified under ASTM C1697 (2016) if they are blends of SCMs that meet specifications. If not, new specifications should be developed in order to facilitate the use of these blended materials in concrete.

It should be noted that fly ash physical, chemical and mineralogical properties can vary widely and influence the behavior of cementitious mixtures differently based off of the coal source, burning conditions and collection and storage conditions (Thomas et al., 2017). Disposal methods and location can also alter these fly ash properties (McCarthy et al., 2017). Reclamation and remediation methods also differ from plant-to-plant. Because of this, the recommendations presented in this report only represent the specific materials tested, not all reclaimed and remediated fly ashes. Testing on a larger sampling of reclaimed and remediated fly ashes can reveal the best reclamation and remediation procedures to obtain a quality fly ash.

In terms of future work, it is suggested that more extensive work for mitigation of ASR and sulfate attack be considered. Although the ASTM C 1567 (2013) accelerated mortar bar method is commonly used in order to predict the ability of an SCM to suppress ASR, it should

only serve as a screening test (Thomas, 2011). Future testing using the concrete prism method, ASTM C 1293 (2015), can give a better indication into the ability of the reclaimed and remediated fly ashes to suppress ASR. It is also recommended that additional work be done to increase SCM replacement for sulfate resistance testing to reveal if the reclaimed fly ashes can protect against sulfate attack.

References

ACAA (2011). *2010 Coal Combustion Product (CCP) Production & Use Survey Report*. Retrieved from https://www.acaa-usa.org/Publications/Production-Use-Reports.

ACAA (2016). *2015 Production and Use Survey Results News Release*. Retrieved from https://www.acaa-usa.org/Publications/Production-Use-Reports.

ACI (2016). *ACI Concrete Terminology,* ACI CT-16, American Concrete Institute, Farmington Hills, Michigan.

ACI Committee 201 (2016). *Guide to Durable Concrete*, ACI 201.2R-16, American Concrete Institute, Farmington Hills, Michigan.

ACI Committee 211 (1991). *Standard Practice for Selecting Proportions for Normal, Heavyweight and Mass Concrete*, ACI 211.1-91, American Concrete Institute, Farmington Hills, Michigan.

ACI Committee 232 (2003). *Use of fly ash in concrete*, ACI 232.2R-03. American Concrete Institute, Farmington Hills, Michigan.

ACI Committee 232 (2000). *Use of Raw or Processed Natural Pozzolans in Concrete*, ACI 232.1R-00, American Concrete Institute, Farmington Hills, Michigan.

Antoni, M., Rossen, J., Martirena, F., Scrivener, K. (2012). Cement substitution by a combination of metakaolin and limestone. *Cement and Concrete Research,* 42, 1579-1589

Arabani, M., Azarhoosh, A.R. (2012). The effect of recycled concerte aggregate and steel slag on the dynamic properties of asphalt mixtures. *Construction and Building Materials,* 35, 1–7.

ARTBA (2015). Production and Use of Coal Combustion Products in the U.S.: Market Forecast through 2033. Retrieved from https://www.acaausa.org/Portals/9/Files/PDFs/ReferenceLibrary/ARTBA-final-forecast.compressed.pdf.

ASTM C39 (2017). Standard Test Method for Compressive Strength of Cylindrical Concrete Specimens, ASTM International, West Conshohocken, Pennsylvania.

ASTM C 109 (2016). Standard Test Method for Compressive Strength of Hydraulic Cement Mortars (Using 2-in. or [50 mm] Cube Specimens), ASTM International, West Conshohocken, Pennsylvania.

ASTM C138 (2017). Standard Test Method for Density (Unit Weight), Yield, and Air Content (Gravimetric) of Concrete, ASTM International, West Conshohocken, Pennsylvania.

ASTM C143 (2015). Standard Test Method for Slump of Hydraulic-Cement Concrete, ASTM International, West Conshohocken, Pennsylvania.

ASTM C 150 (2017). Standard Specification for Portland Cement, ASTM International (2017) West Conshohocken, Pennsylvania.

ASTM C 151 (2016). Standard Test Method for Autoclave Expansion of Hydraulic Cement, ASTM International, West Conshohocken, Pennsylvania.

ASTM C192 (2016). Standard Practice for Making and Curing Concrete Test Specimens in the Laboratory, ASTM International, West Conshohocken, Pennsylvania.

ASTM C230 (2014). Standard Specification for Flow Table for Use in Tests of Hydraulic Cement, ASTM International, West Conshohocken, Pennsylvania.

ASTM C231 (2017). Standard Test Method for Air Content of Freshly Mixed Concrete by the Pressure Method, ASTM International, West Conshohocken, Pennsylvania.

ASTM C305 (2014). Standard Practice for Mechanical Mixing of Hydraulic Cement Pastes and Mortars of Plastic Consistency, ASTM International, West Conshohocken, Pennsylvania.

ASTM C311 (2016). Standard Test Method for Sampling and Testing Fly Ash or Natural Pozzolans for Use in Portland-Cement Concrete, ASTM International, West Conshohocken, Pennsylvania.

ASTM C403 (2016). Standard Test Method for Time of Setting of Concrete Mixtures by Penetration Resistance, ASTM International, West Conshohocken, Pennsylvania.

ASTM C430 (2015). Standard Test Method for Fineness of Hydraulic Cement by the 45-μm (No. 325) Sieve, ASTM International, West Conshohocken, Pennsylvania.

ASTM C618 (2015). Standard Specification for Coal Fly Ash and Raw or Calcined Natural Pozzolan for Use in Concrete, ASTM International, West Conshohocken, Pennsylvania.

ASTM C1012 (2015). Standard Test Method for Length Change of Hydraulic-Cement Mortars Exposed to a Sulfate Solution, ASTM International, West Conshohocken, Pennsylvania.

ASTM C1202 (2017). Standard Test Method for Electrical Indication of Concrete's Ability to Resist Chloride Ion Penetration, ASTM International, West Conshohocken, Pennsylvania.

ASTM C 1260 (2014). Standard Test Method for Potential Alkali Reactivity of Aggregates (Mortar-Bar Method), ASTM International, West Conshohocken, Pennsylvania.

ASTM C1437 (2015). Standard Test Method for Flow of Hydraulic Cement Mortar, ASTM International, West Conshohocken, Pennsylvania.

ASTM C1567 (2013). Standard Test Method for Determining the Potential Alkali-Silica Reactivity of Combinations of Cementitious Materials and Aggregate (Accelerated Mortar-Bar Method), ASTM International, West Conshohocken, Pennsylvania.

ASTM C1697 (2016). Standard Specification for Blended Supplementary Cementitious Materials, ASTM International, West Conshohocken, Pennsylvania.

ASTM C1738 (2014). Standard Practice for High-Shear Mixing of Hydraulic Cement Pastes, ASTM International, West Conshohocken, Pennsylvania.

Bentz, D.P., Ferraris, C.F., Jones, S.Z., Lootens, D., Zunino, F. (2017). Limestone and silica powder replacements for cement: Early-age performance. *Cement and Concrete Composites*, 78, 43-56.

Berry E.E., Hemmings R.T., Langley W.S., Carette G.G. (1989). Beneficiated Fly Ash: Hydration, Microstructure, and Strength Development in Portland Cement Systems. In V.M. Malhotra (Ed), *ACI Special Publication SP-114* (pp. 241-273). Trondheim, Norway: American Concrete Institute.

Cheerarot, R., Jaturapitakkul, C. (2004). A study of disposed fly ash from landfill to replace Portland cement. *Waste Management*, *24*, 701-709.

Diaz-Loya, I., Juenger, M., Seraj, S., Minkara, R. (2017). Extending supplementary cementitious material resources: Reclaimed and remediated fly ash and natural pozzolans. *Cement and Concrete Composites*, 1-8.

Elfert, R. J. (1974). "Bureau of Reclamation Experiences with Flyash and Other Pozzolans in Concrete," Information Circular No. 8640, U.S. Bureau of Mines, Washington, D.C., pp. 80-93.

EPA. *Frequent Questions about the Coal Ash Disposal Rule*. Retrieved July 15, 2017, from https://www.epa.gov/coalash/frequent-questions-about-coal-ash-disposal-rule#2.

Fajun, W., Grutzeck, M.W., Roy, D.M. (1985). The Retarding Effects of Fly Ash upon the Hydration of Cement Pastes: The first 24 hours. *Cement and Concrete Research*, 15, 174-184.

Farny, J., Kerkhoff, B. (2007). *Diagnosis and Control of Alkali-Aggregate Reactions in Concrete*. Portland Cement Association, Skokie, Illinois.

Fedorka, W.F., Knowles, J., Castleman, J. (2015). Reclaiming and Recycling Coal Fly Ash for Beneficial Reuse with the STAR[TM] Process. *2015 World of Coal Ash (WOCA) Conference*. Retrieved from http://www.flyash.info/2015/168-fedorka-2015.pdf.

Flett, J. (1911). Dacite. Encyclopedia Britannica 11th edtion. p. 728.

Folliard, K., Hover, K., Harris, N., Ley, T., Naranjo, A. (2009). *Effects of Texas Fly Ash on Air-Entrainment in Concrete: Comprehensive Report*. CTR Technical Report 0-5207-1. Austin, TX: Center for Transportation Research at The University of Texas at Austin.

Geology.com (2015). Rhyolite. Accessed on December 17th, 2015 from
http://geology.com/rocks/rhyolite.shtml.

Hamley, P., Lester, E., Thompson, A., Cloke, M., Poliakoff, M. (2001). The removal of carbon from fly ash using supercritical water oxidation. *2001 International Ash Utilization Symposium*. Retrieved from http://www.flyash.info/2001/benef1/85lester.pdf.

Han, D., Ferron, R. (2016). Influence of high mixing intensity on rheology, hydration and microstructure of fresh state cement paste. *Cement and Concrete Research*, 84, 95–106.

Howard, C., Kabis, S., Farrington, S.A. (2013). Advances in Chemical Beneficiation of Fly Ashes Containing Natural Carbon or Powdered Activated Carbon. *2013 World of Coal Ash (WOCA) Conference*. Retrieved from http://www.flyash.info/2013/148-Kabis-2013.pdf.

Industrial Minerals Association North America (IMANA), What is Feldspar (2015). Accessed on December 17th, 2015 from http://www.ima-na.org/?page=what_is_feldspar.

Juenger, M.C.G., Siddique, R. (2015). Recent advances in understanding the role of supplementary cementitious materials in concrete. *Cement and Concrete Research*, 78, 71-80.

Kabay, N., Tufekci, M.M., Kizilkanat, A.B., Oktay, D., (2015) Properties of concrete with pumice powder and fly ash as cement replacement materials. *Construction and Building Materials*, 85, 1–8. doi: 10.1016/j.conbuildmat.2015.03.026.

Kayali, O. (2008). Fly ash lightweight aggregates in high performance concrete, *Construction and Building Materials,* 22, 2393–2399.

Kim, T., Olek, J. (2012). Effects of Sample Preparation and Interpretation of Thermogravimetric Curves on Calcium Hydroxide in Hydrated Pastes and Mortars. *Journal of the Transportation Research Board*, 2290, 10-18.

Ladwig, K.J., Blythe, G.M. (2017). Flue-gas desulfurization products and other air emissions controls. In T. Robl, A. Oberlink & R. Jones (Eds.), *Coal Combustion Products (CCP's): Characteristics, Utilization and Beneficiation* (pp. 67-95). Duxford, UK: Woodhead Publishing.

Lieber, O. (1856). Report on the Survey of South Carolina. South Carolina General Assembly., p. 33.

Lothenbach, B., Scrivener, K., Hooton, R.D. (2011) Supplementary cementitious materials. *Cement and Concrete Research*, 41 (12), 1244-1256

McCarthy M.J., Robl, T., Csetenyi, L.J. (2017). Recovery, processing, and usage of wet-stored fly ash. In T. Robl, A. Oberlink & R. Jones (Eds.), *Coal Combustion Products (CCP's): Characteristics, Utilization and Beneficiation* (pp. 343-367). Duxford, UK: Woodhead Publishing.

McLemore, V. (2006). Nepheline Syenite, *Industrial Minerals and Rocks*, 653-670.

Mechtcherine, V., Gram, A., Krenzer, K., Schwabe, J.H., Shyshko, S., Roussel, N. (2014). Simulation of fresh concrete flow using Discrete Element Method (DEM): theory and applications. *Materials and Structures*, 47, 615-630.

Nocun-Wczelik, W. (2001). Heat evolution in Hydrated Cementitious Systems admixture with Fly Ash, *Journal of Thermal Analysis and Calorimetry,* 65, 613-619.

Oxford Dictionaries. Retrieved July 15, 2017, from https://en.oxforddictionaries.com/.

Ramachandran, V.S. (1995). *Concrete Admixtures Handbook, Properties, Science and Technology*. Noyes Publications, Park Ridge, New Jersey.

Ranganath, R.V., Bhattacharjee, B., Krishnamoorthy, S. (1998). Influence of Size Fraction of Ponded Ash on its Pozzolanic Activity. *Cement and Concrete Research*, 28 (5), 749-761.

Robl, T. (2017). Ash beneficiation, quality, and standard criteria. In T. Robl, A. Oberlink & R. Jones (Eds.), *Coal Combustion Products (CCP's): Characteristics, Utilization and Beneficiation* (pp. 217-224). Duxford, UK: Woodhead Publishing.

Seraj, S., Cano, R., Liu, S., Whitney, D., Fowler, D., Ferron, R., Zhu, J., and Juenger, M. (2014). Evaluating the Performance of Alternative Supplementary Cementing Material in Concrete, Technical Report 0-6717-1, Center for Transportation Research, The University of Texas at Austin.

Sobolev, K.G., Batrakov, V.G. (2007). Effect of a Polyethylhydrosiloxane Admixture on the Durability of Concrete with Supplementary Cementitious Materials. *Journal of Materials in Civil Engineering*, 19 (10), 809-819.

Spencer, L. (1911). Nepheline. Encyclopedia Britannica 11th edtion.

Sutter, L.L., Bentz, D.P. (2017). Assessing ash quality and performance. In T. Robl, A. Oberlink & R. Jones (Eds.), *Coal Combustion Products (CCP's): Characteristics, Utilization and Beneficiation* (pp. 121-154). Duxford, UK: Woodhead Publishing.

Texas Department of Transportation (TxDOT) (2014). *Standard Specifications for Construction and Maintenance of Highways, Streets, and Bridges*. Adopted November 1, 2014. Retreived from ftp://ftp.dot.state.tx.us/pub/txdot-info/des/spec-book-1114.pdf

Thomas, M. (2011). The effect of supplementary cementing materials on alkali-silica reaction: A review. *Cement and Concrete Research*, 41, 1224-1231.

Thomas, M., Jewell, R., Jones, R. (2017). Coal fly ash as a pozzolan. In T. Robl, A. Oberlink & R. Jones (Eds.), *Coal Combustion Products (CCP's): Characteristics, Utilization and Beneficiation* (pp. 121-154). Duxford, UK: Woodhead Publishing.

U.S. Energy Information Administration (EIA) (2017). *Annual Energy Outlook 2017: with projections to 2050*. Retrieved from https://www.eia.gov/outlooks/aeo/.

U.S. Geological Survey (2017). *Mineral commodity summaries 2017*. Retrieved from https://doi.org/10.3133/70180197.

Vogt, C. (2010). *Ultrafine particles in concrete*. Doctoral Thesis. Royal Institute of Technology.

White, D.J. (2006). Reclaimed Hydrated Fly Ash as a Geomaterial. *Journal of Materials in Civil Engineering*, 18 (2), 206-213.

Želinková, M., Sičáková, A., Holub, M. (2013). Influence of Selected Grinding Specifications on the Fly Ash Granulometry. *Procedia Engineering*, 65, 39-44.

Appendix A. Environmental Scanning Electron Microscopy Images

A.1 Supplier A
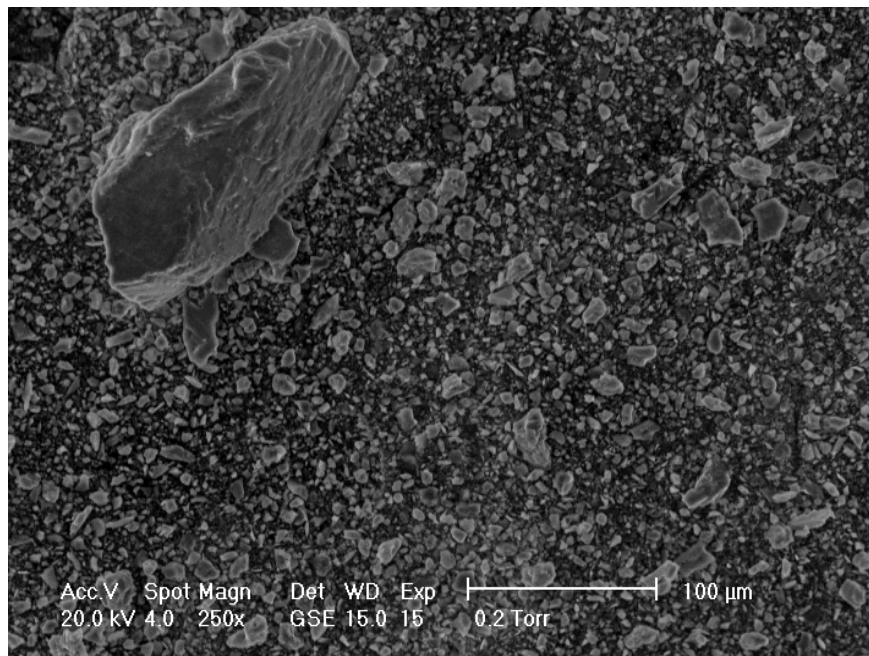
Figure A.1: ESEM image of D-L at 250x
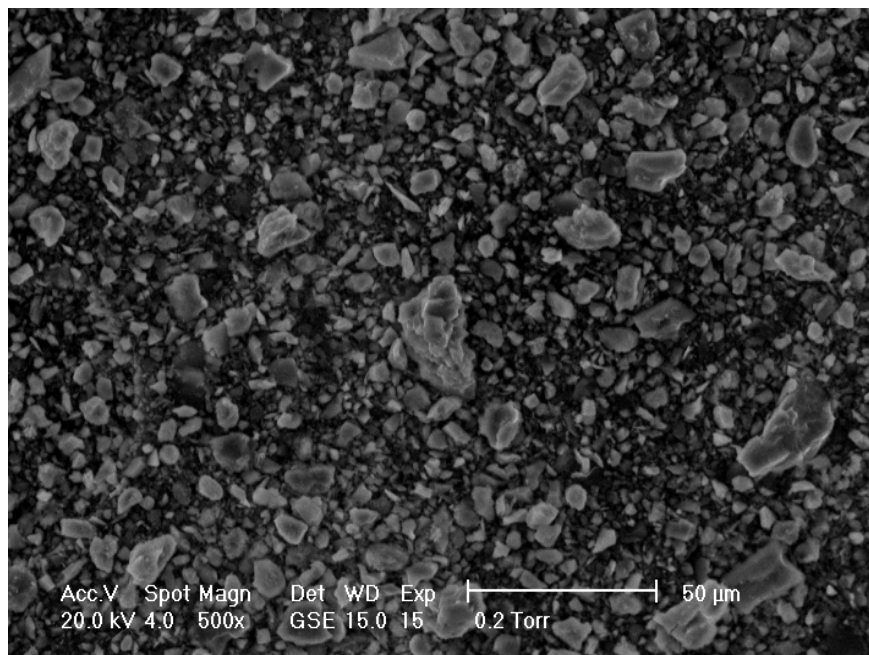
Figure A.2: ESEM image of D-L at 500x
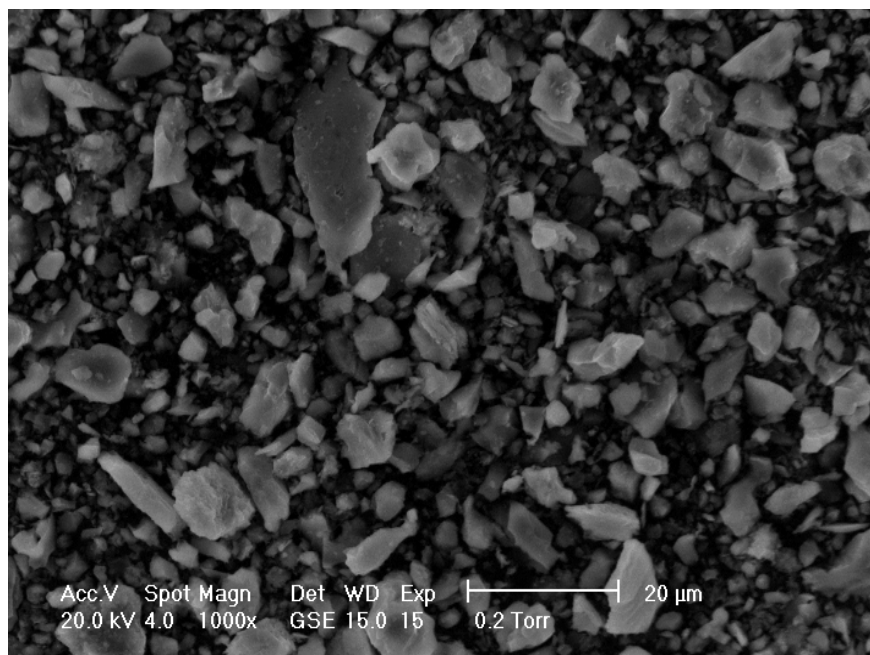
Figure A.3: ESEM image of D-L at 1000x
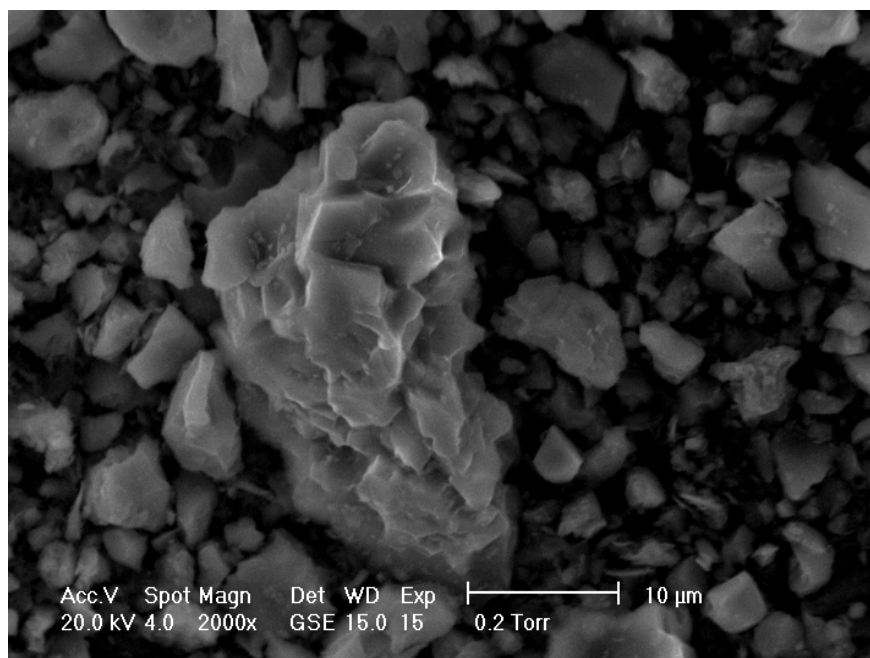
Figure A.4: ESEM image of D-L at 2000x
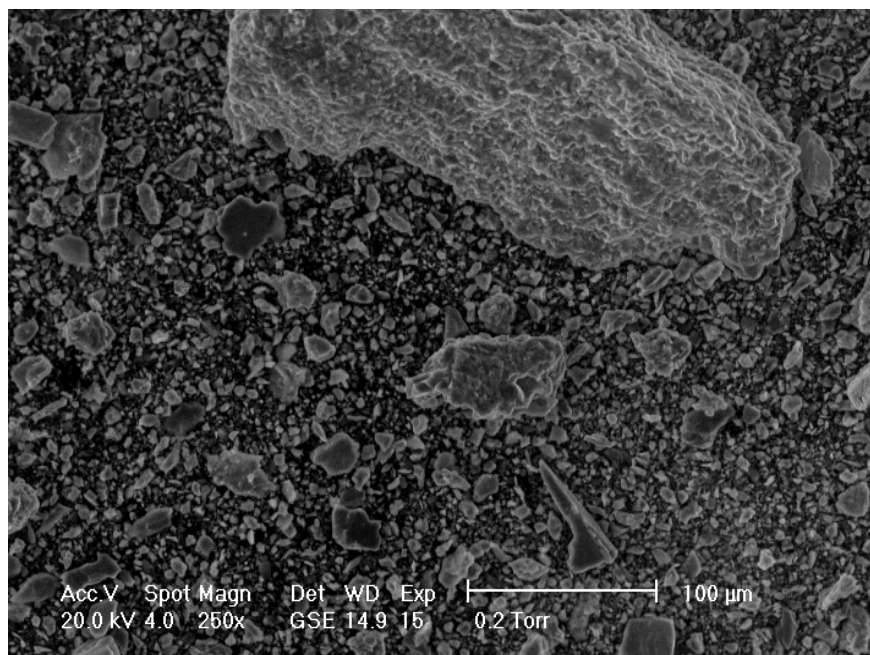
Figure A.5: ESEM image of D-S at 250x
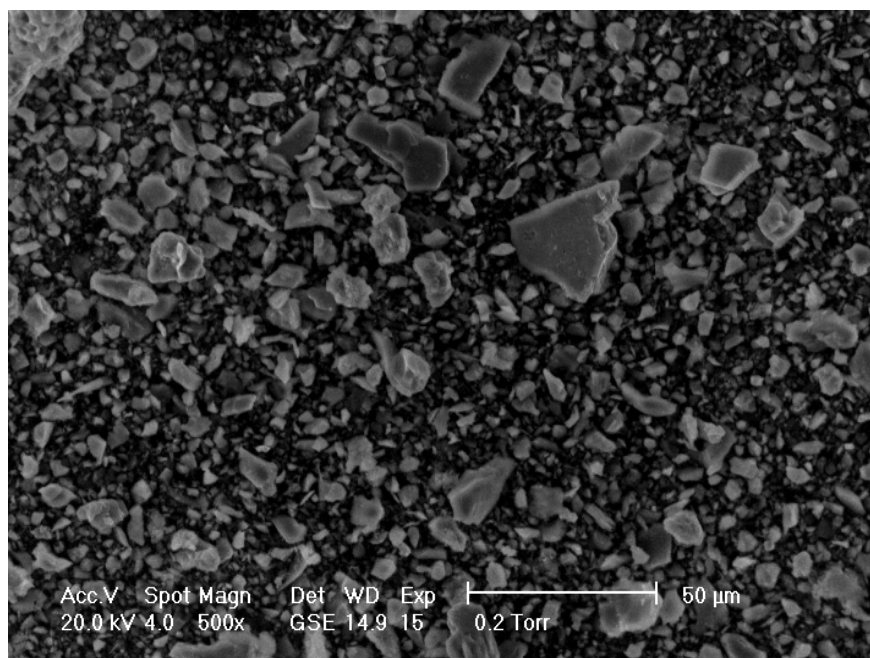
Figure A.6: ESEM image of D-S at 500x
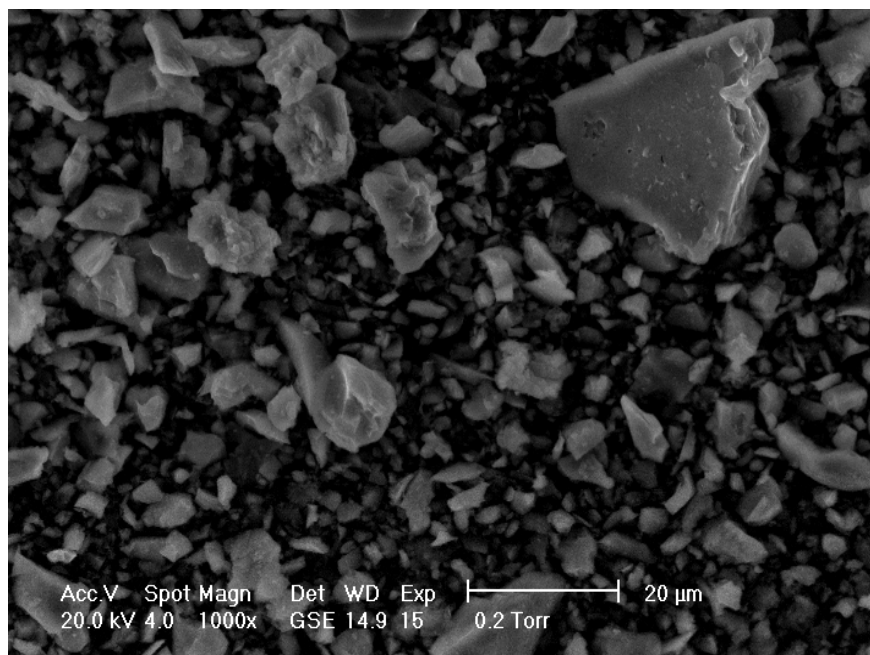
Figure A.7: ESEM image of D-S at 1000x
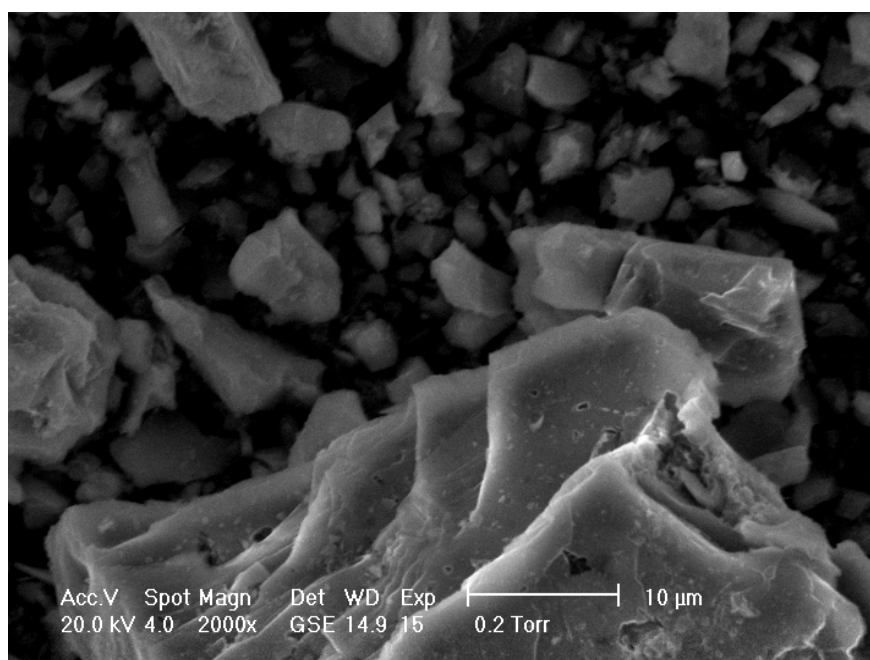
Figure A.8: ESEM image of D-S at 2000x
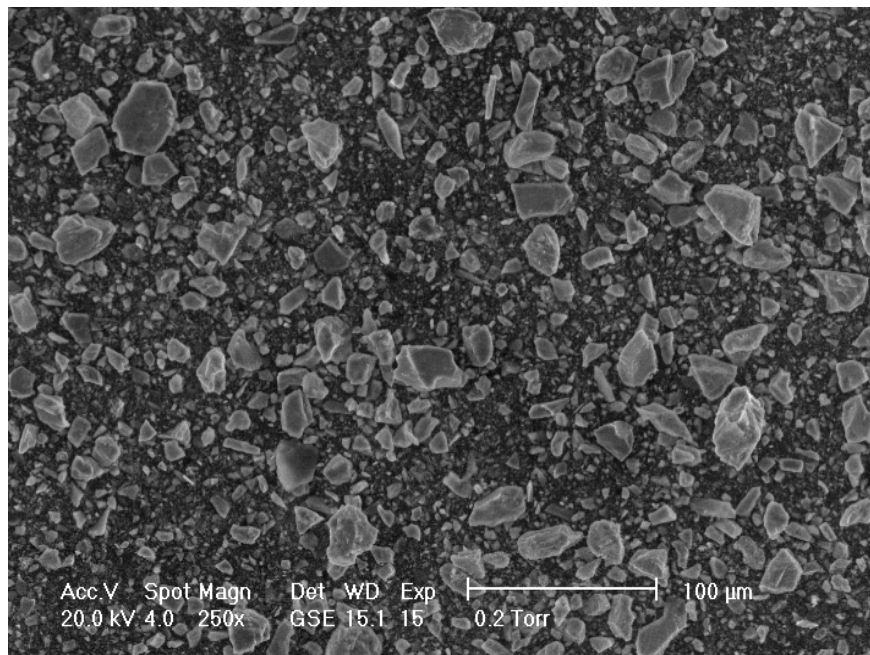
Figure A.9: ESEM image of NS-I at 250x
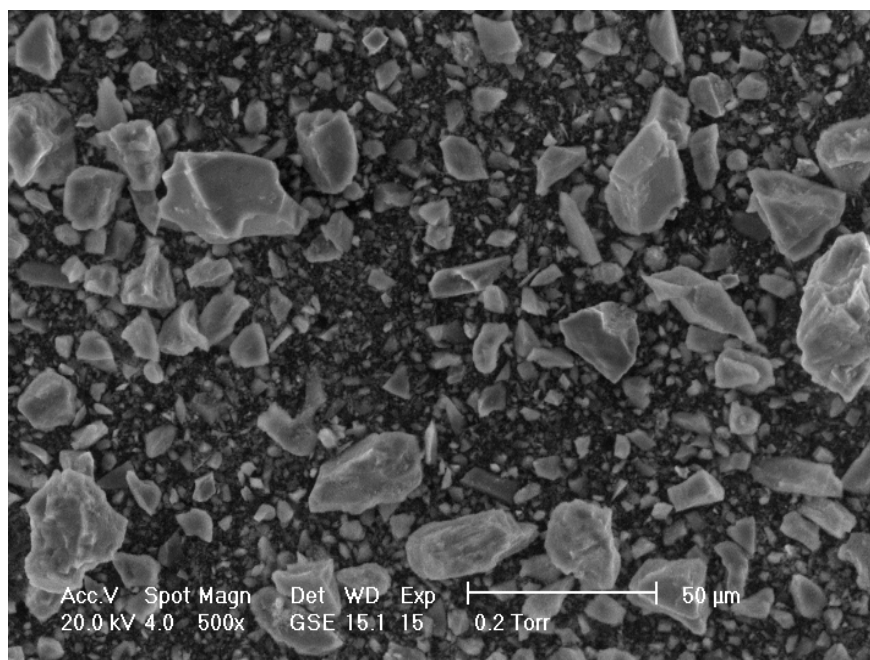
Figure A.10: ESEM image of NS-I at 500x
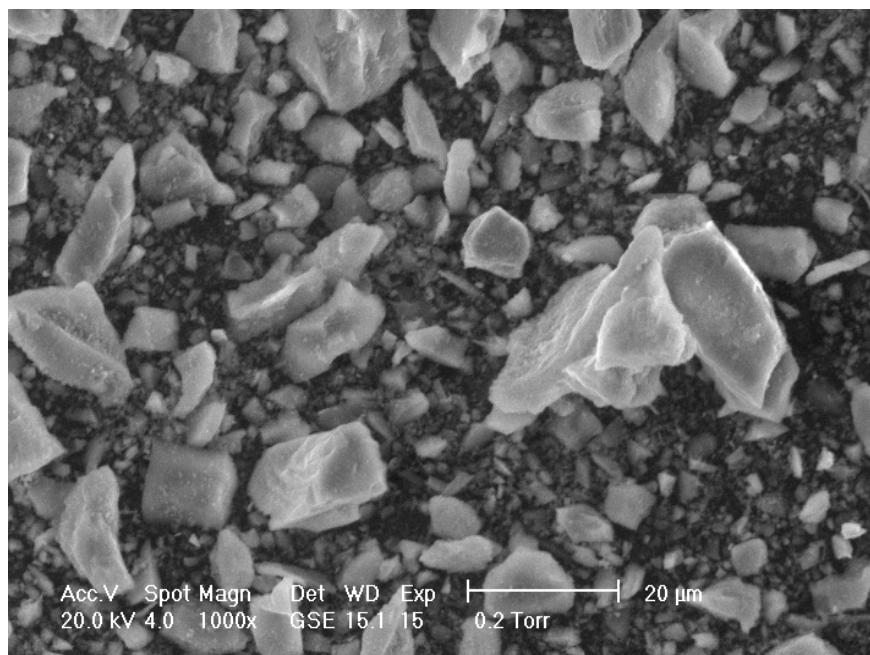
Figure A.11: ESEM image of NS-I at 1000x
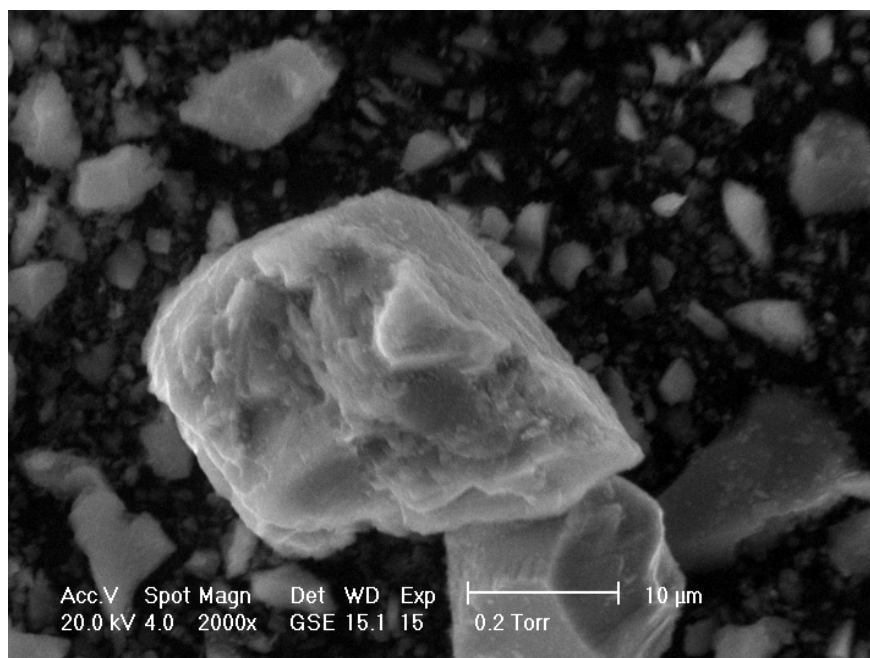
Figure A.12: ESEM image of NS-I at 2000x
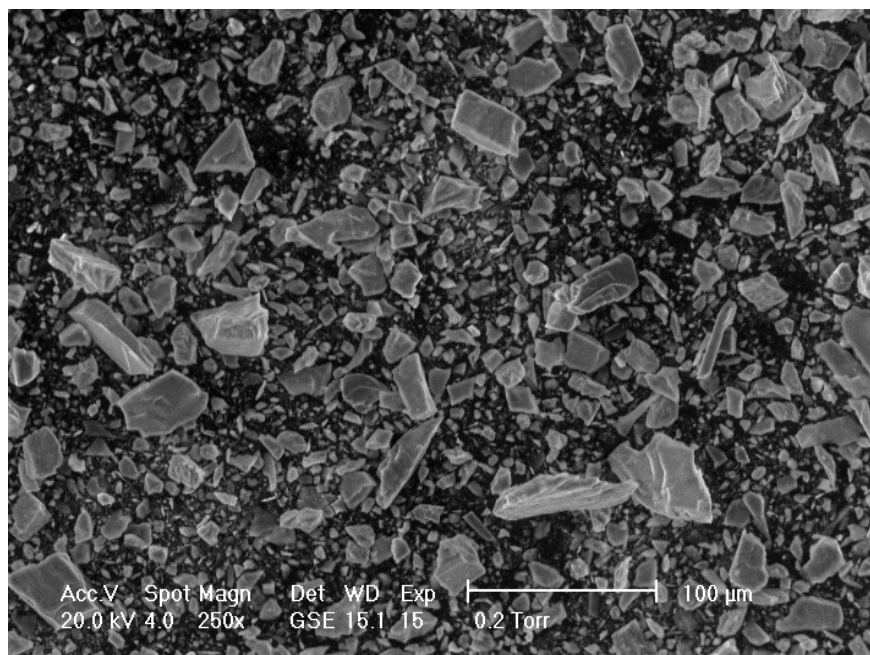
Figure A.13: ESEM image of NS-L at 250x
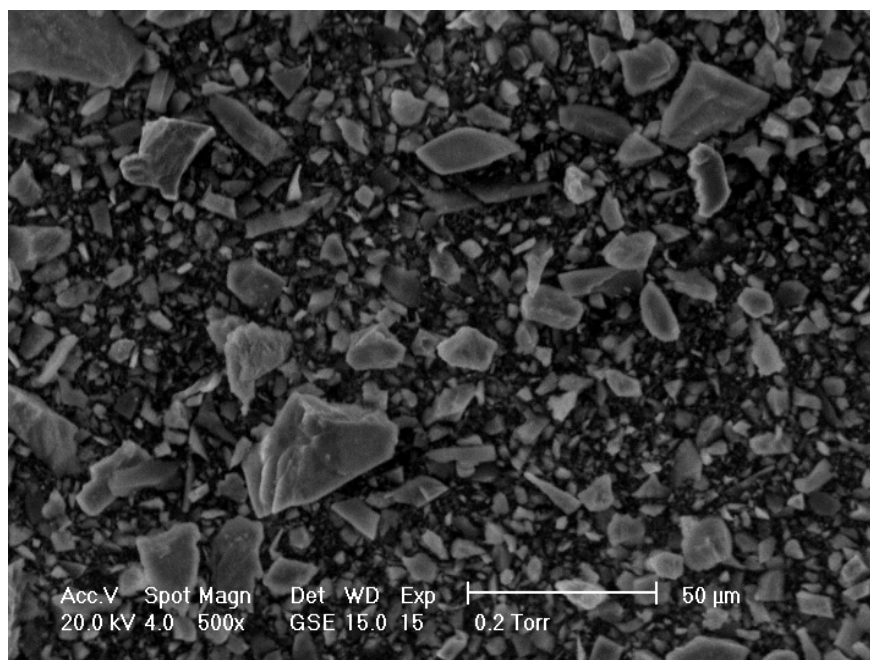
Figure A.14: ESEM image of NS-L at 500x
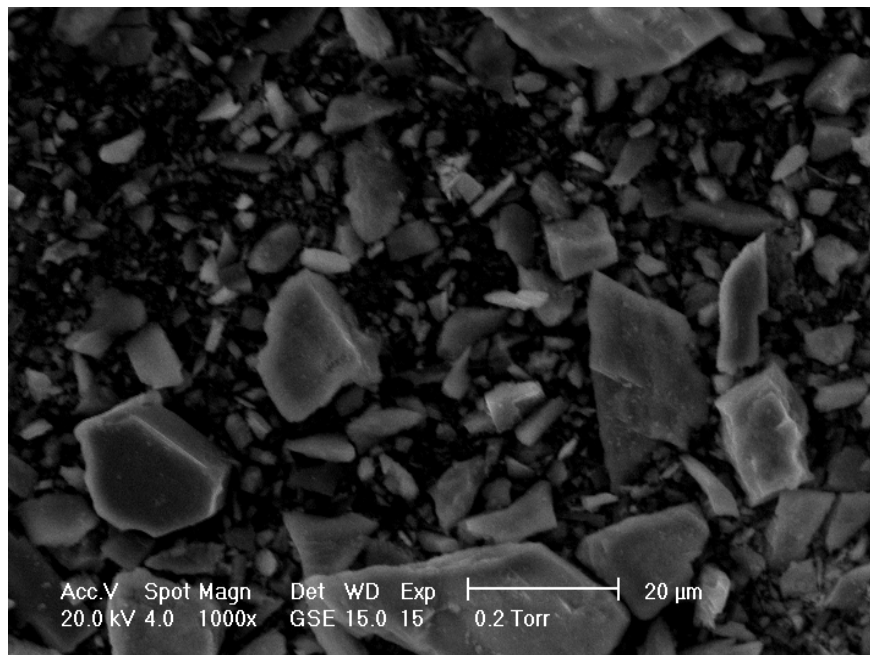
Figure A.15: ESEM image of NS-L at 1000x
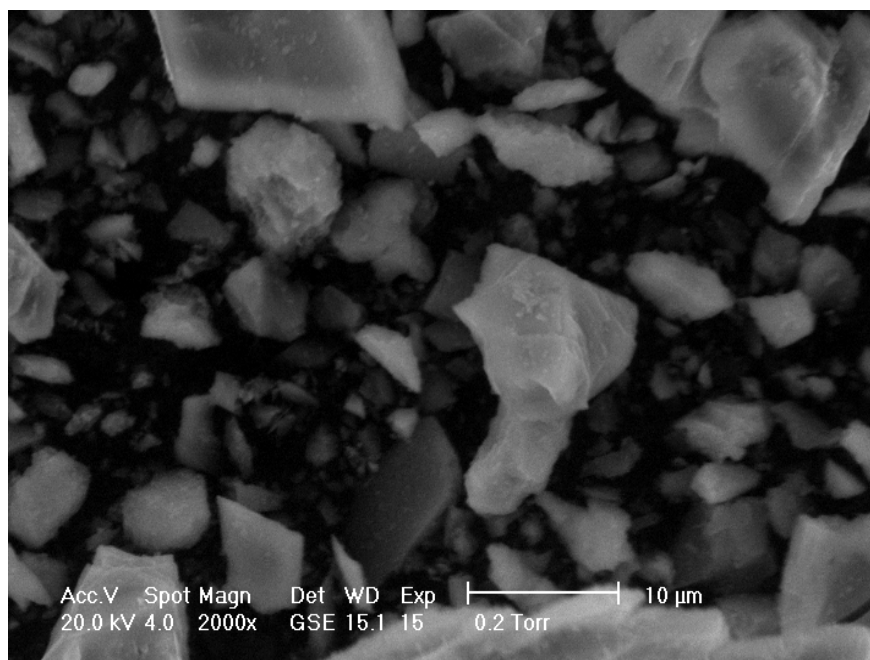
Figure A.16: ESEM image of NS-L at 2000x
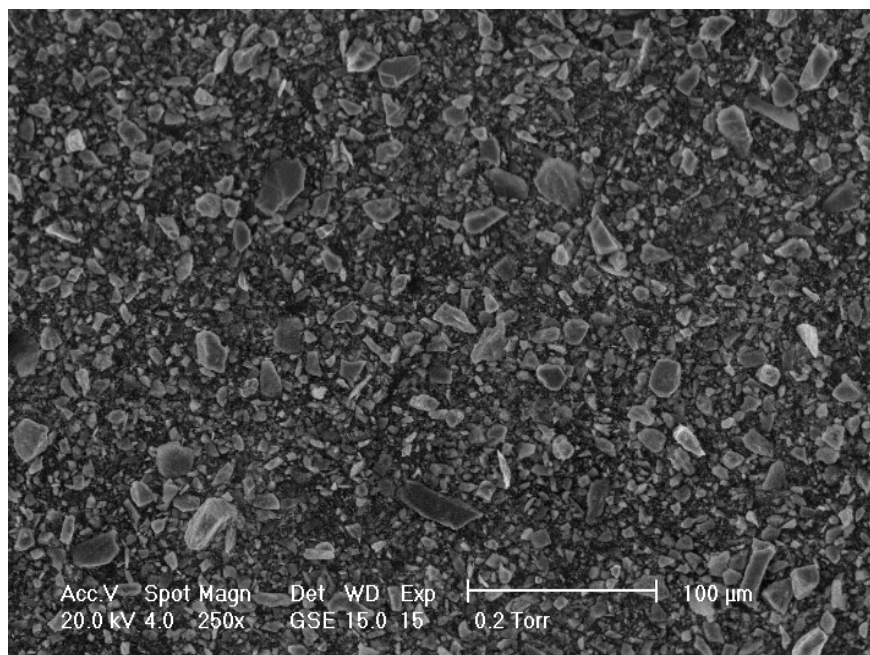
Figure A.17: ESEM image of NS-S at 250x
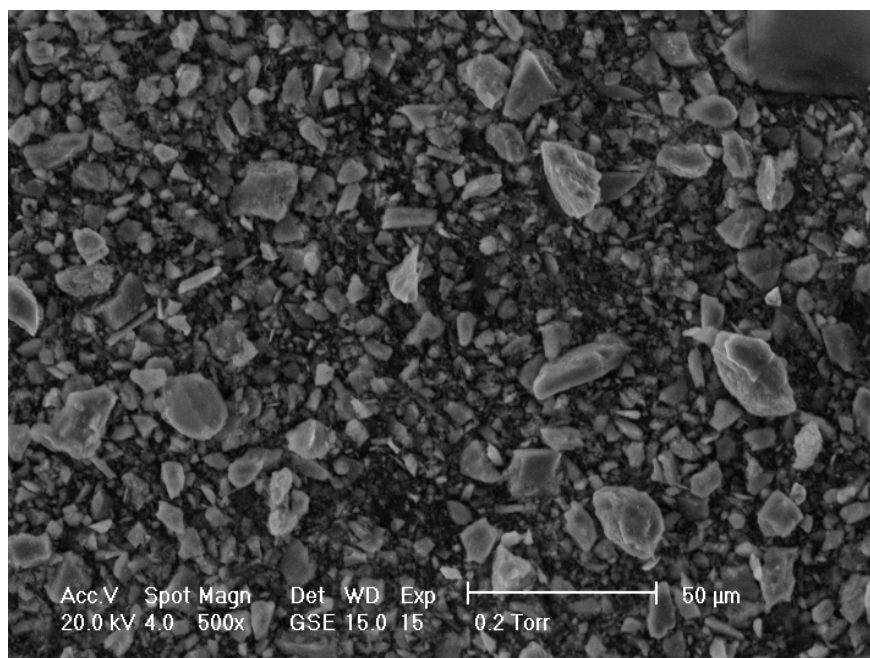
Figure A.18: ESEM image of NS-S at 500x
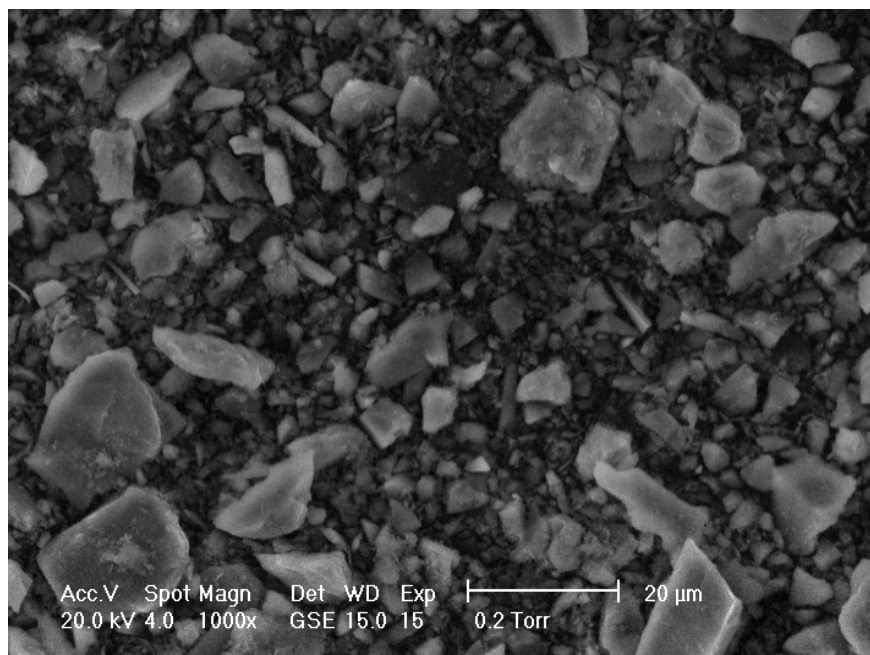
Figure A.19: ESEM image of NS-S at 1000x
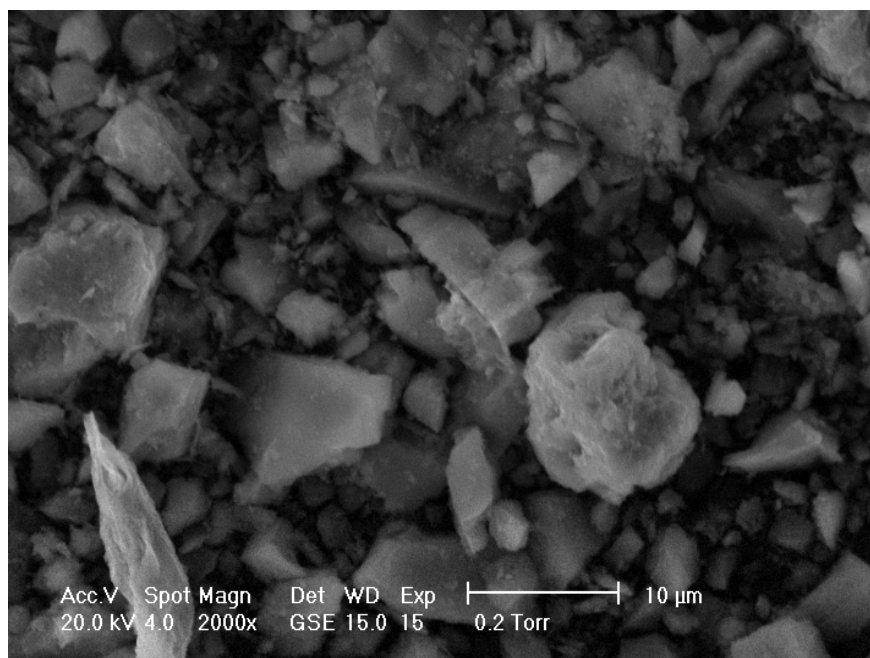
Figure A.20: ESEM image of NS-S at 2000x
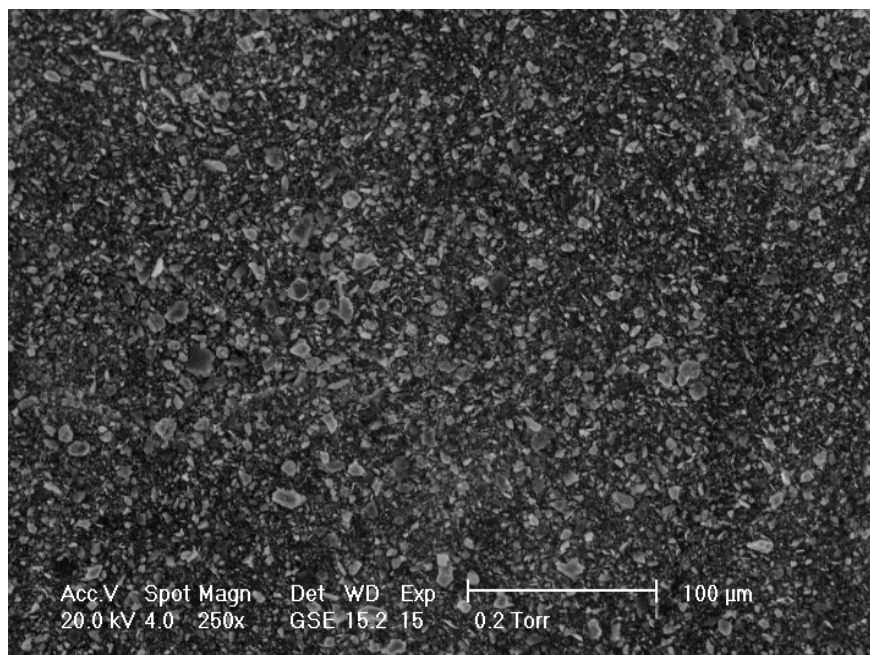
Figure A.21: ESEM image of R-O at 250x
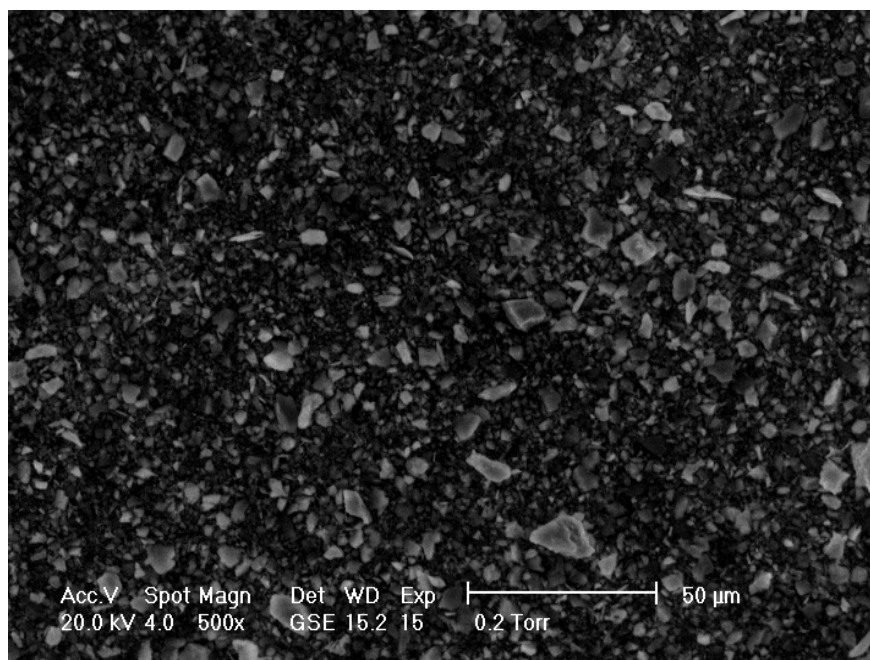
Figure A.22: ESEM image of R-O at 500x
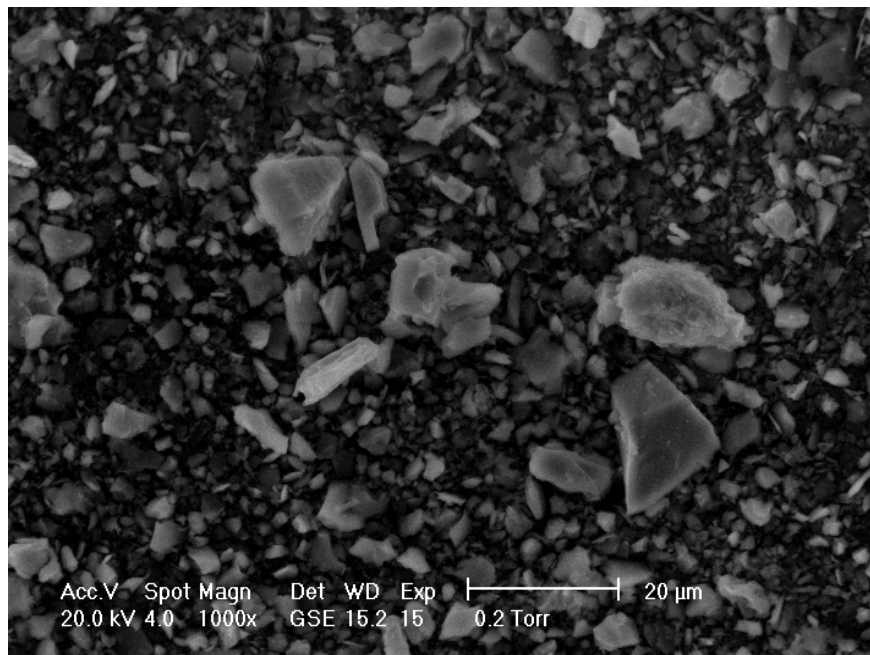
Figure A.23: ESEM image of R-O at 1000x
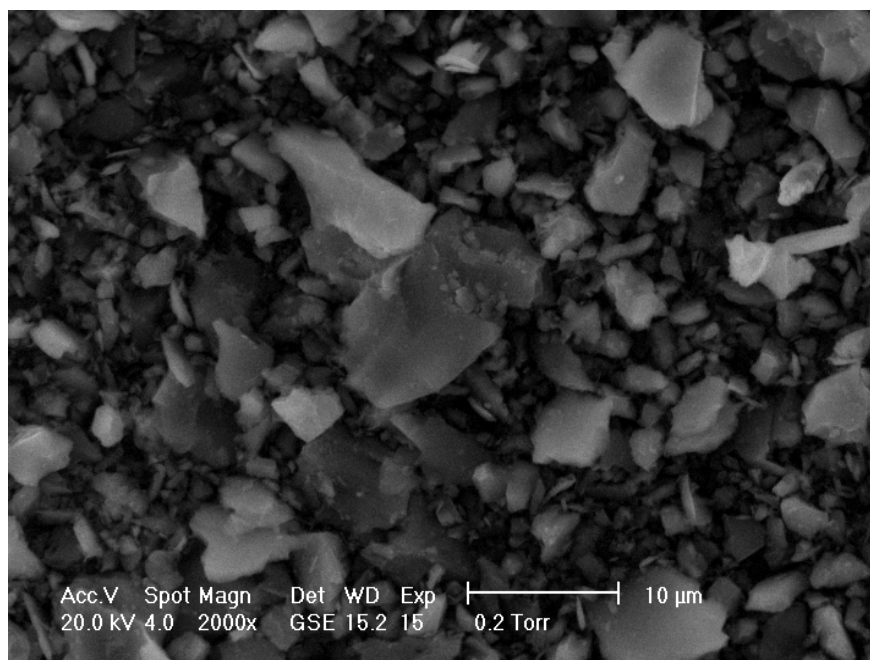
Figure A.24: ESEM image of R-O at 2000x

A.2 Supplier B
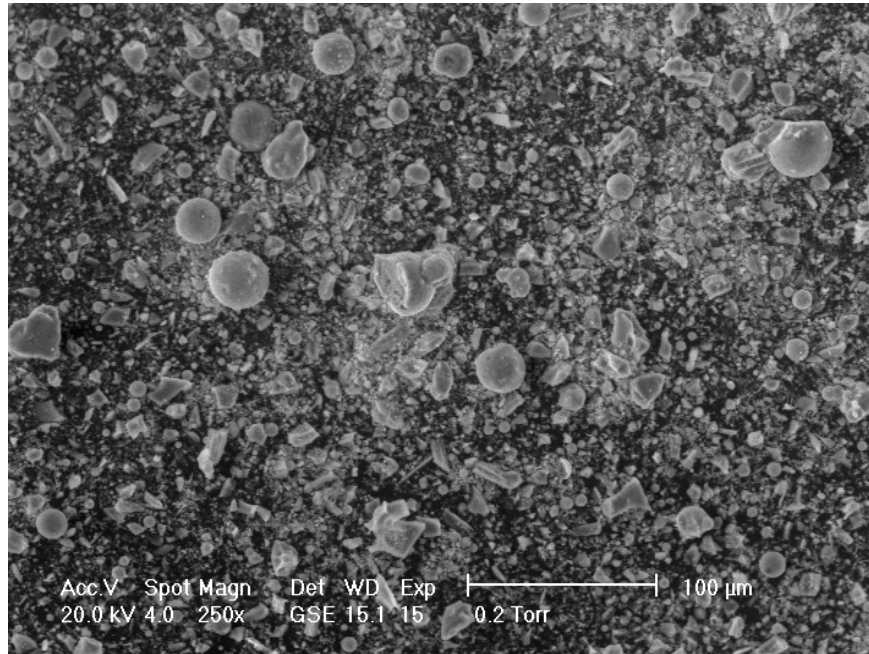
Figure A.25: ESEM image of RM-C at 250x
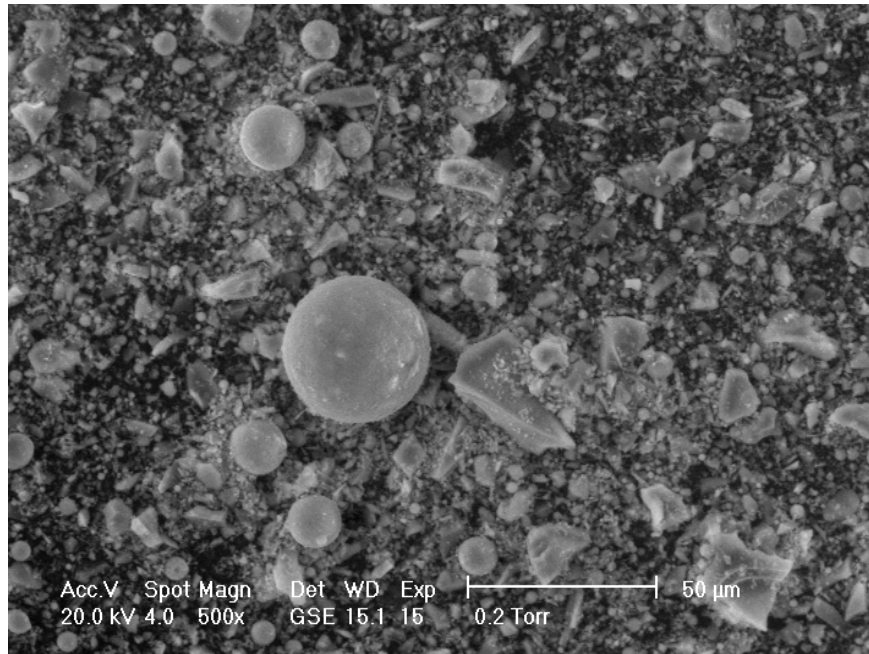
Figure A.26: ESEM image of RM-C at 500x
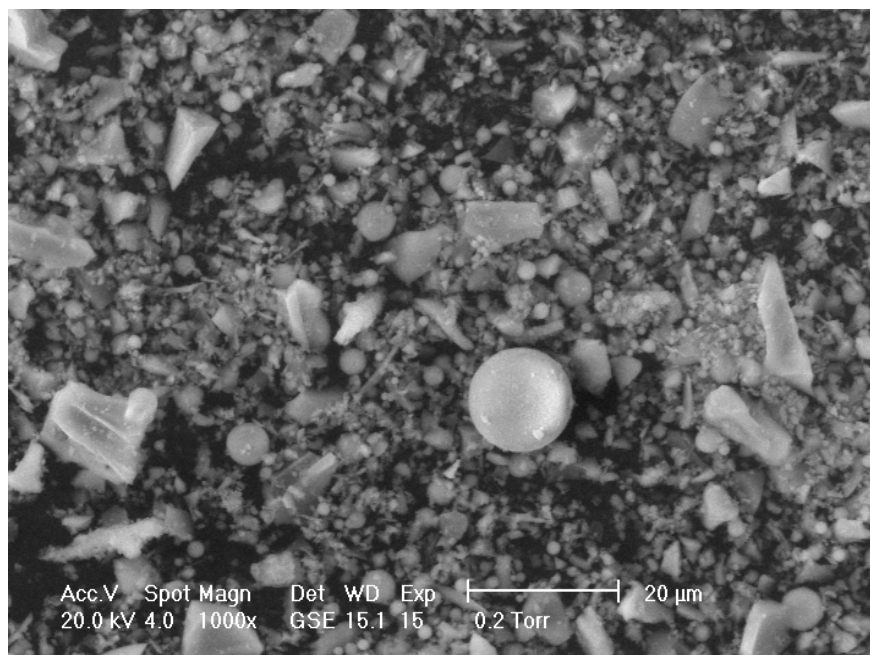
Figure A.27: ESEM image of RM-C at 1000x
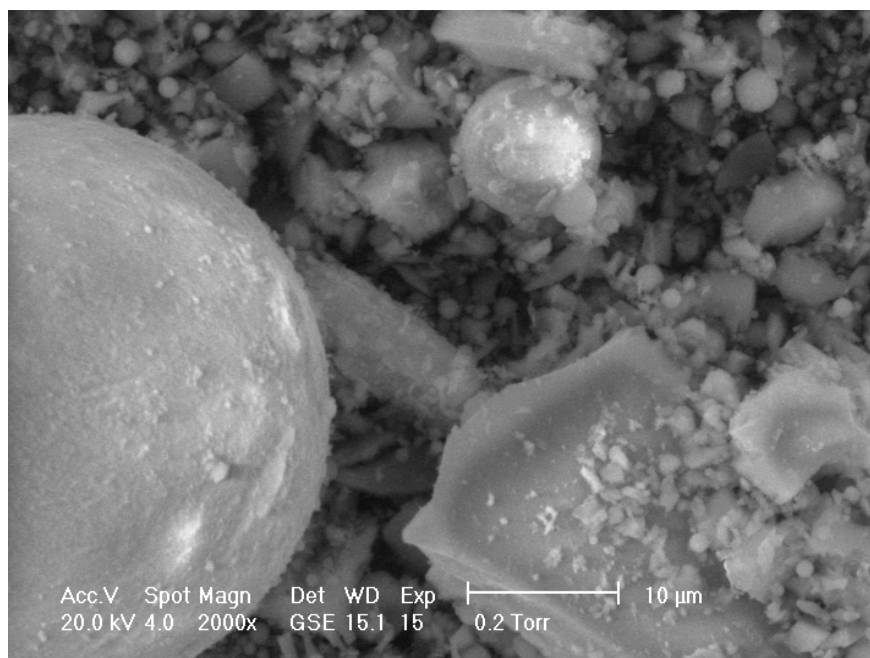
Figure A.28: ESEM image of RM-C at 2000x
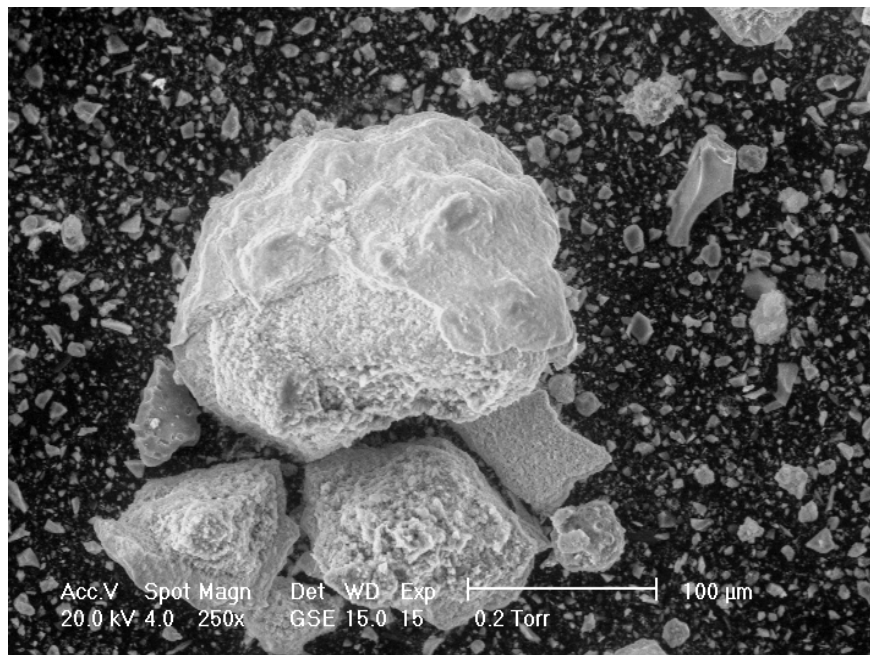
Figure A.29: ESEM image of RM-L at 250x
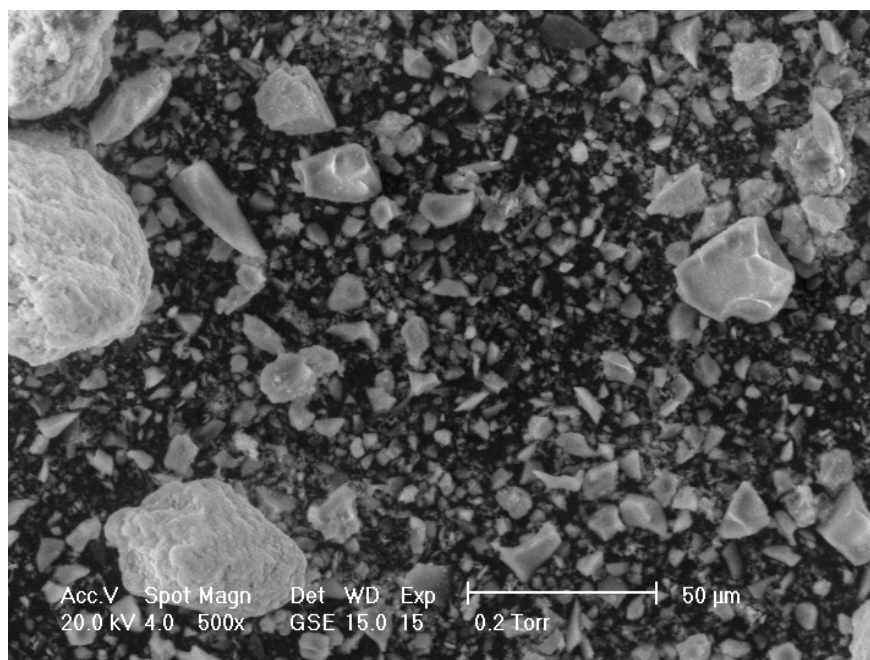
Figure A.30: ESEM image of RM-L at 500x

84
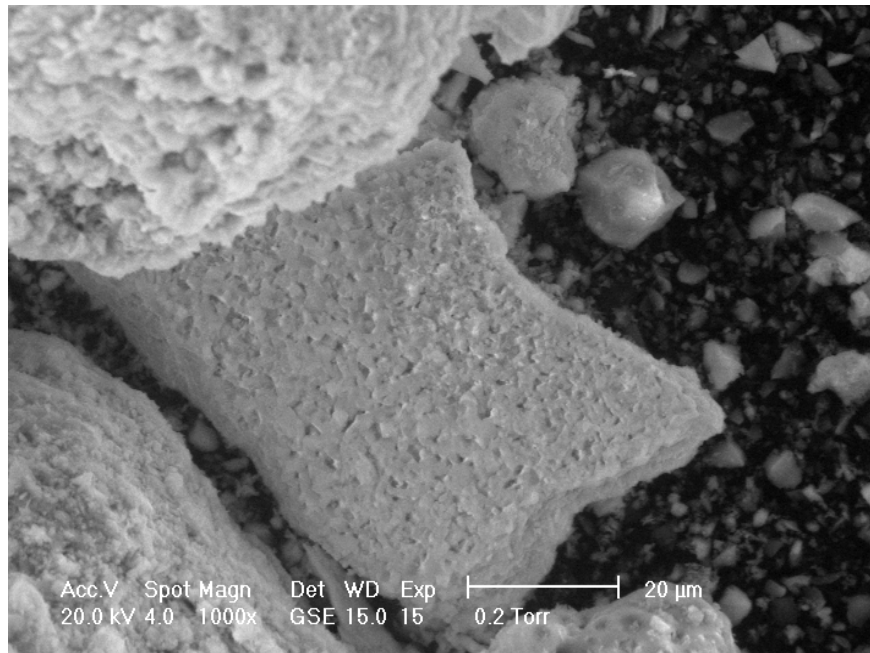
Figure A.31: ESEM image of RM-L at 1000x
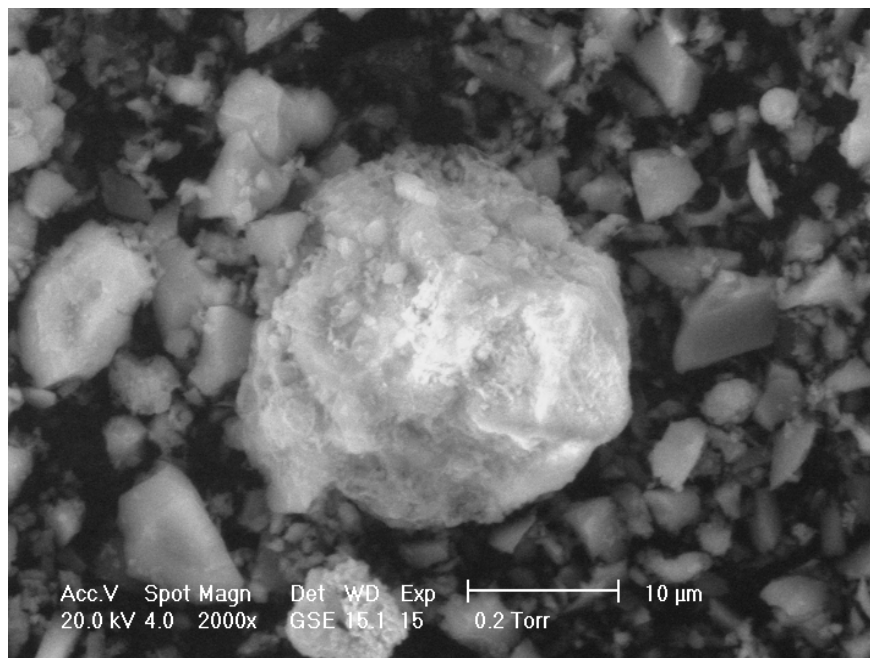
Figure A.32: ESEM image of RM-L at 2000x
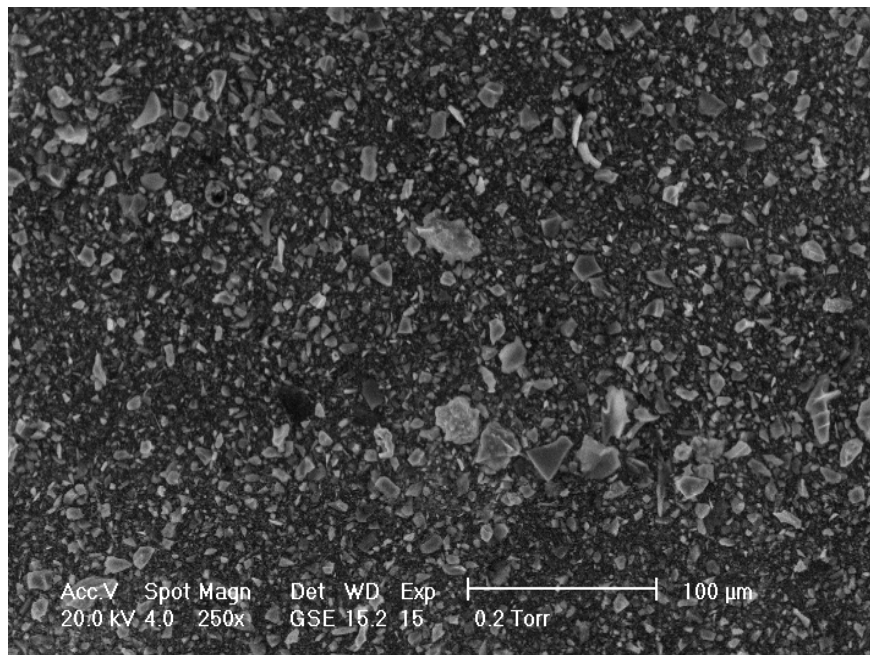
Figure A.33: ESEM image of RM-S at 250x
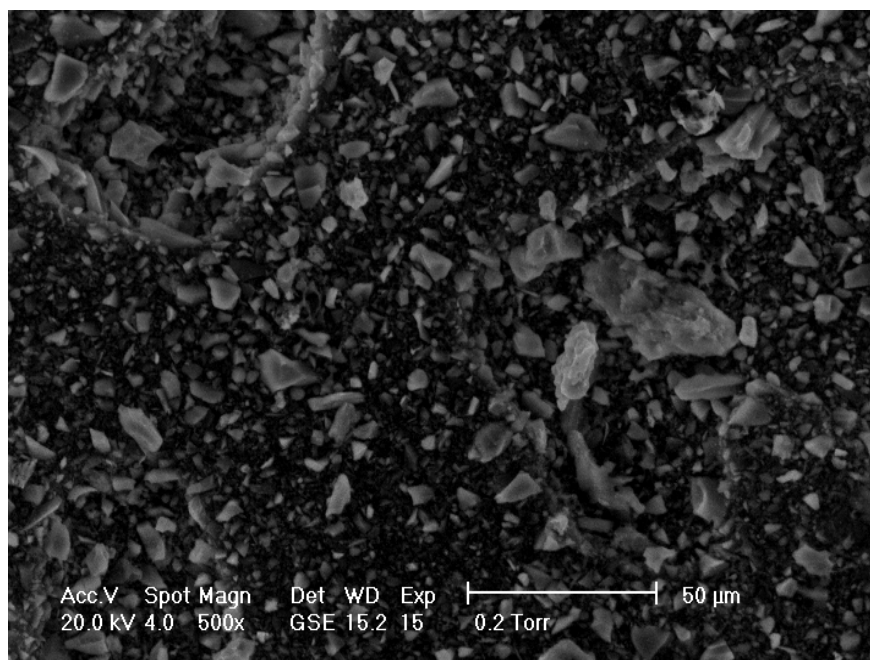
Figure A.34: ESEM image of RM-S at 500x
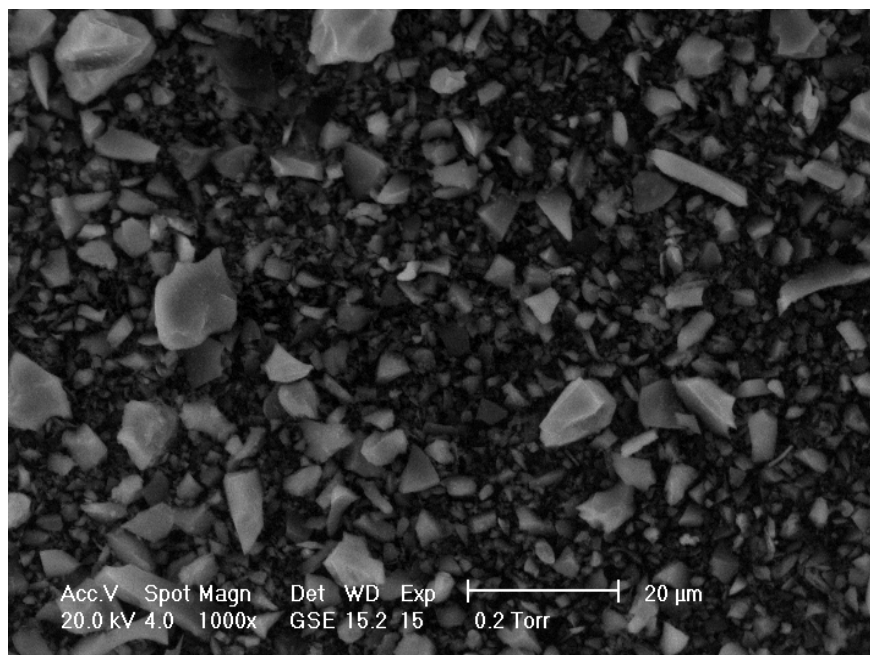
Figure A.35: ESEM image of RM-S at 1000x
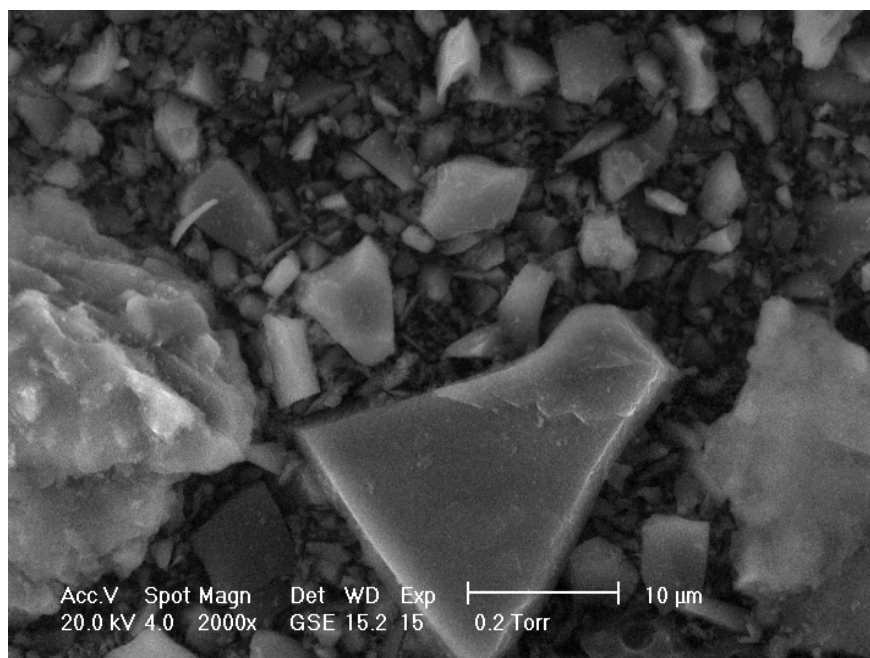
Figure A.36: ESEM image of RM-S at 2000x
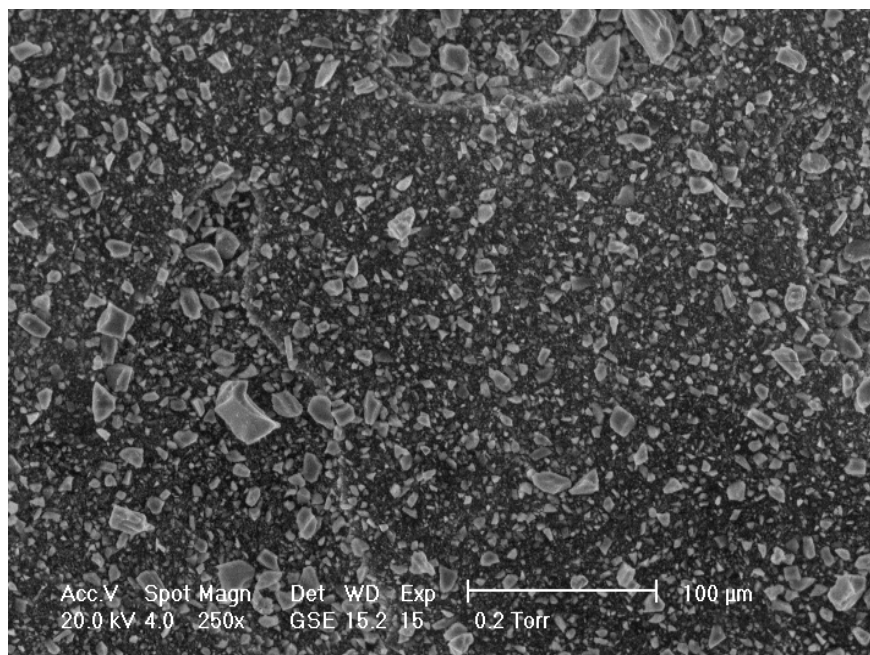
Figure A.37: ESEM image of P-B at 250x
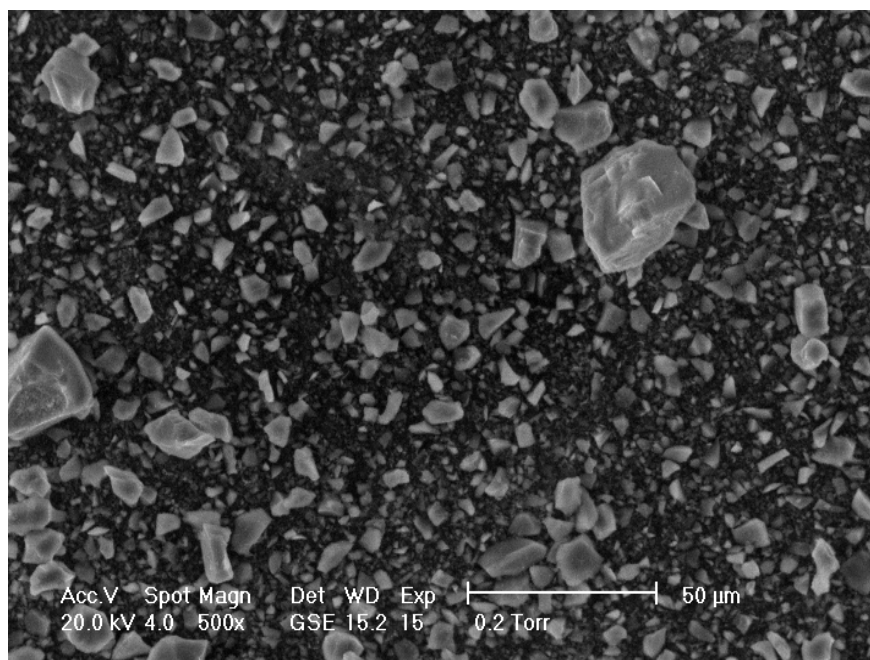
Figure A.38: ESEM image of P-B at 500x
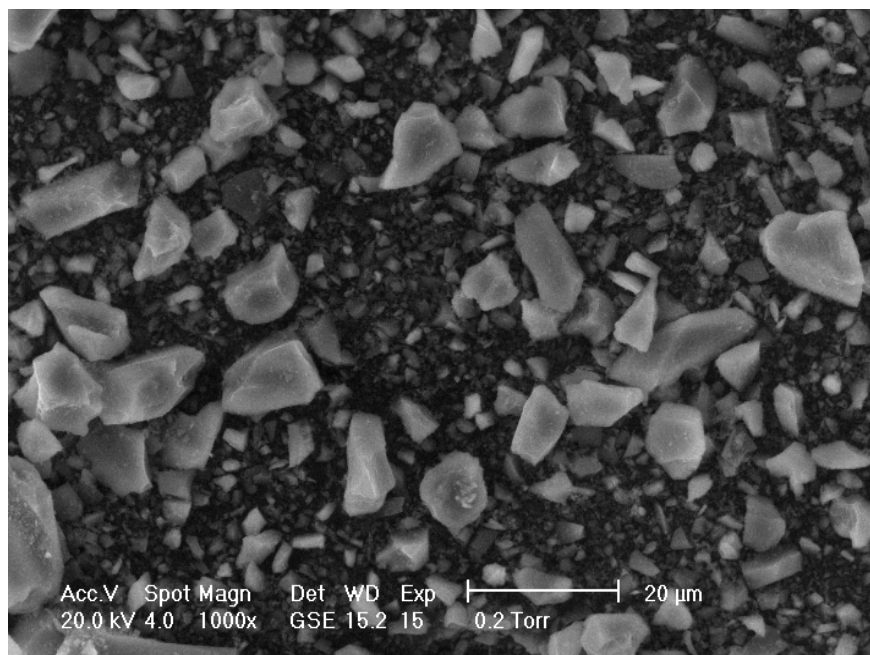
Figure A.39: ESEM image of P-B at 1000x
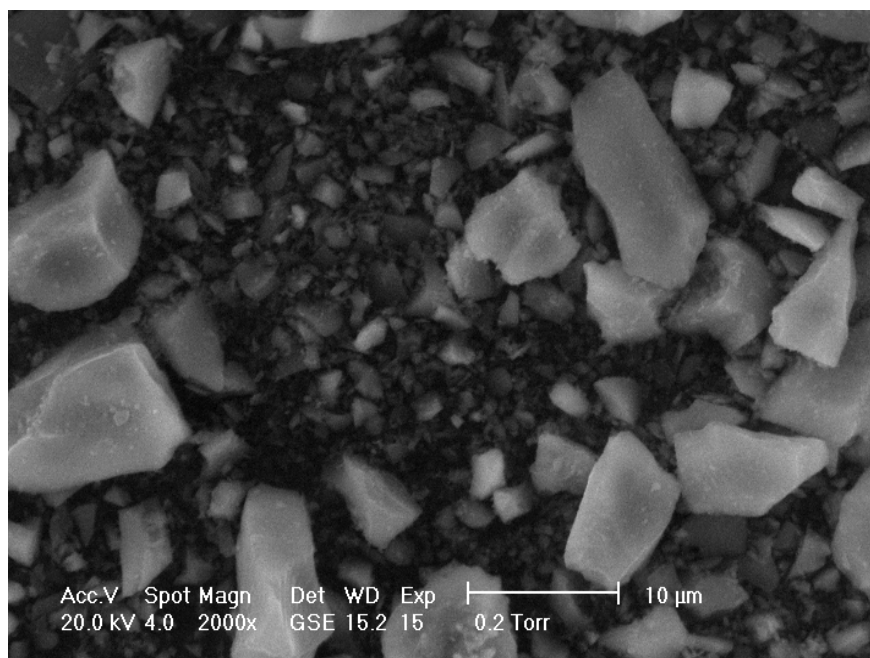
Figure A.40: ESEM image of P-B at 2000x
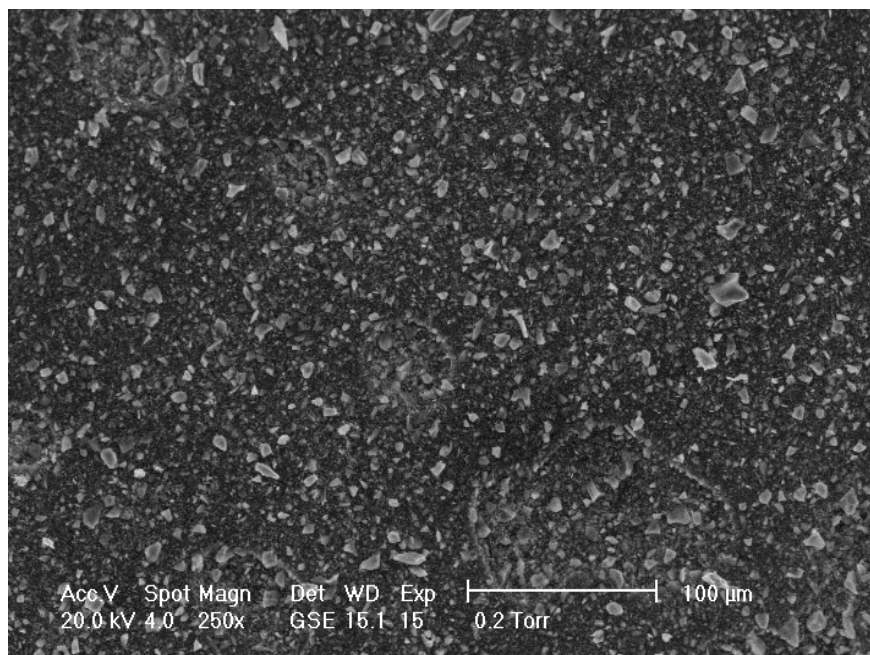
Figure A.41: ESEM image of P-W at 250x
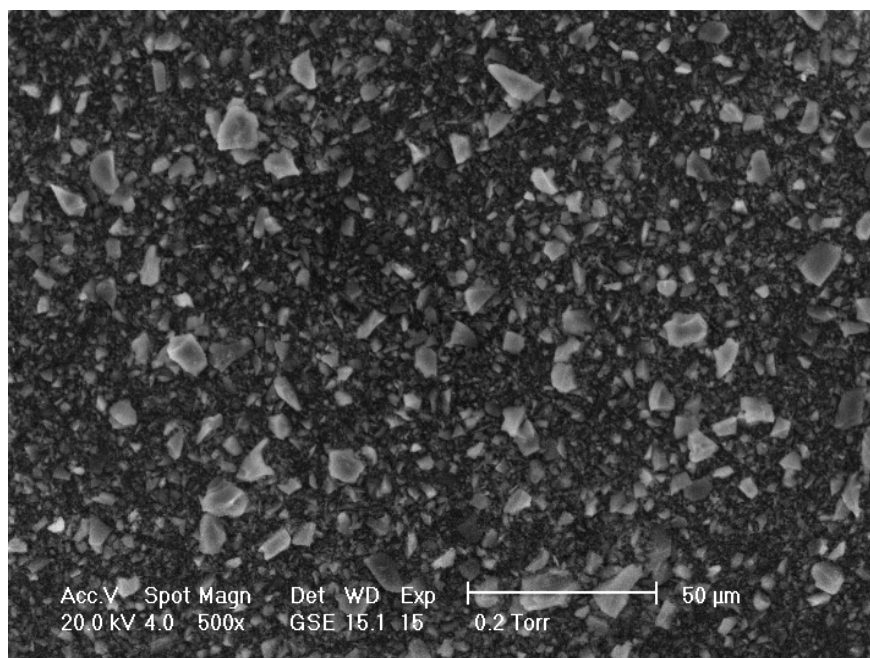
Figure A.42: ESEM image of P-W at 500x
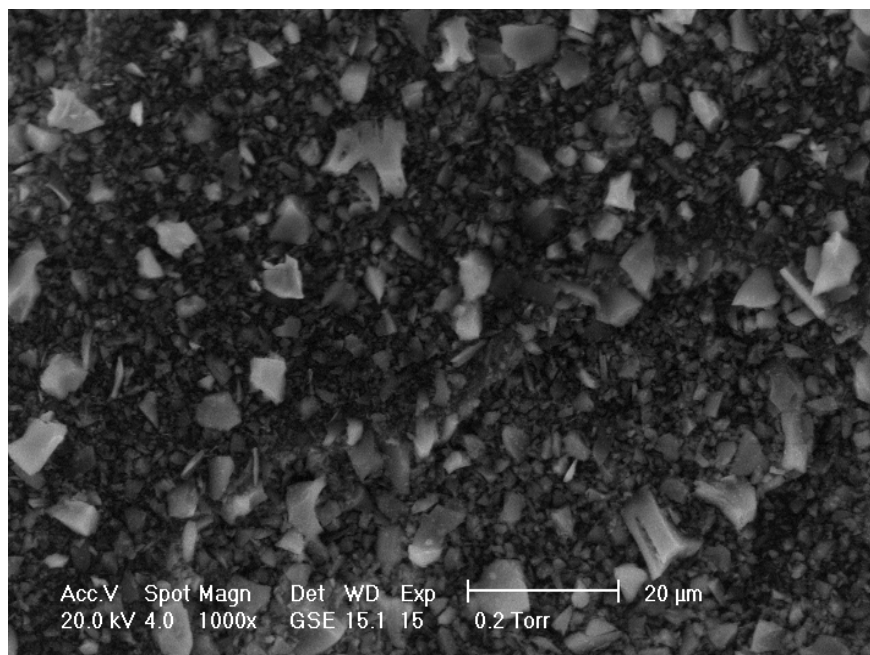
Figure A.43: ESEM image of P-W at 1000x
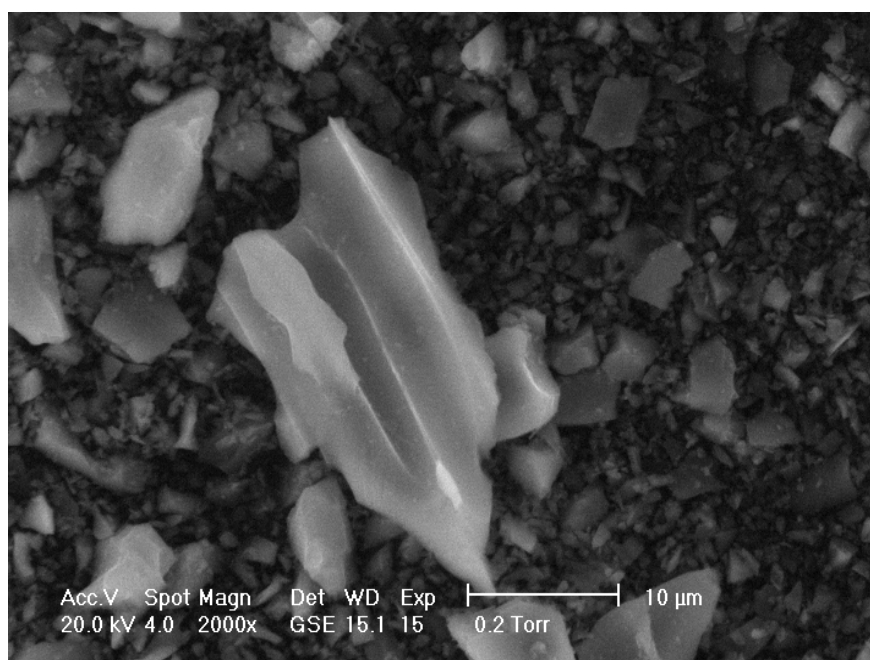
Figure A.44: ESEM image of P-W at 2000x

A.3 Supplier C
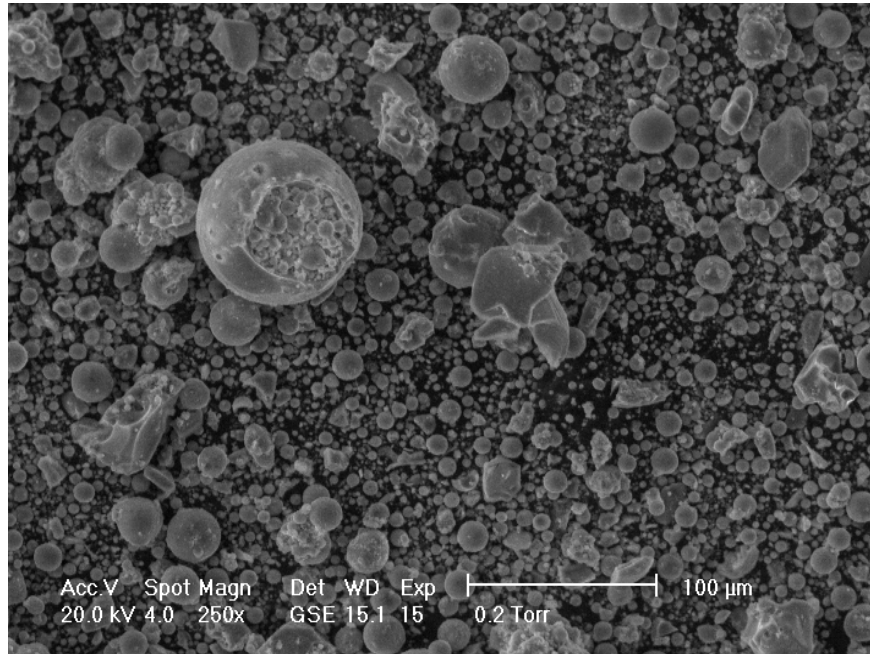
Figure A.45: ESEM image of RC-G at 250x
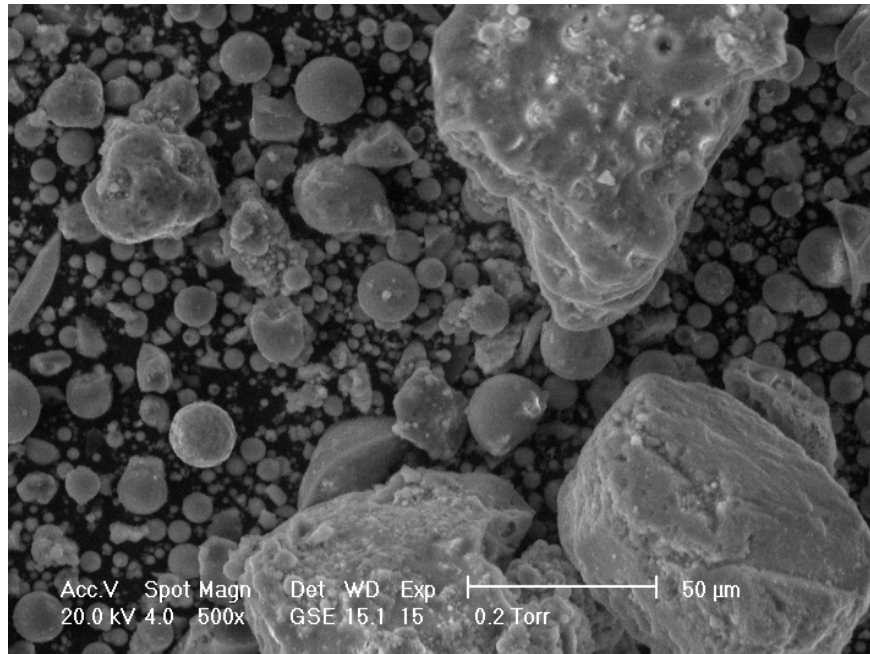
Figure A.46: ESEM image of RC-G at 500x
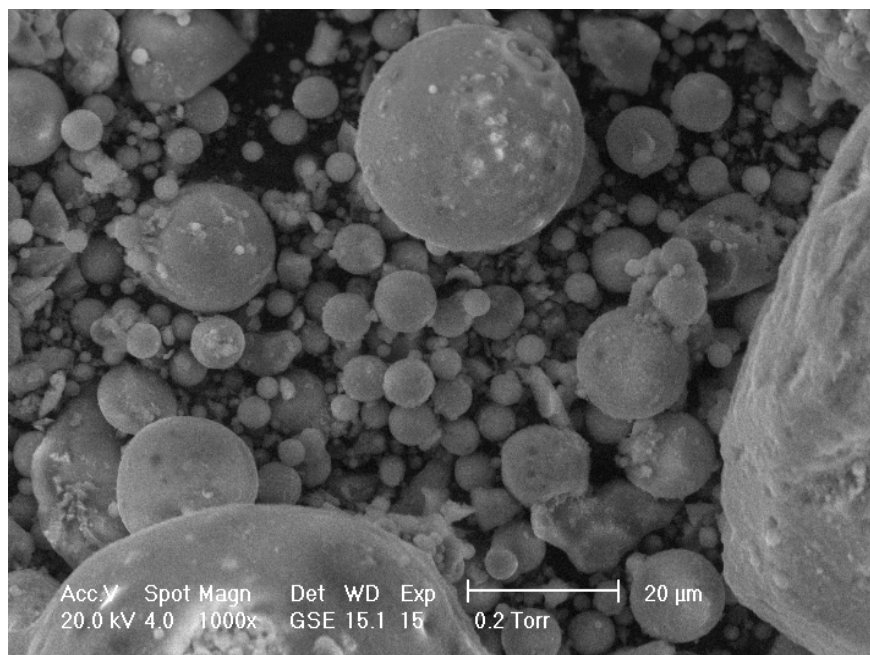
Figure A.47: ESEM image of RC-G at 1000x
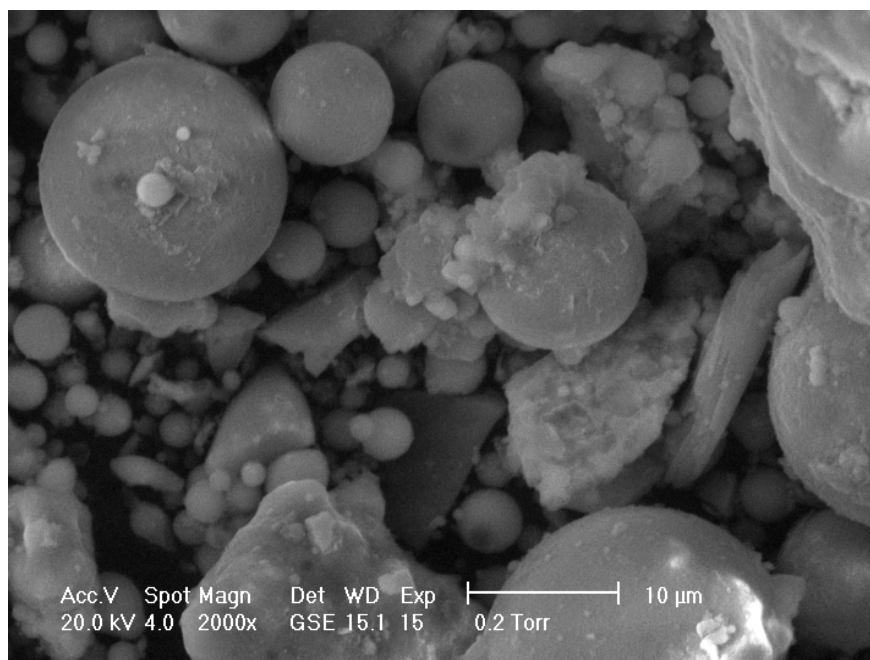
Figure A.48: ESEM image of RC-G at 2000x
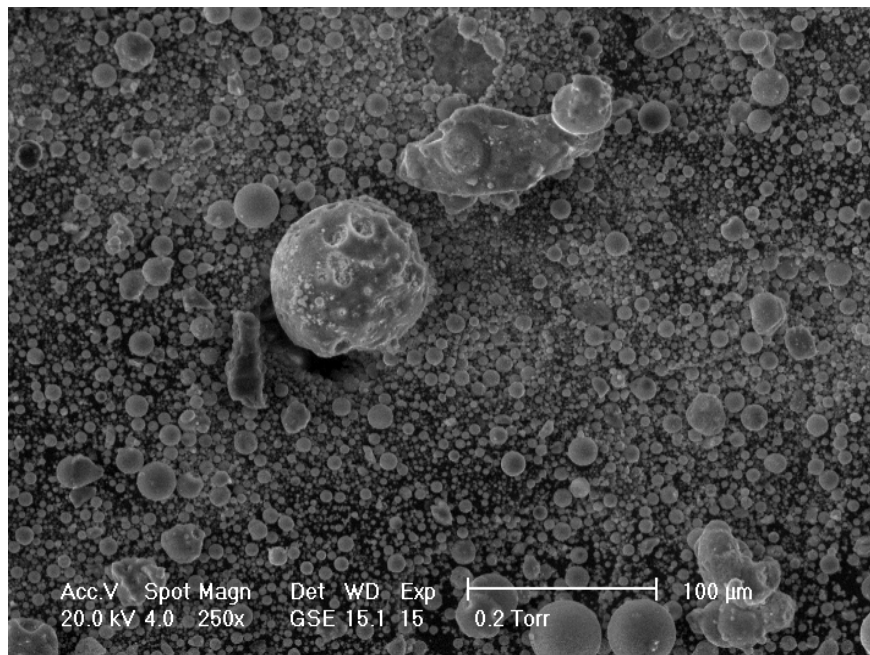
Figure A.49: ESEM image of RC-M at 250x
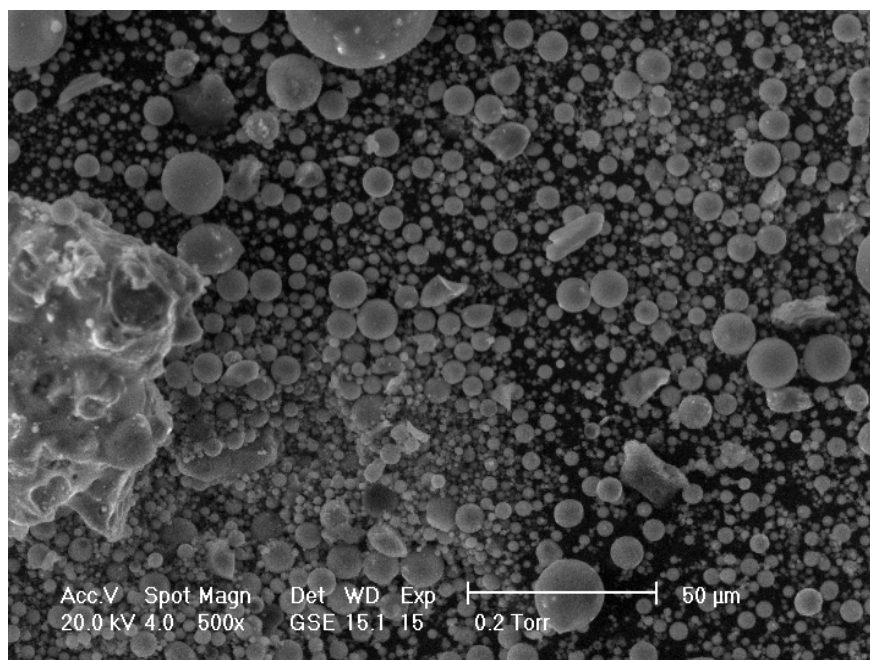
Figure A.50: ESEM image of RC-M at 500x
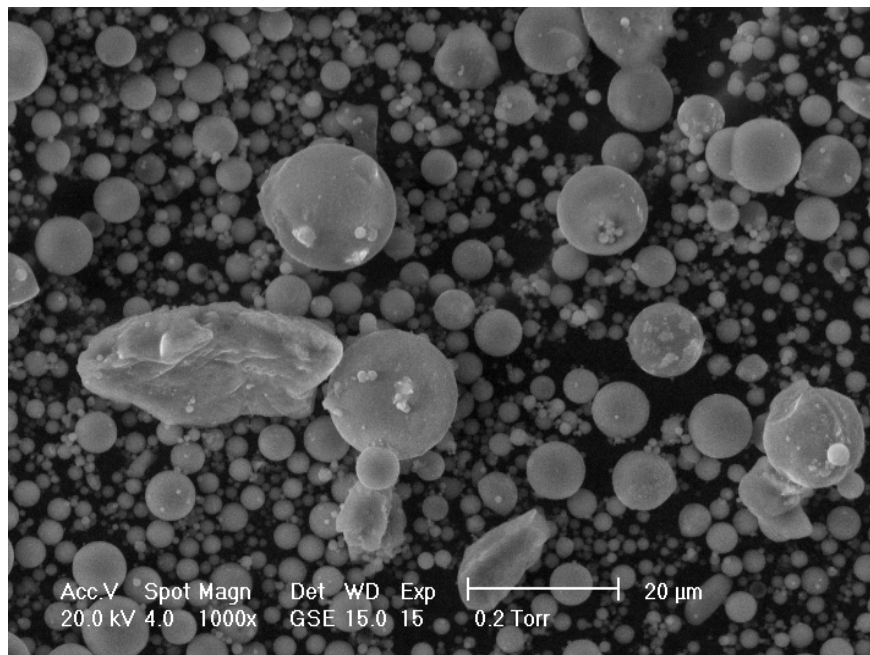
Figure A.51: ESEM image of RC-M at 1000x
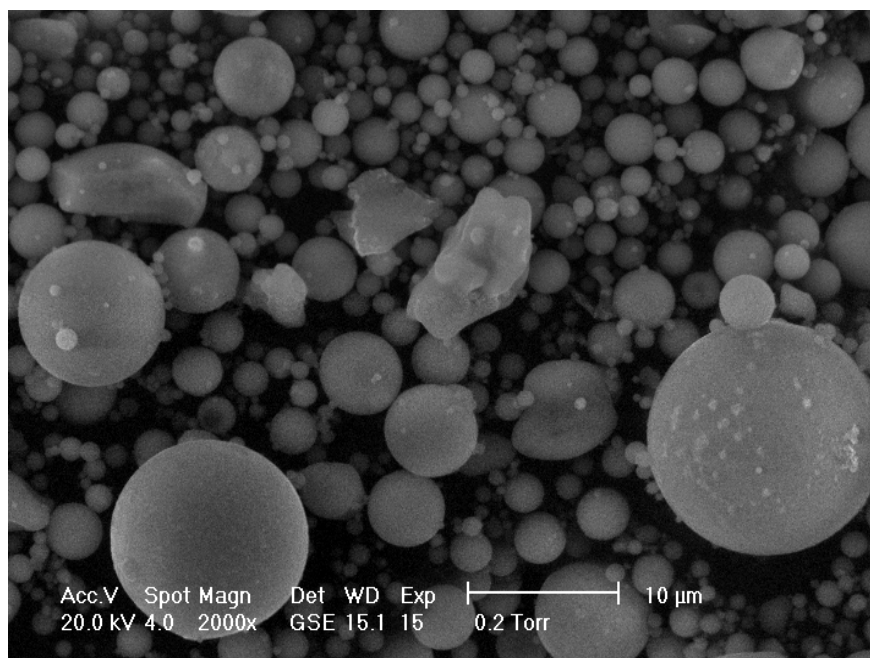
Figure A.52: ESEM image of RC-M at 2000x
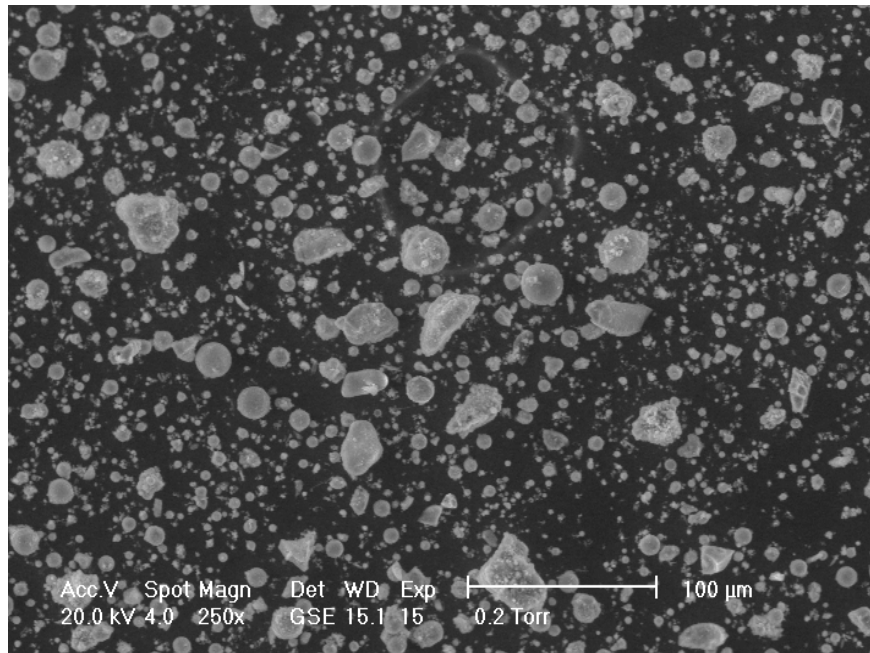
Figure A.53: ESEM image of RC-P at 250x
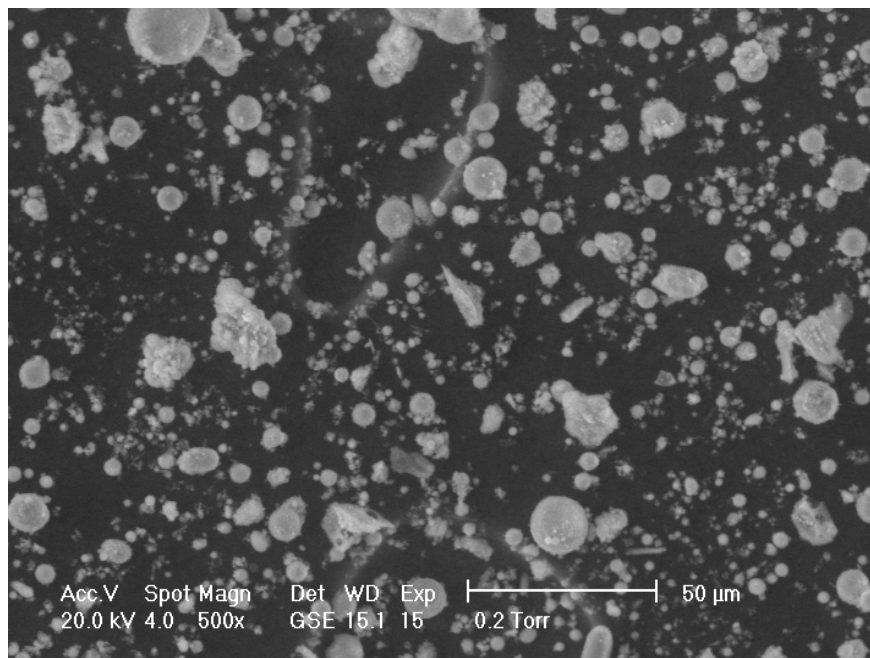
Figure A.54: ESEM image of RC-P at 500x
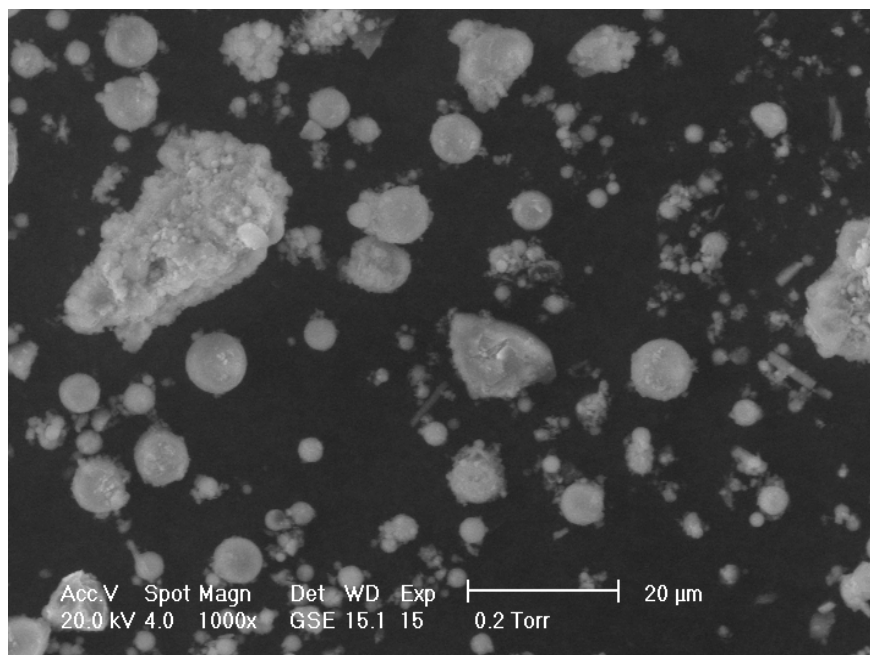
Figure A.55: ESEM image of RC-P at 1000x
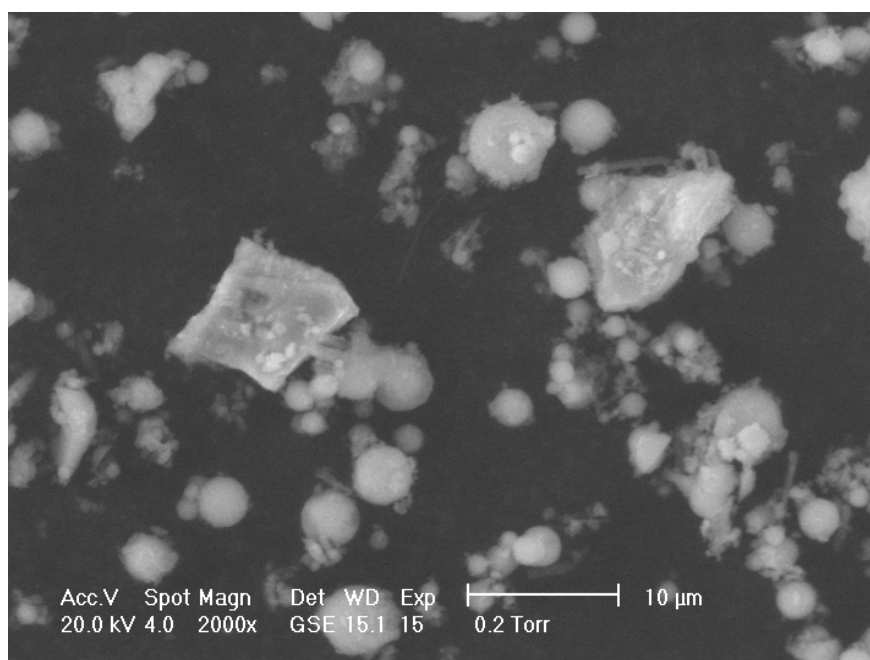
Figure A.56: ESEM image of RC-P at 2000x
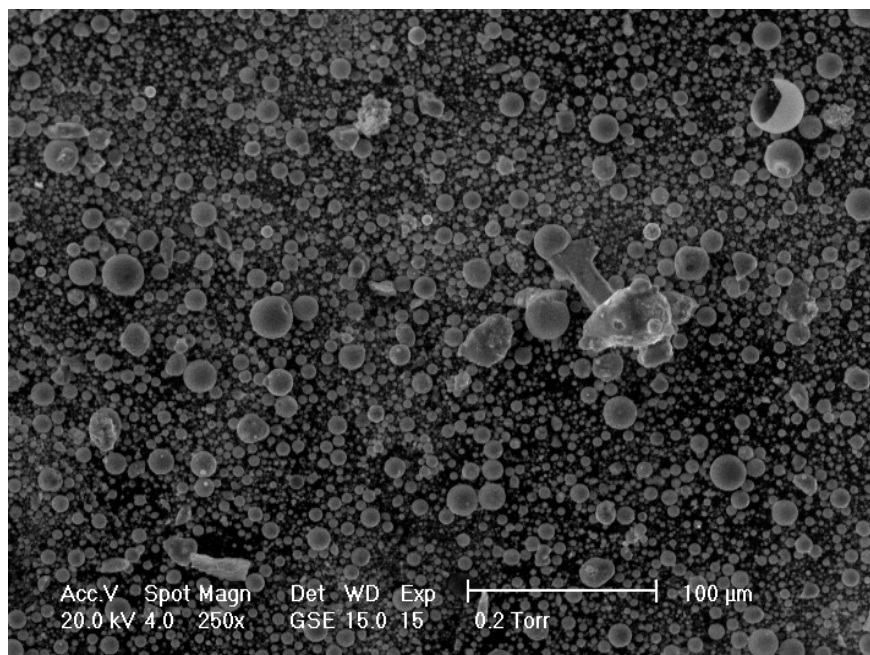
Figure A.57: ESEM image of RM-M at 250x
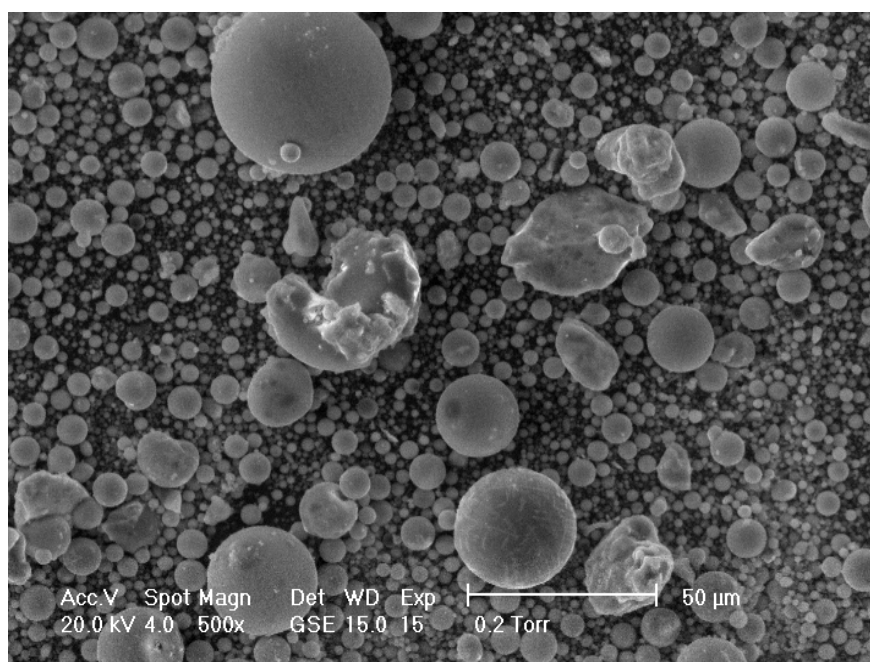
Figure A.58: ESEM image of RM-M at 500x
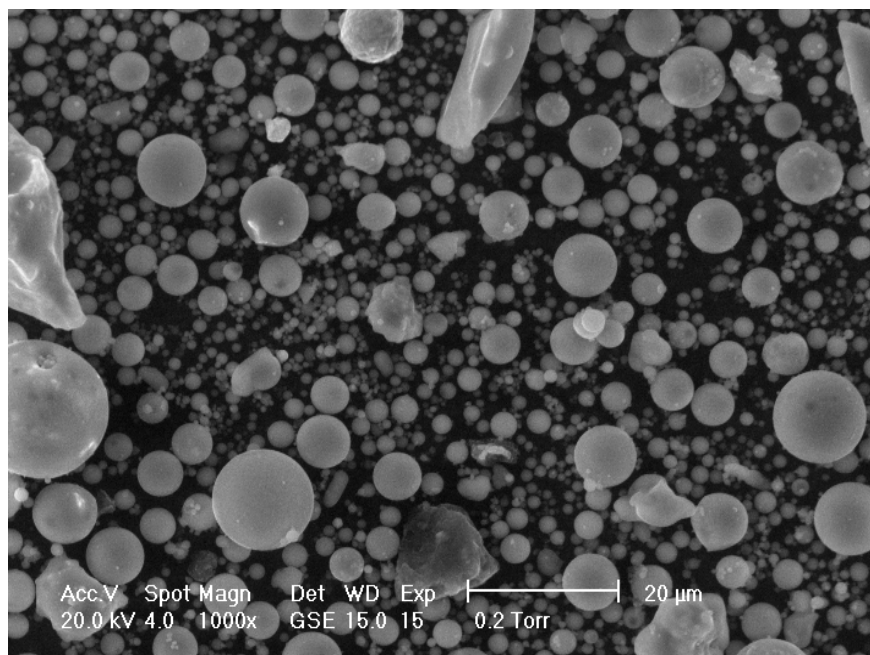
Figure A.59: ESEM image of RM-M at 1000x
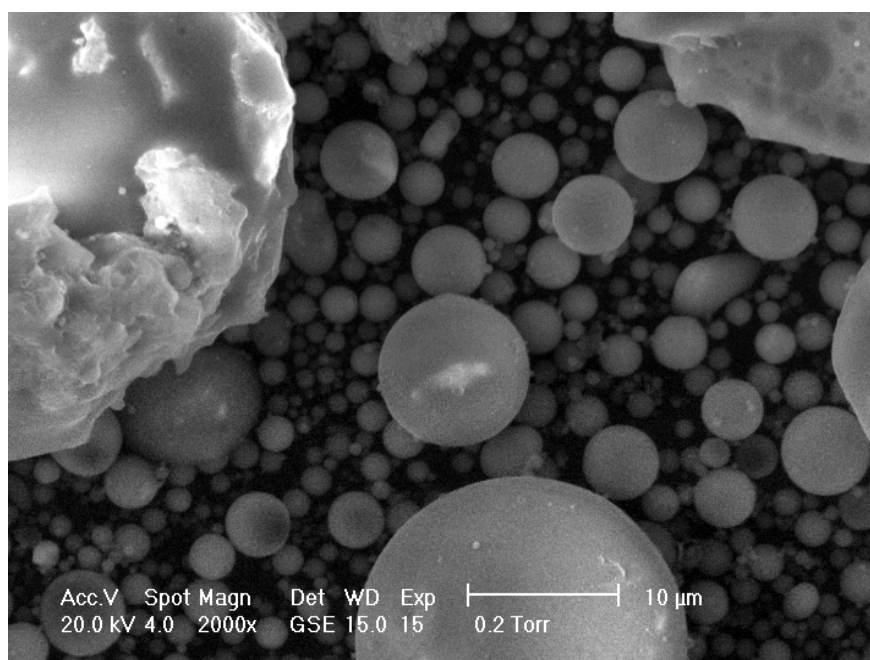
Figure A.60: ESEM image of RM-M at 2000x

Appendix B. X-Ray Diffractograms

B.1 Controls
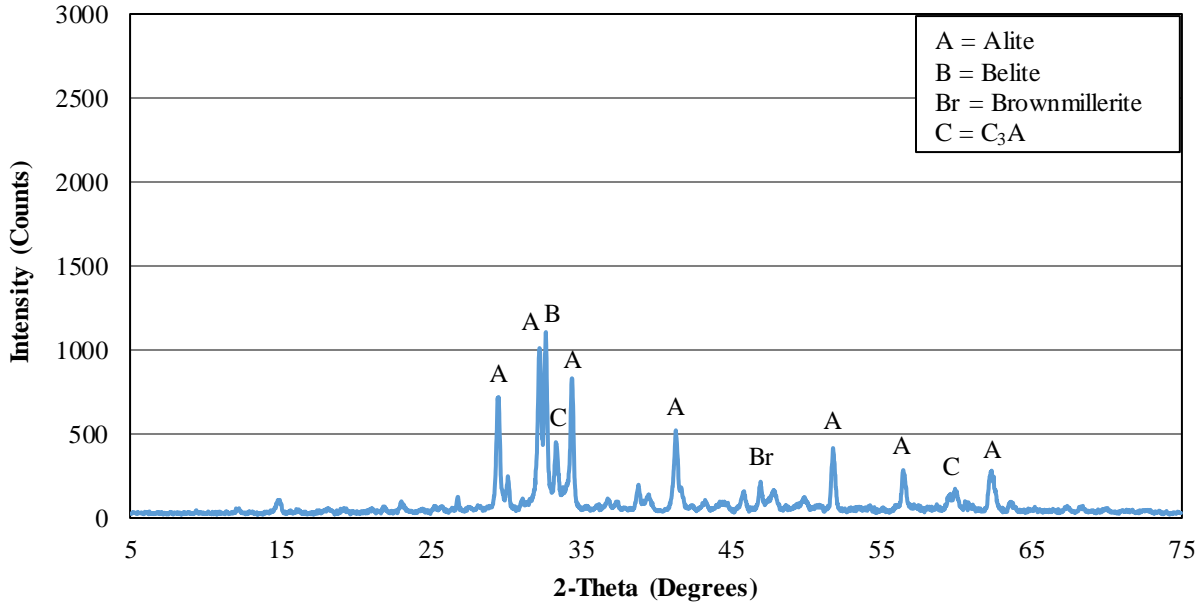
Figure B.1: X-ray diffraction pattern of OPC
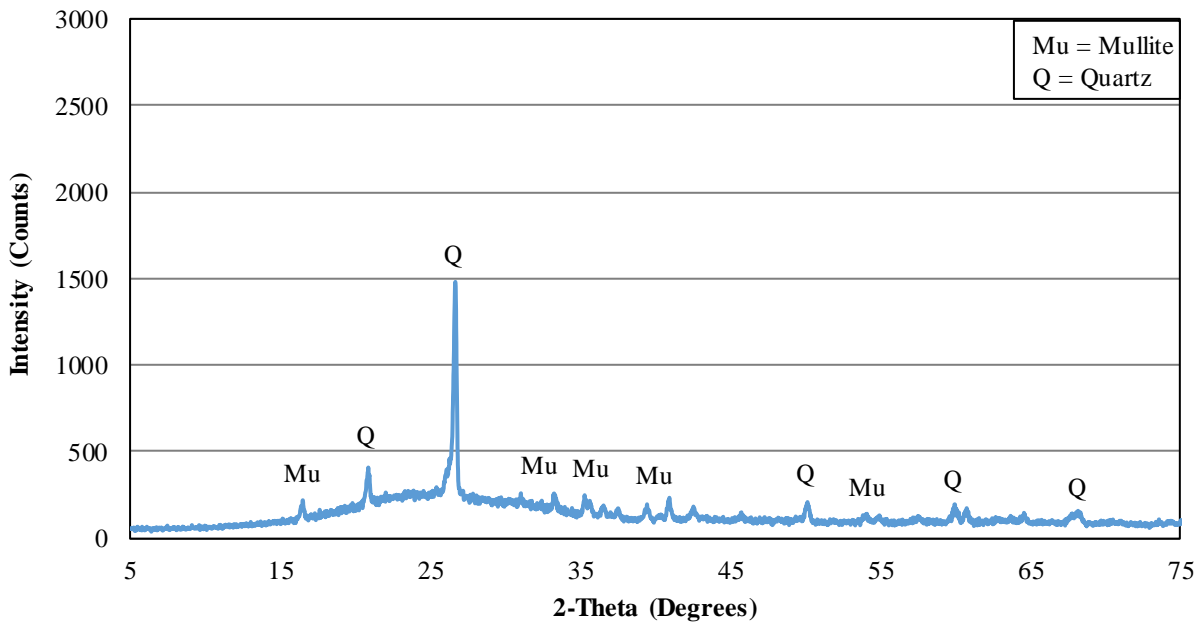
Figure B.2: X-ray diffraction pattern of FA

B.2 Supplier A
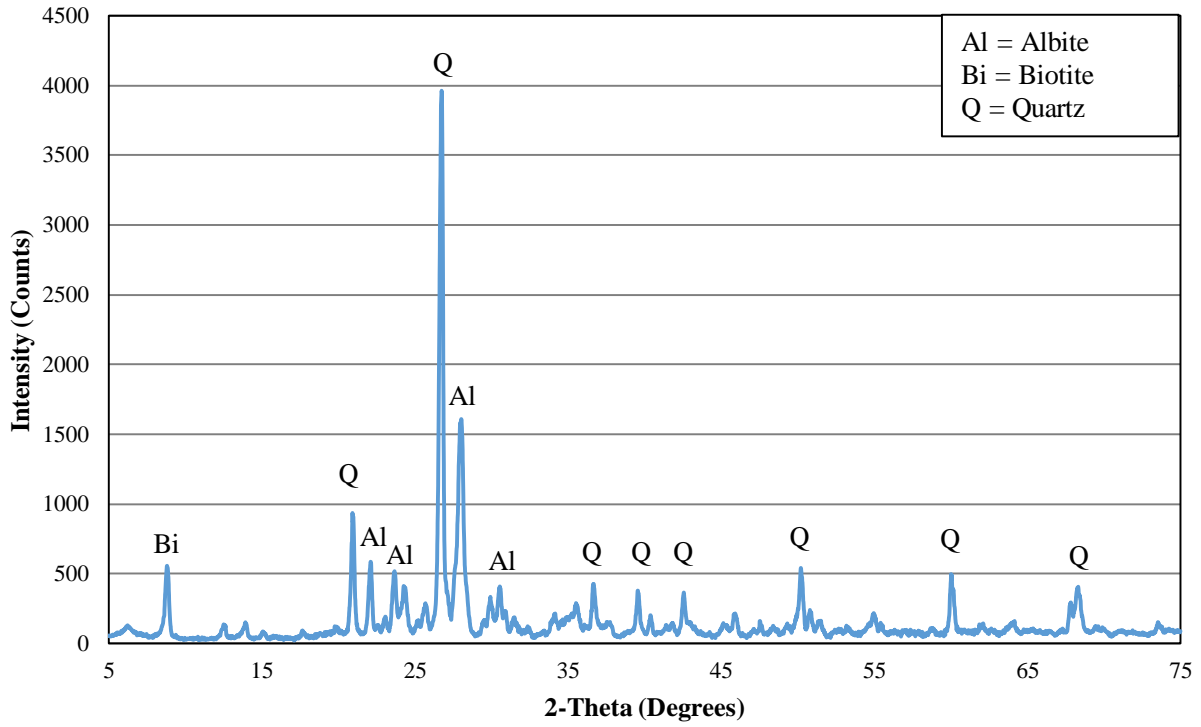
Figure B.3: X-ray diffraction pattern of D-L
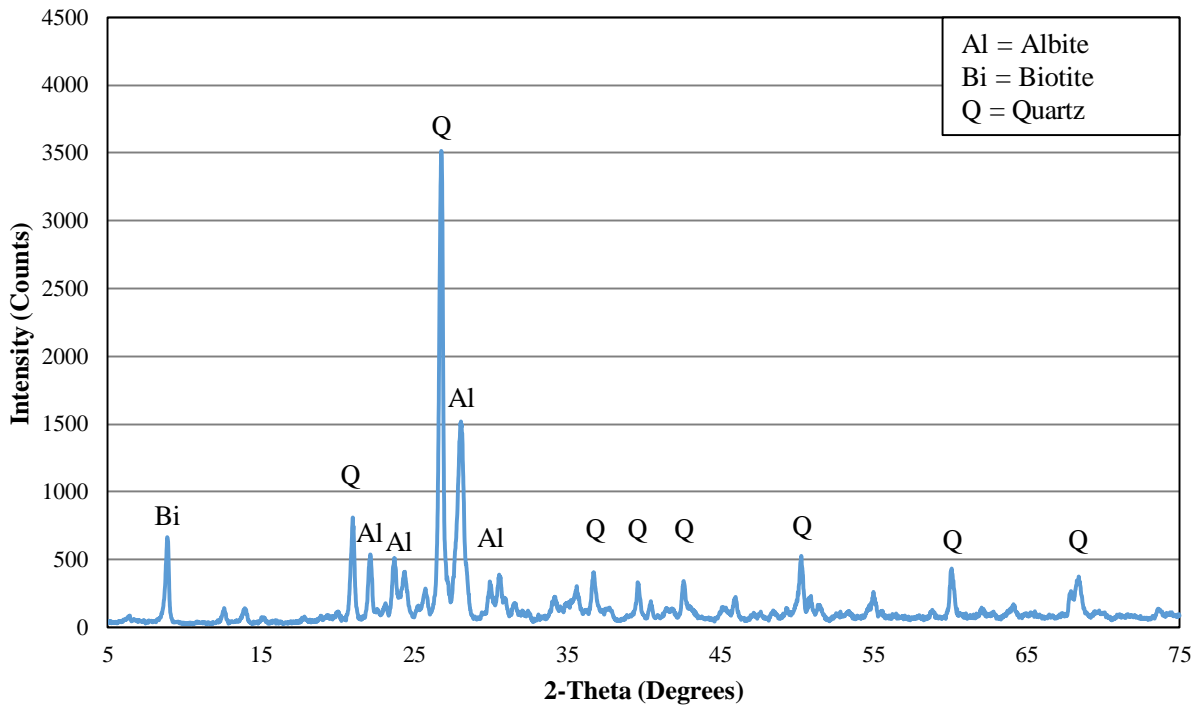
Figure B.4: X-ray diffraction pattern of D-S
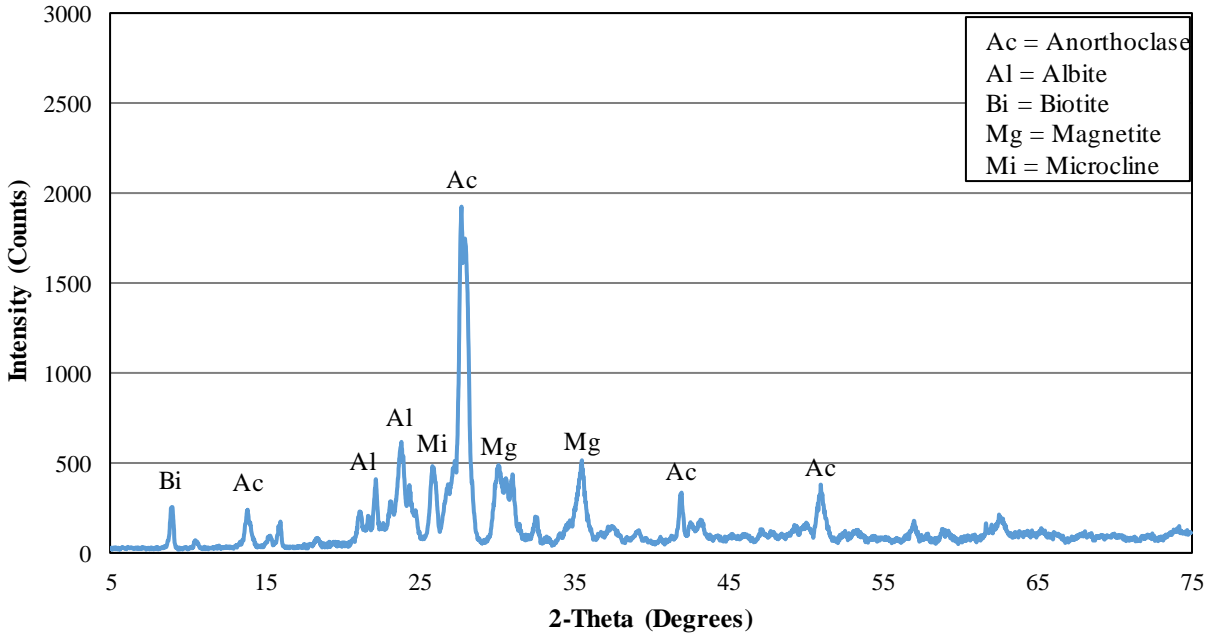
Figure B.5: X-ray diffraction pattern of NS-I
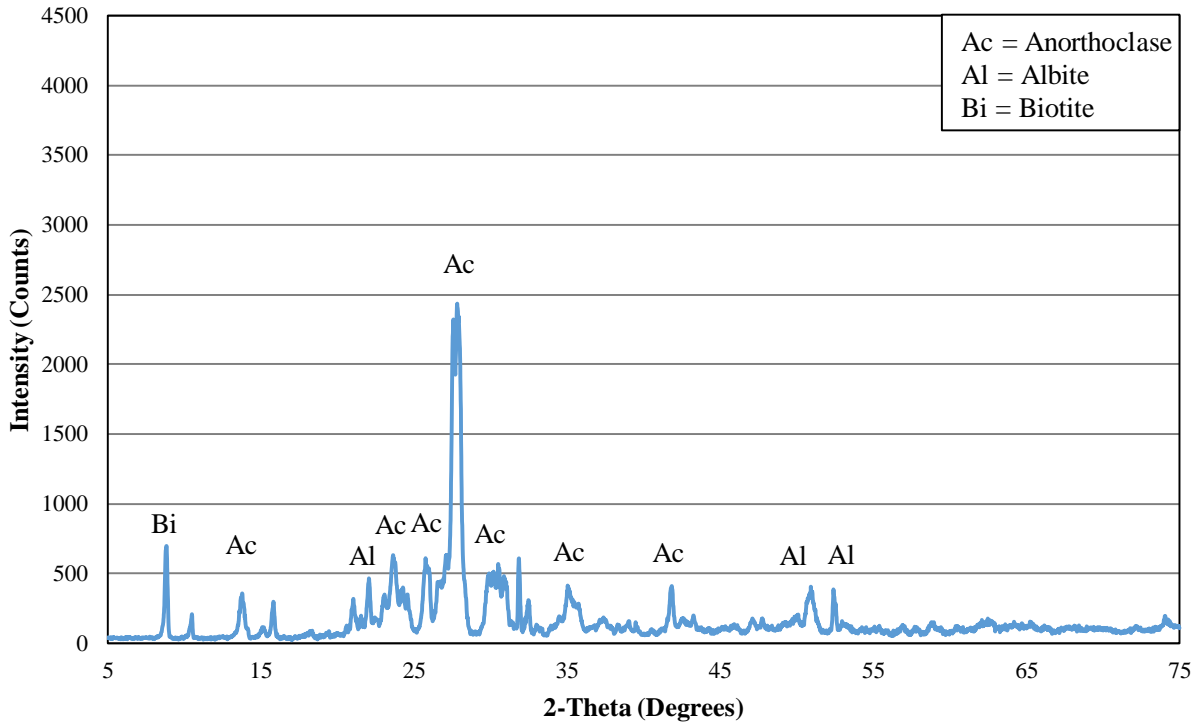
Figure B.6: X-ray diffraction pattern of NS-L
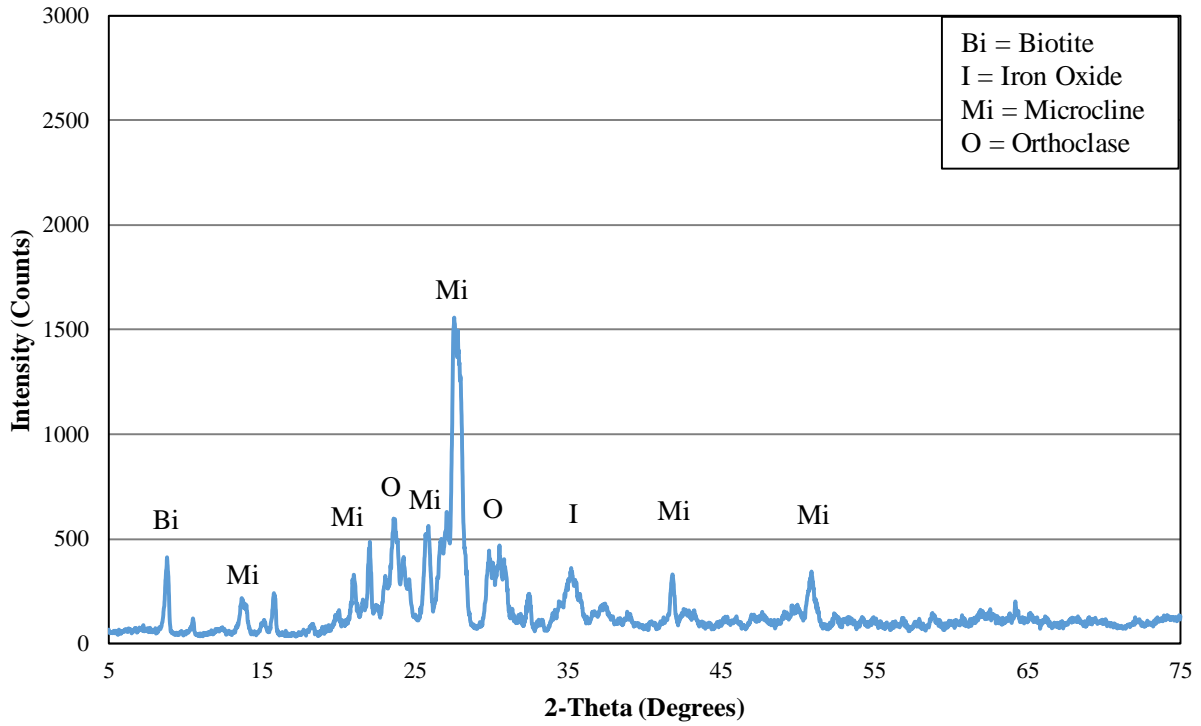
Figure B.7: X-ray diffraction pattern of NS-S
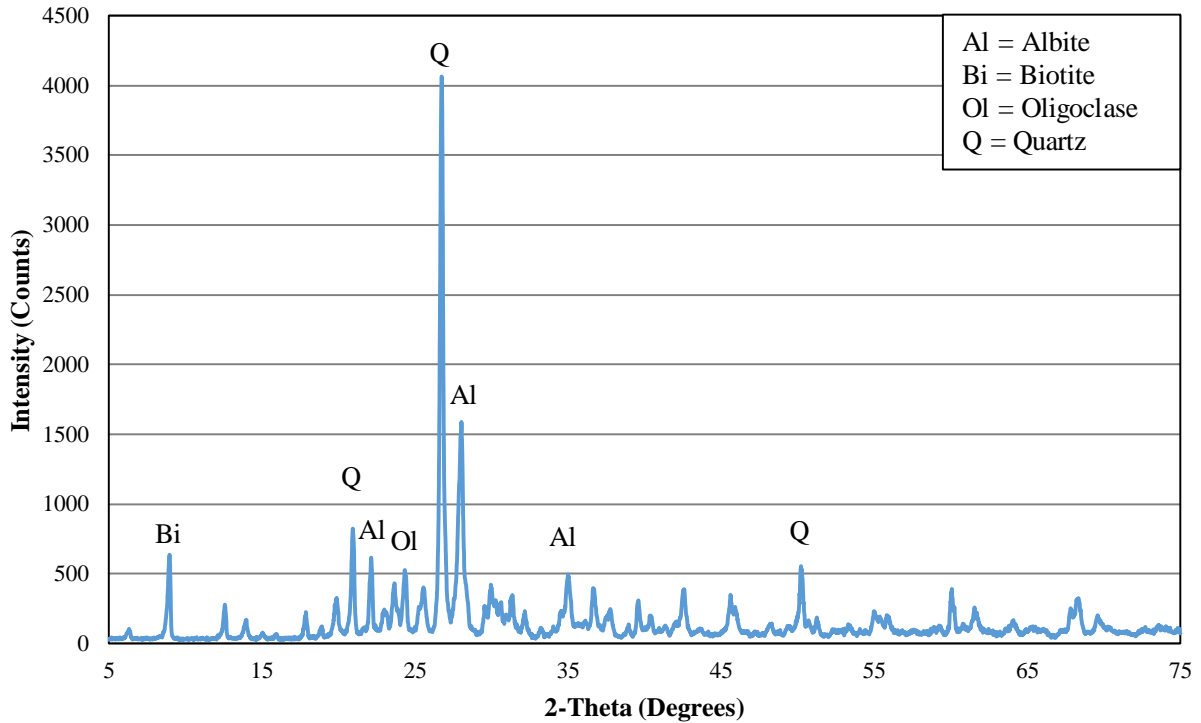
Figure B.8: X-ray diffraction pattern of R-O

B.3 Supplier B
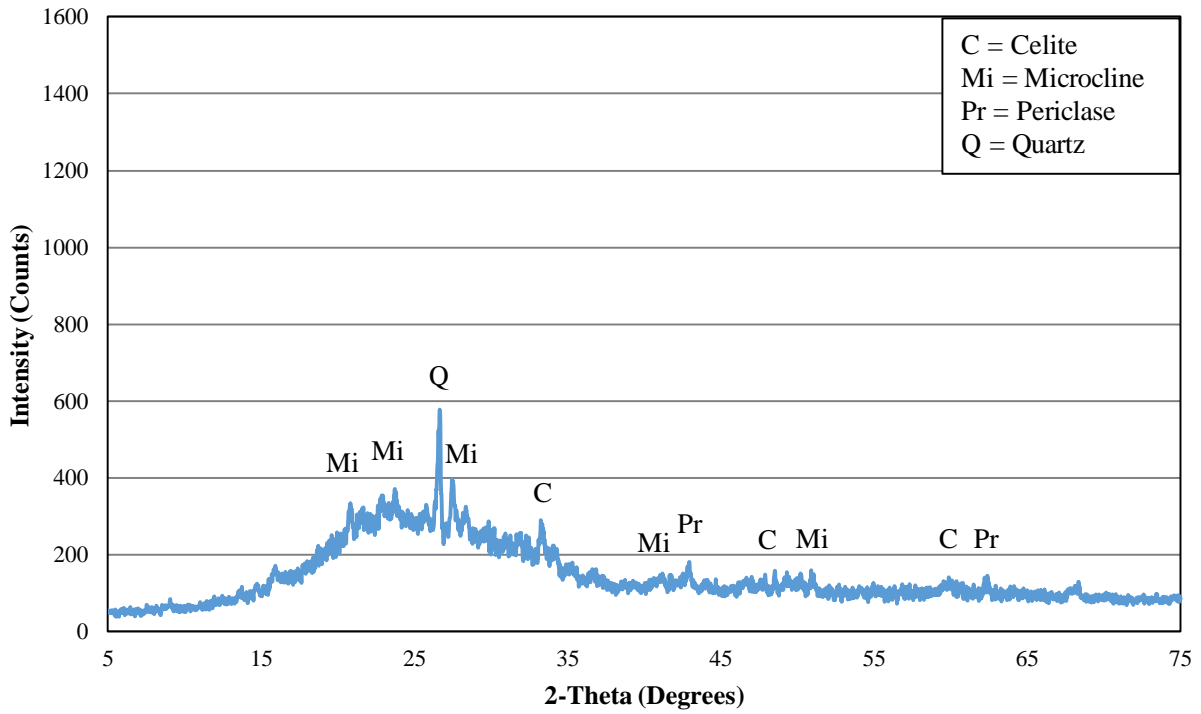
Figure B.9: X-ray diffraction pattern of RM-C
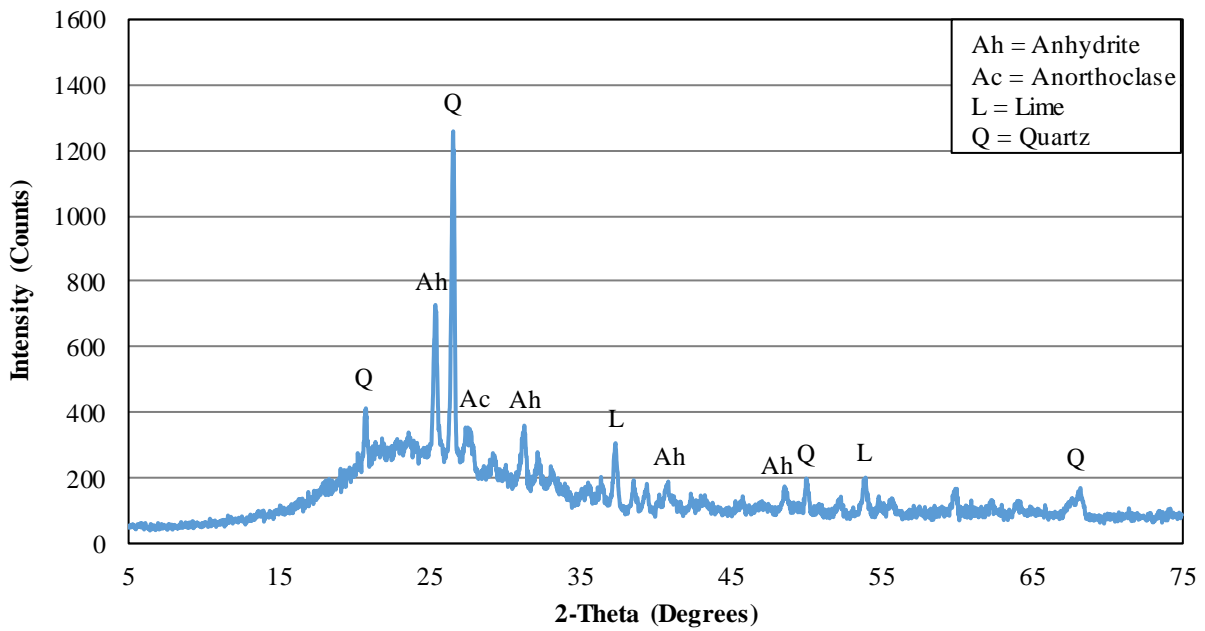
Figure B.10: X-ray diffraction pattern of RM-L
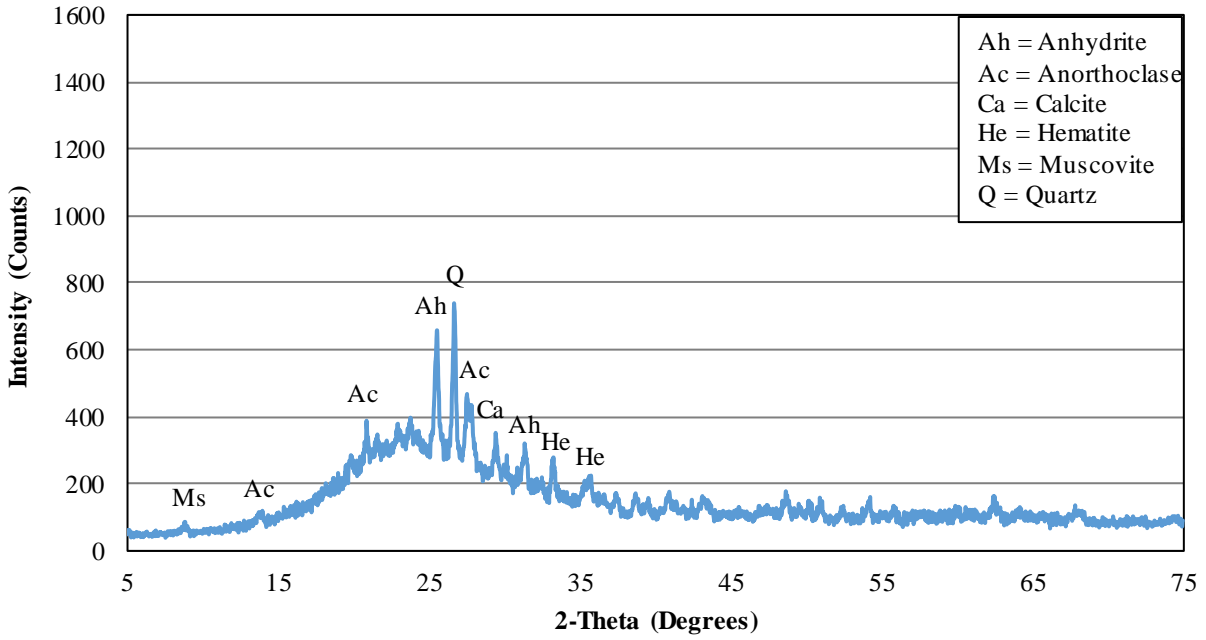
Figure B.11: X-ray diffraction pattern of RM-S
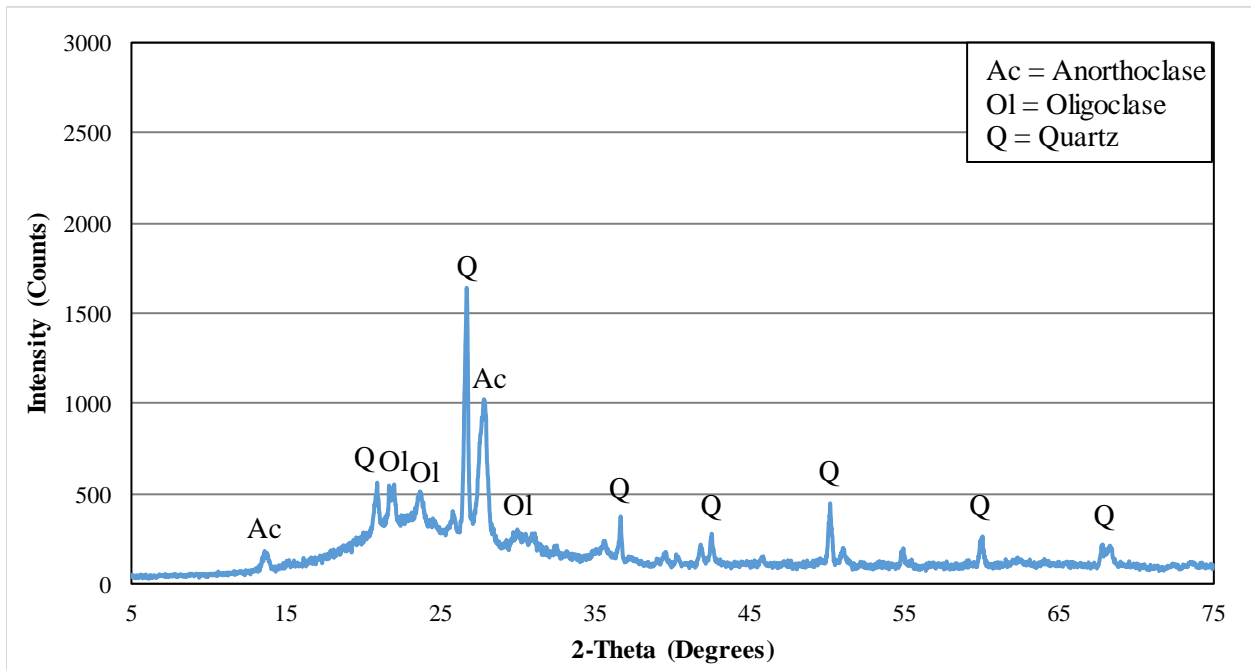
Figure B.12: X-ray diffraction pattern of P-B
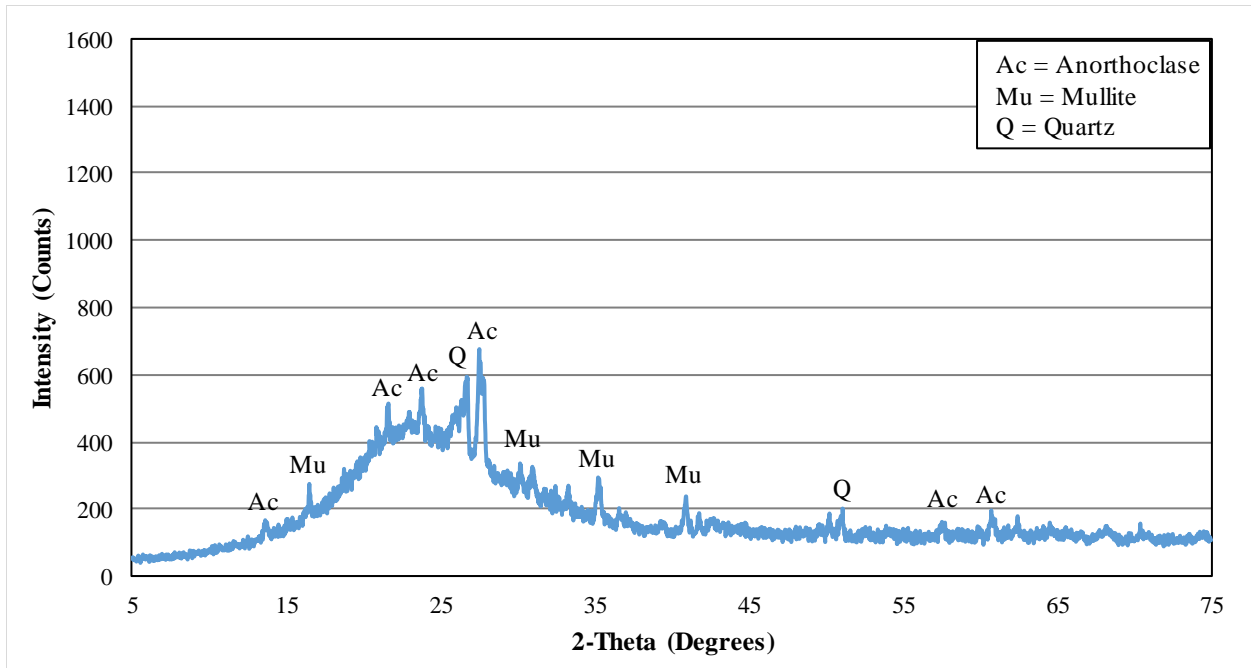
Figure B.13: X-ray diffraction pattern of P-W

B.3 Supplier C
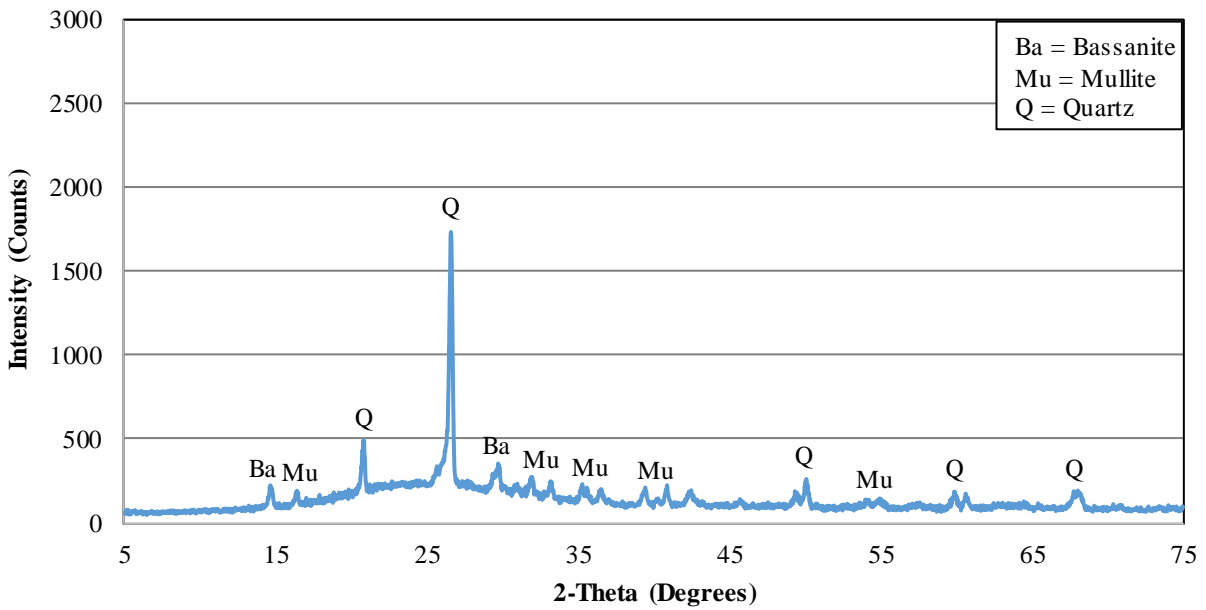
Figure B.14: X-ray diffraction pattern of RC-G
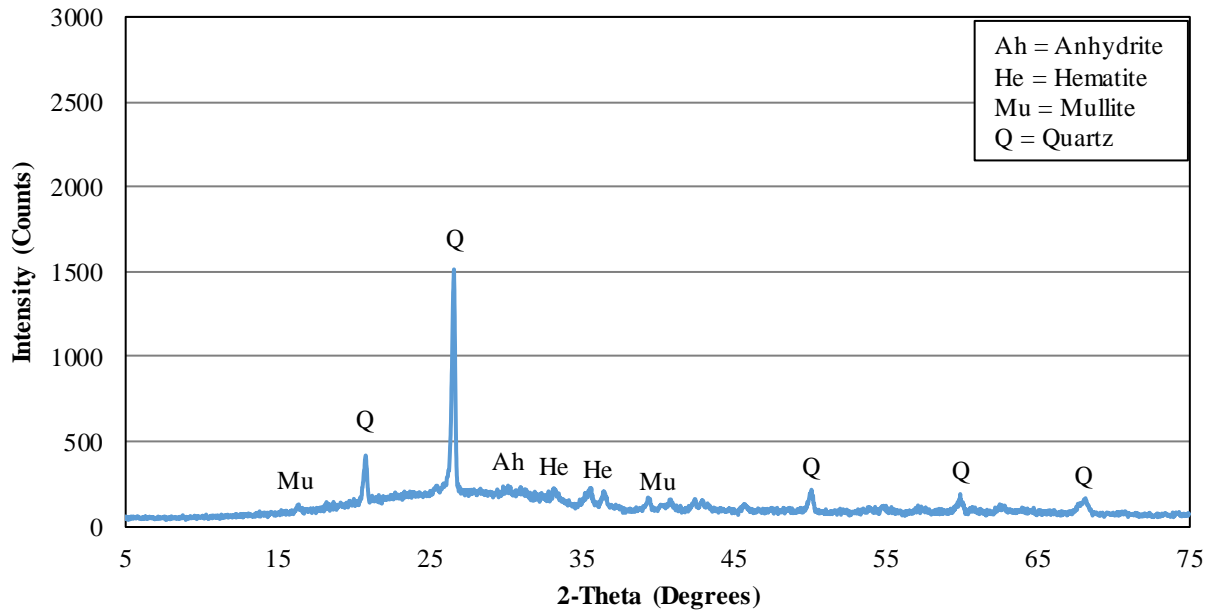
Figure B.15: X-ray diffraction pattern of RC-M
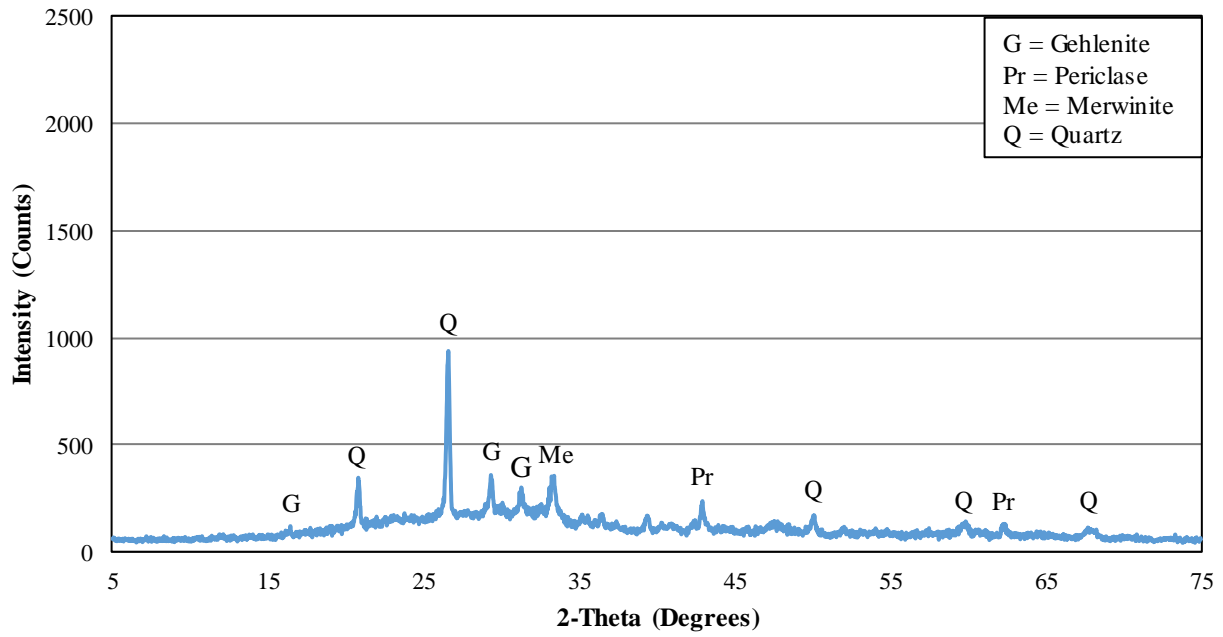
Figure B.16: X-ray diffraction pattern of RC-P
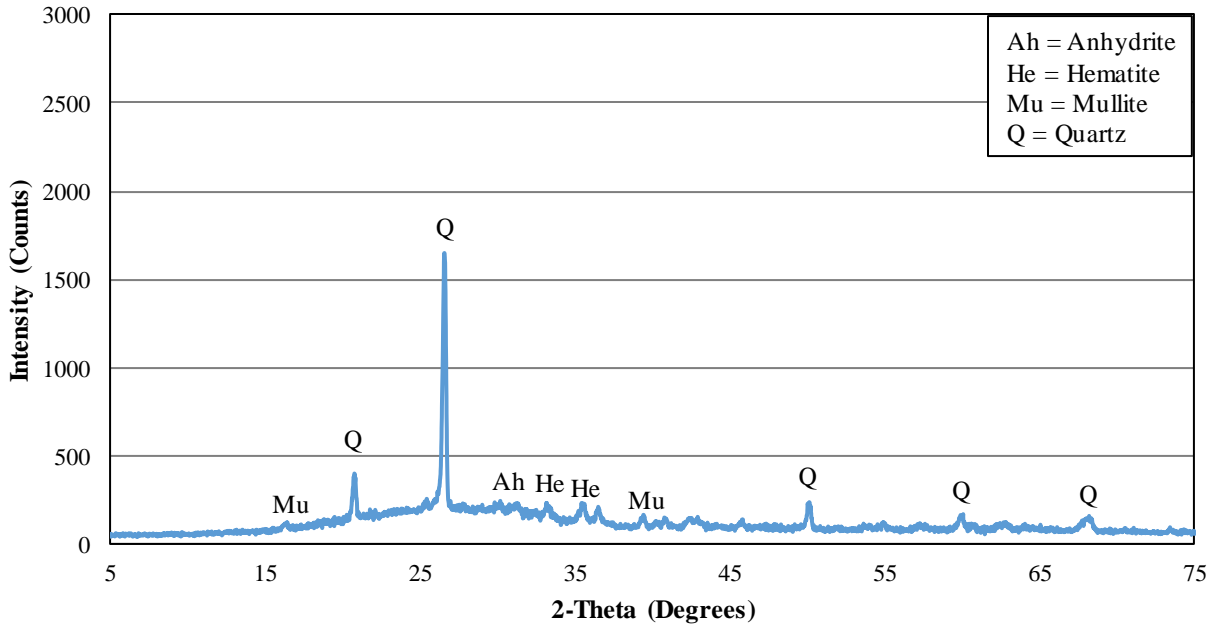
Figure B.17: X-ray diffraction pattern of RM-M

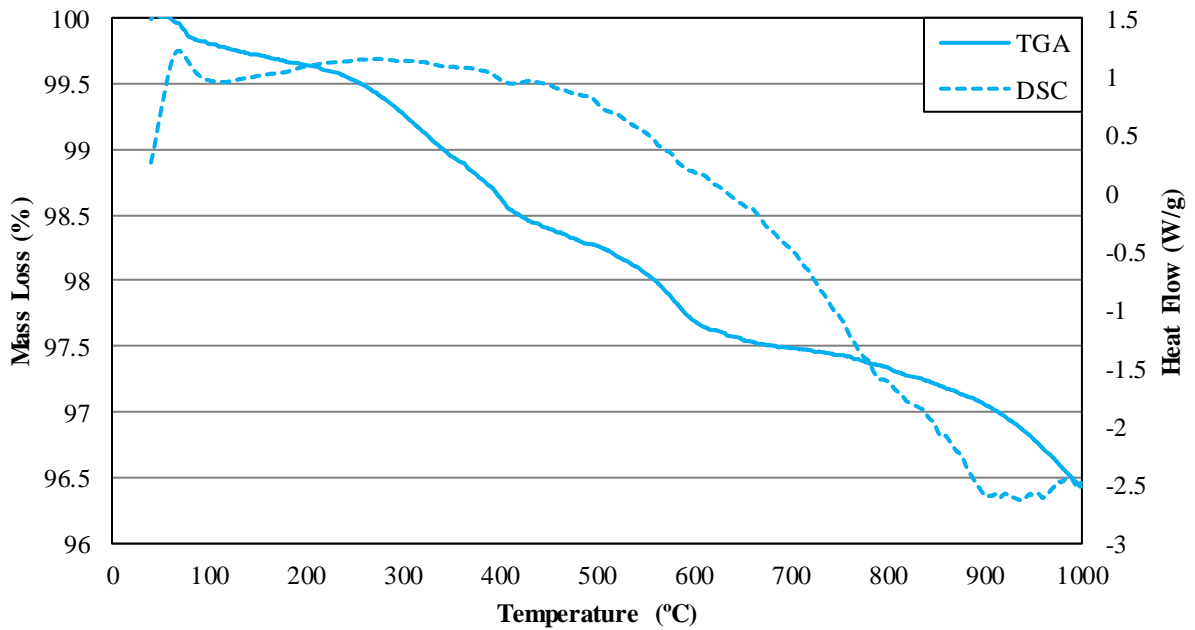# Appendix C. DSC/TGA Plots of SCMs

C.1 Supplier A
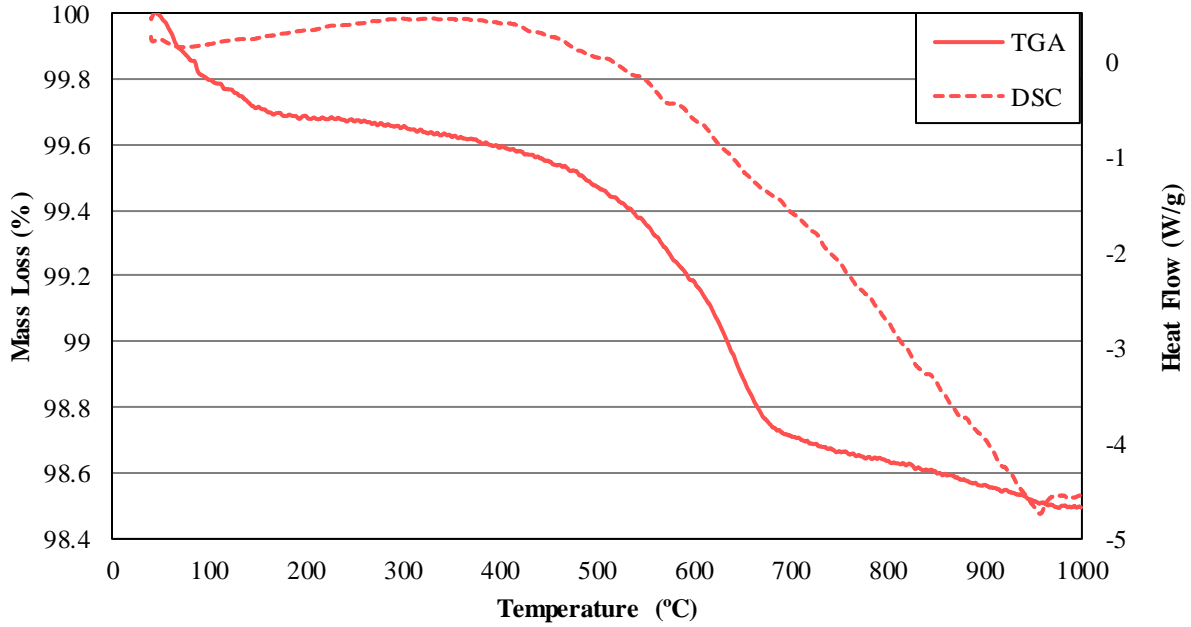
Figure C.1: DSC/TGA plot of D-L
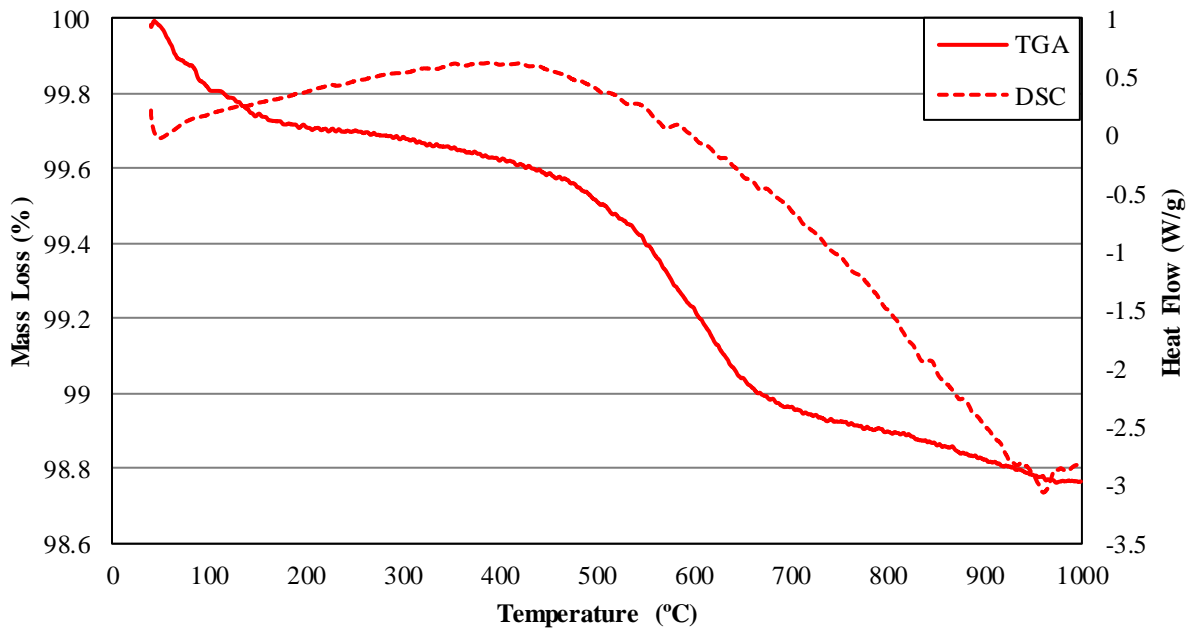
Figure C.2: DSC/TGA plot of D-S
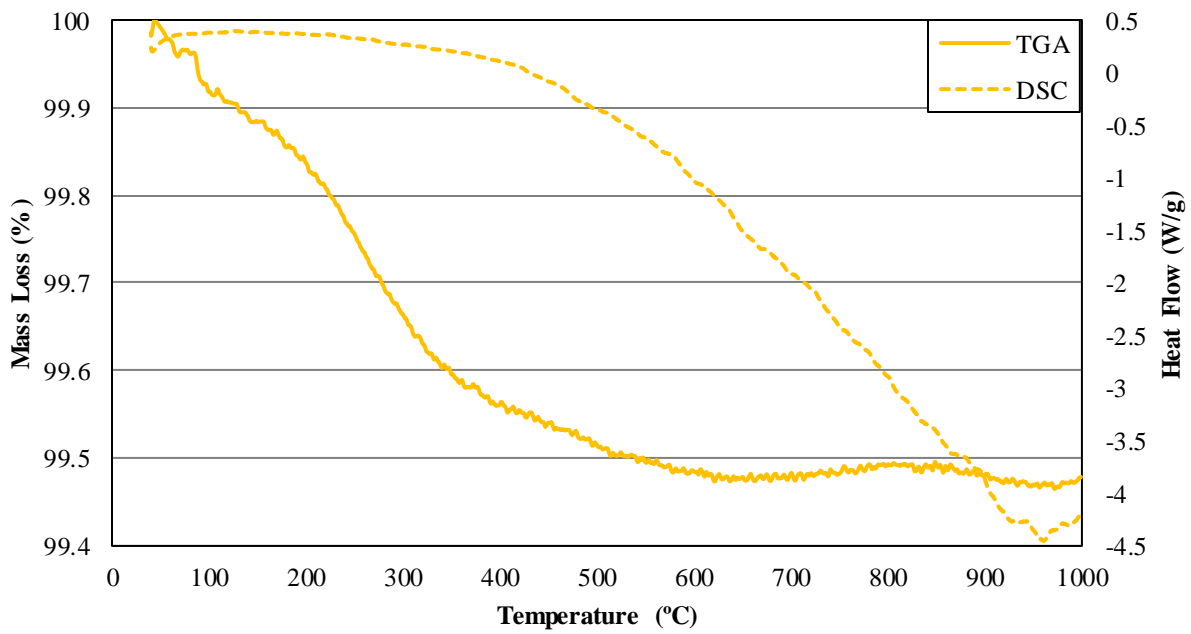
Figure C.3: DSC/TGA plot of NS-I
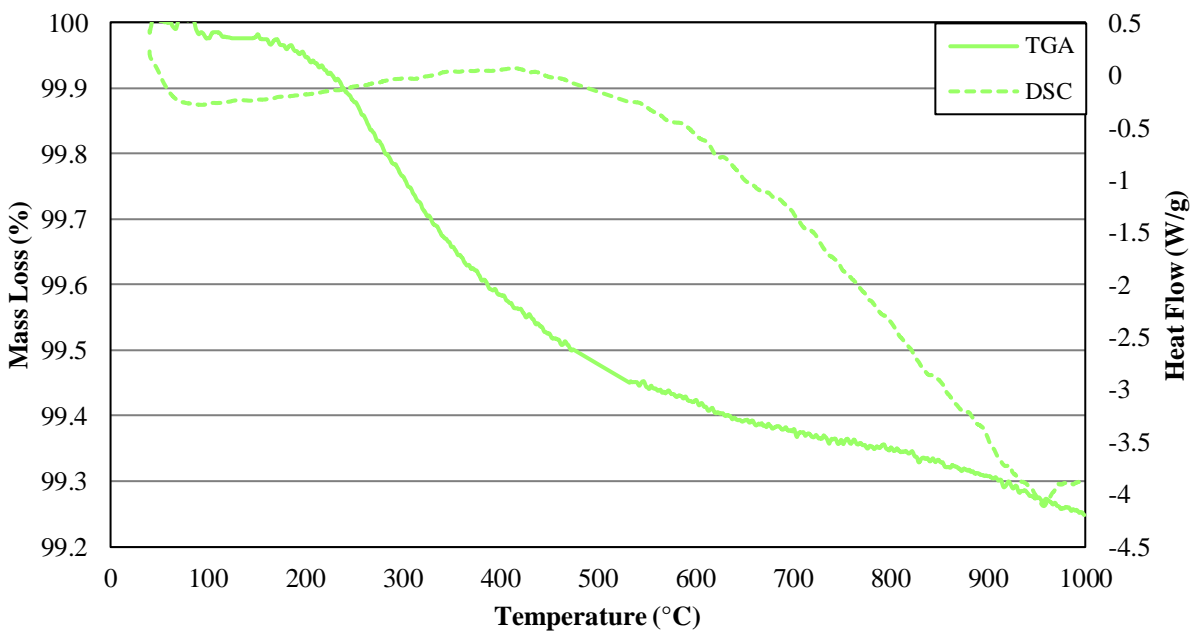
Figure C.4: DSC/TGA plot of NS-L
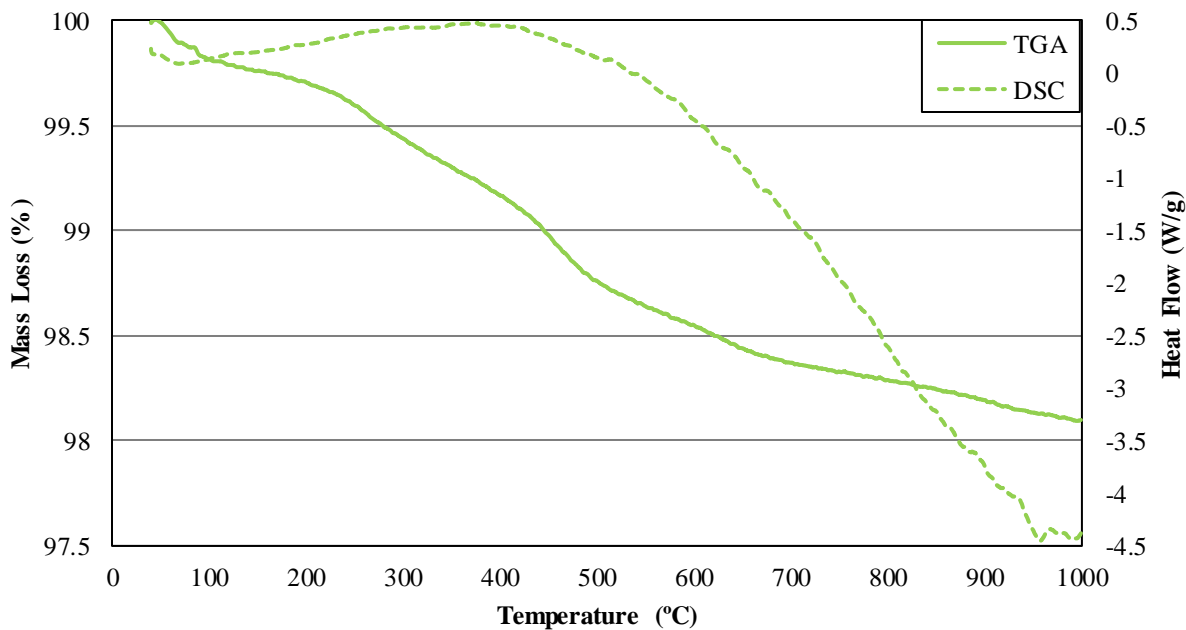
Figure C.5: DSC/TGA plot of NS-S
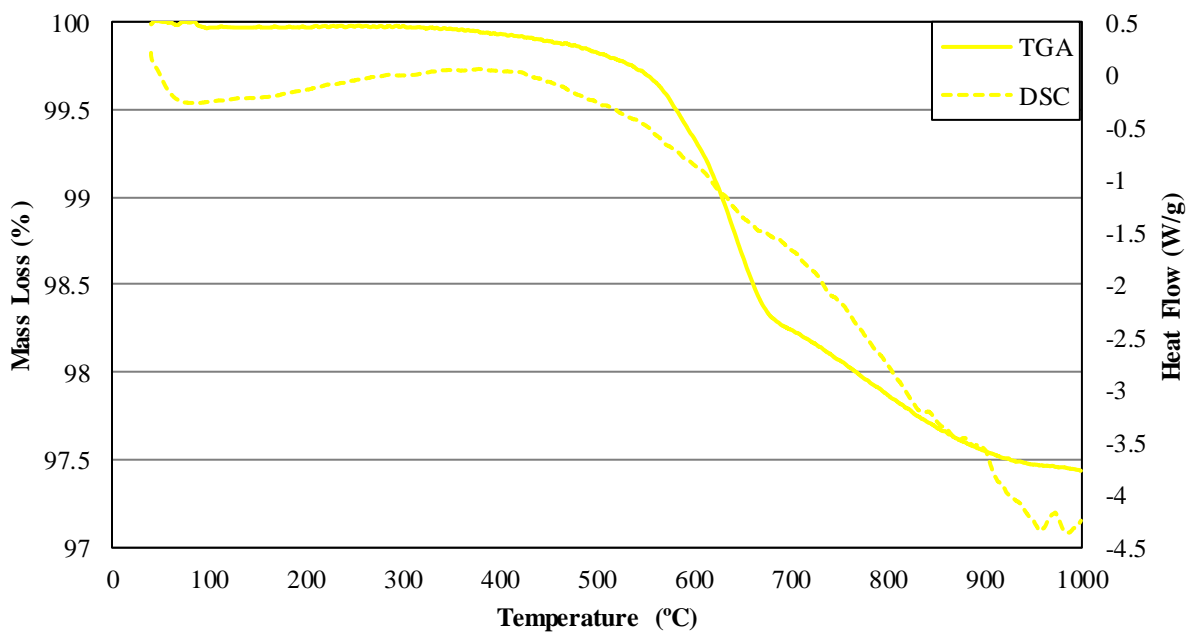
Figure C.6: DSC/TGA plot of R-O

111
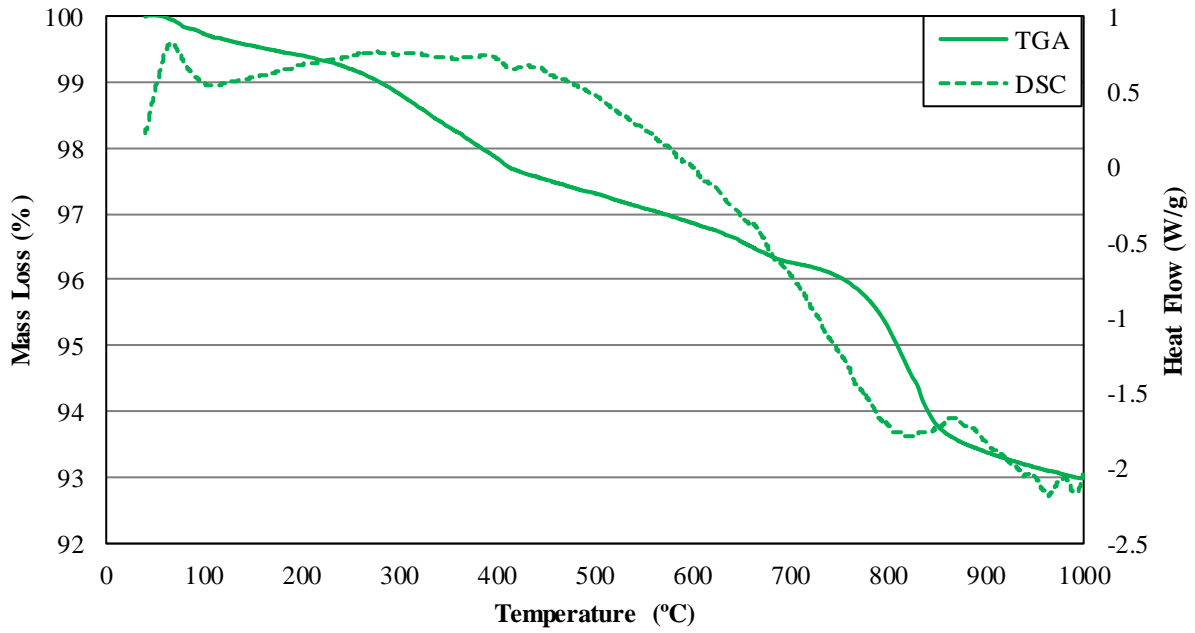
C.2 Supplier B

Figure C.7: DSC/TGA plot of RM-C

Figure C.8: DSC/TGA plot of RM-L
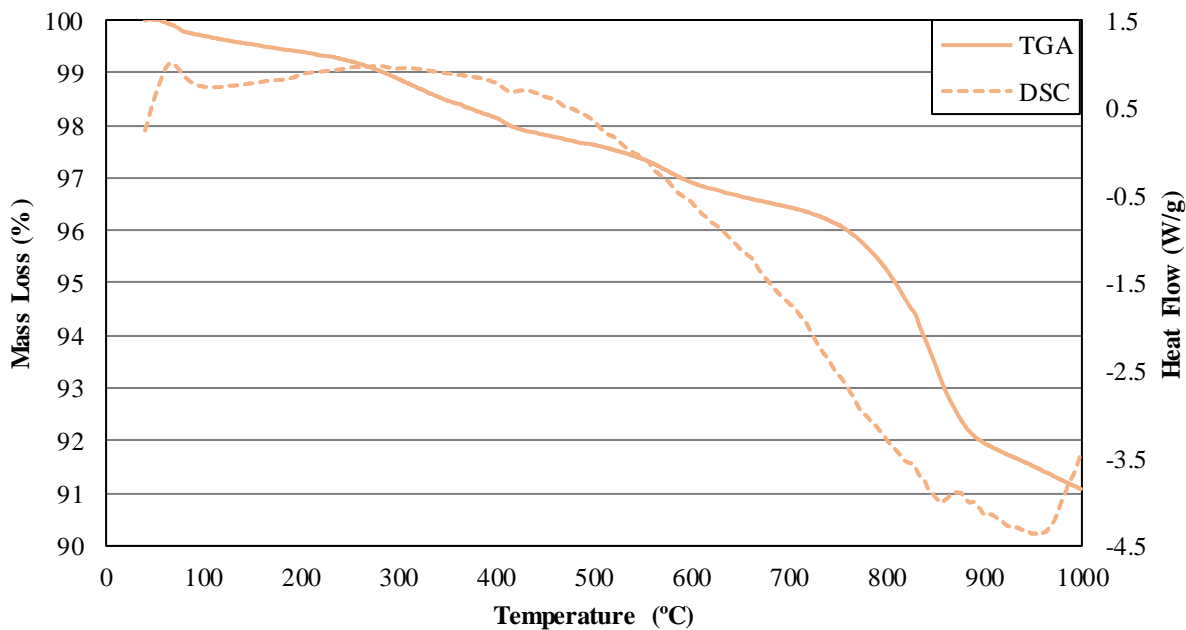
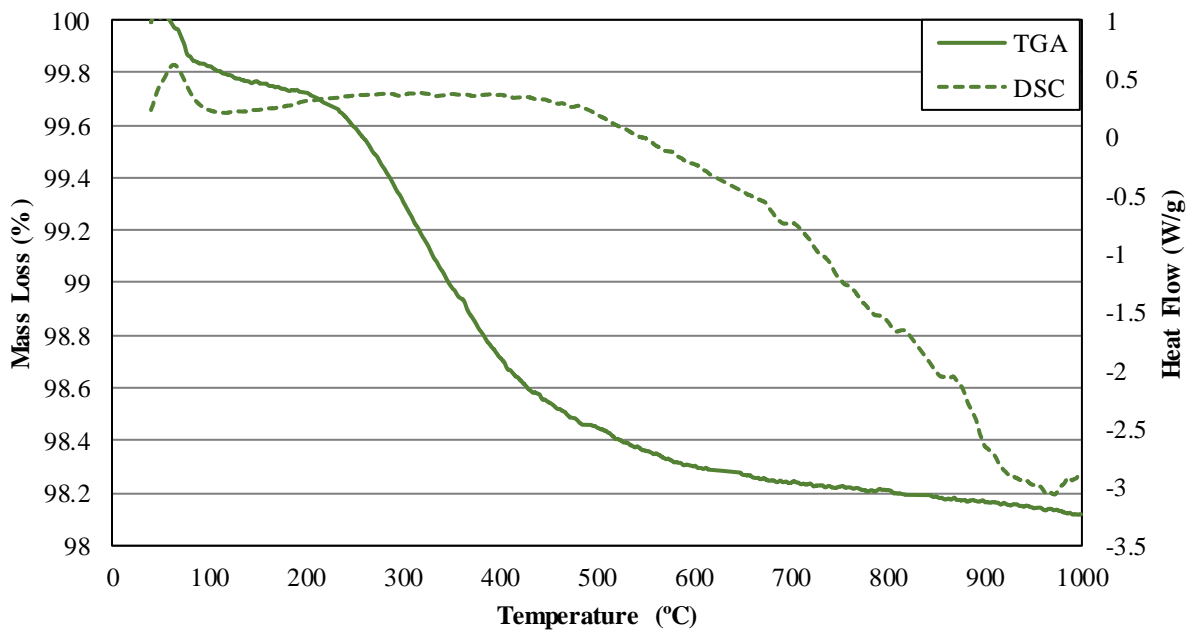*Figure C.9: DSC/TGA plot of RM-S*
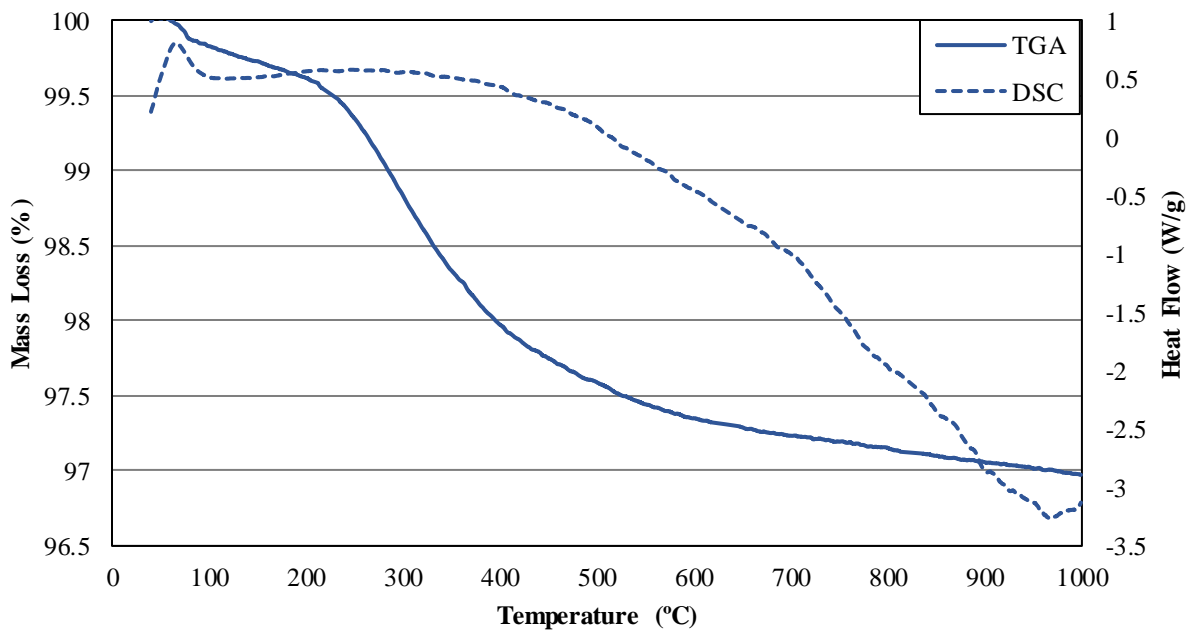

Figure C.10: DSC/TGA plot of P-B

Figure C.11: DSC/TGA plot of P-W
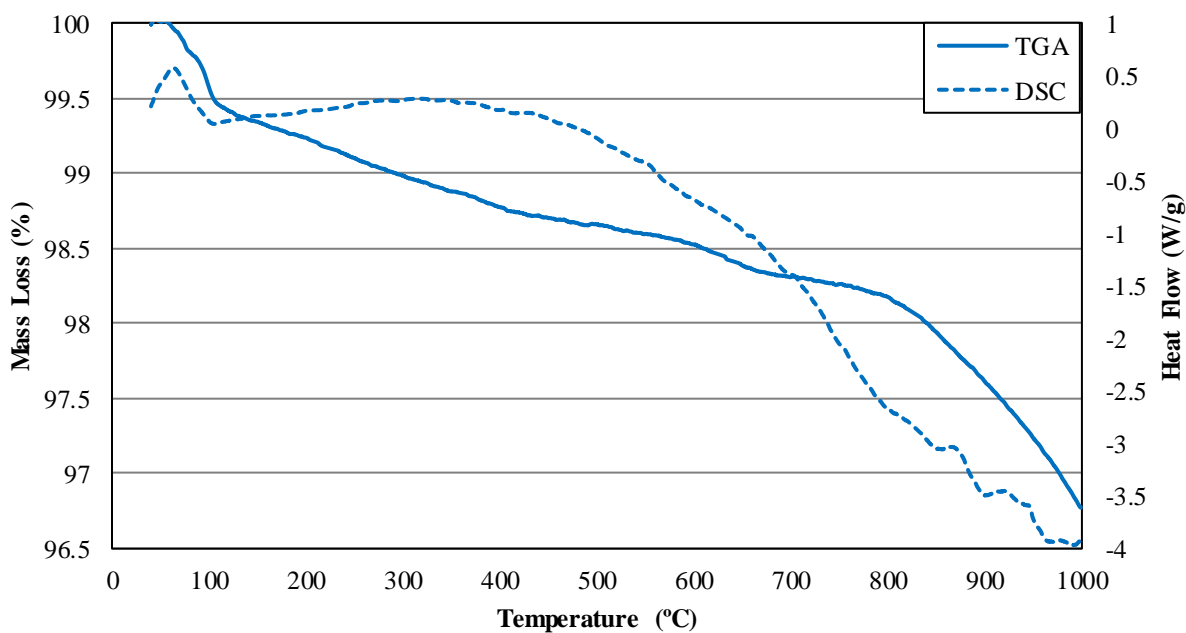
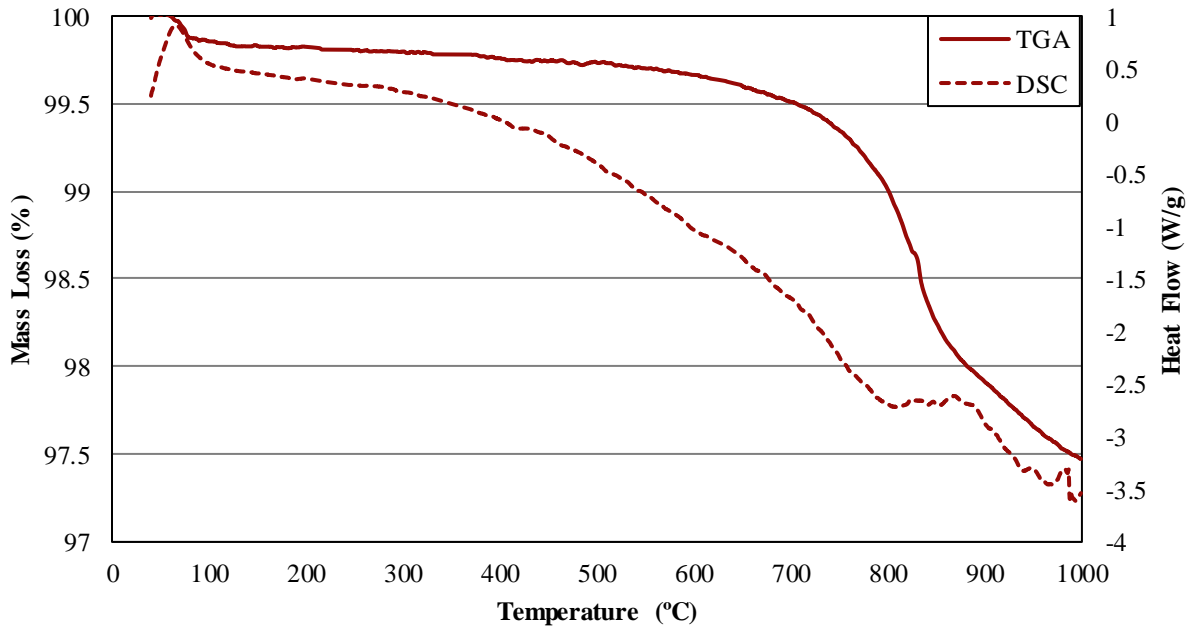## C.3 Supplier C

Figure C.12: DSC/TGA plot of RC-G
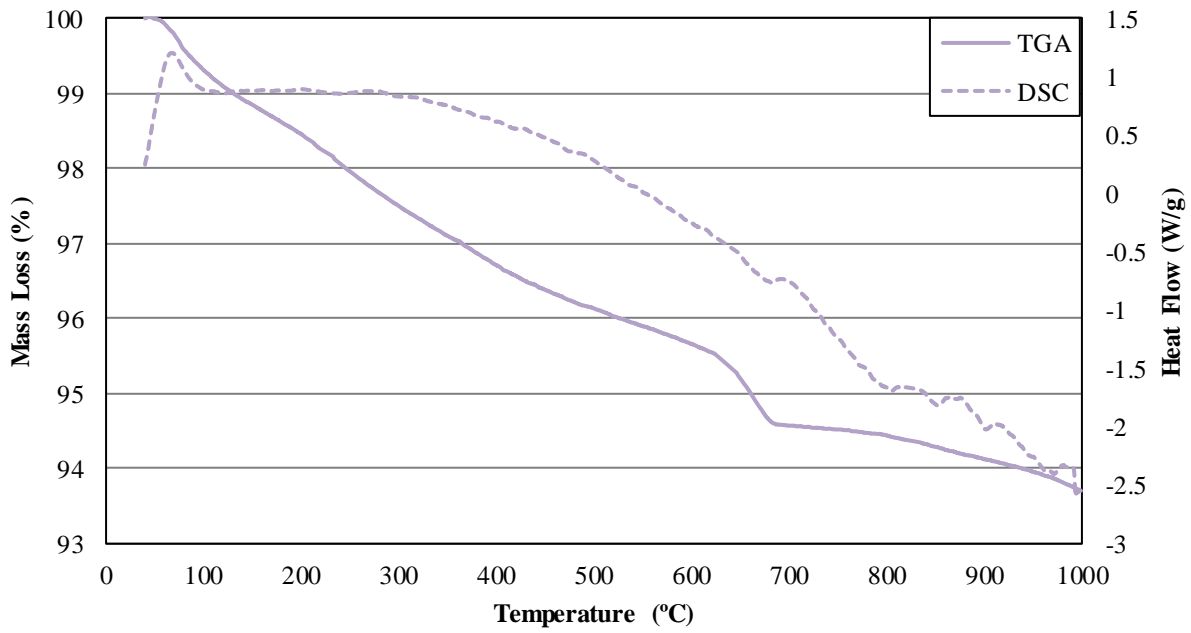
Figure C.13: DSC/TGA plot of RC-M
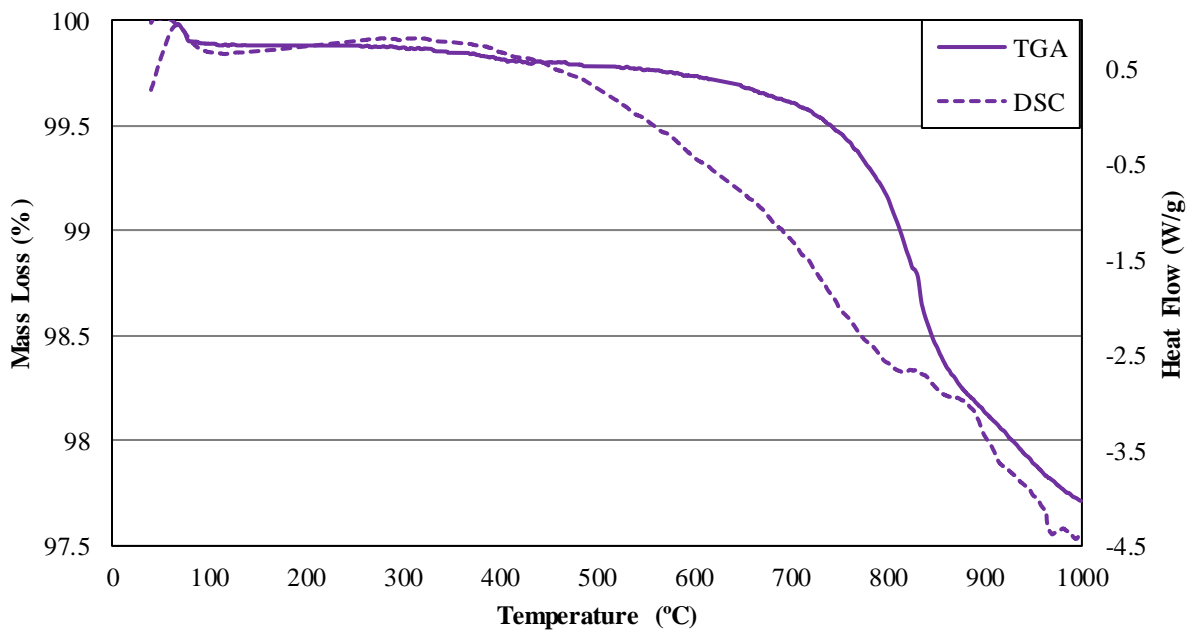

Figure C.14: DSC/TGA plot of RC-P

Figure C.15: DSC/TGA plot of RM-M

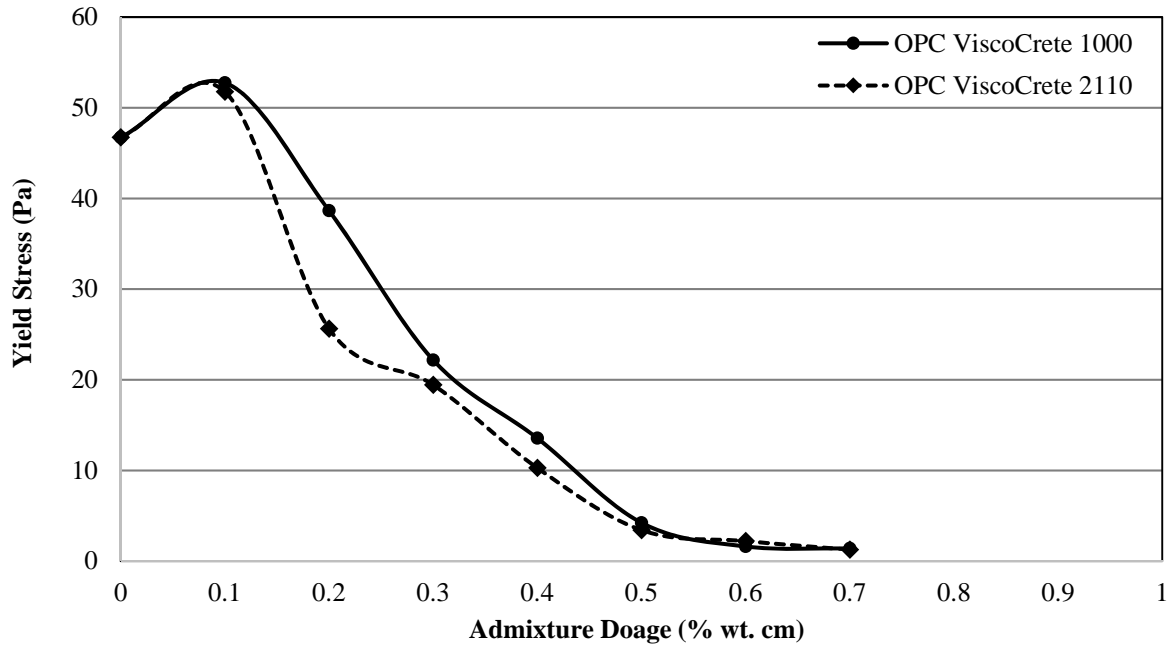# Appendix D. Admixture Interaction
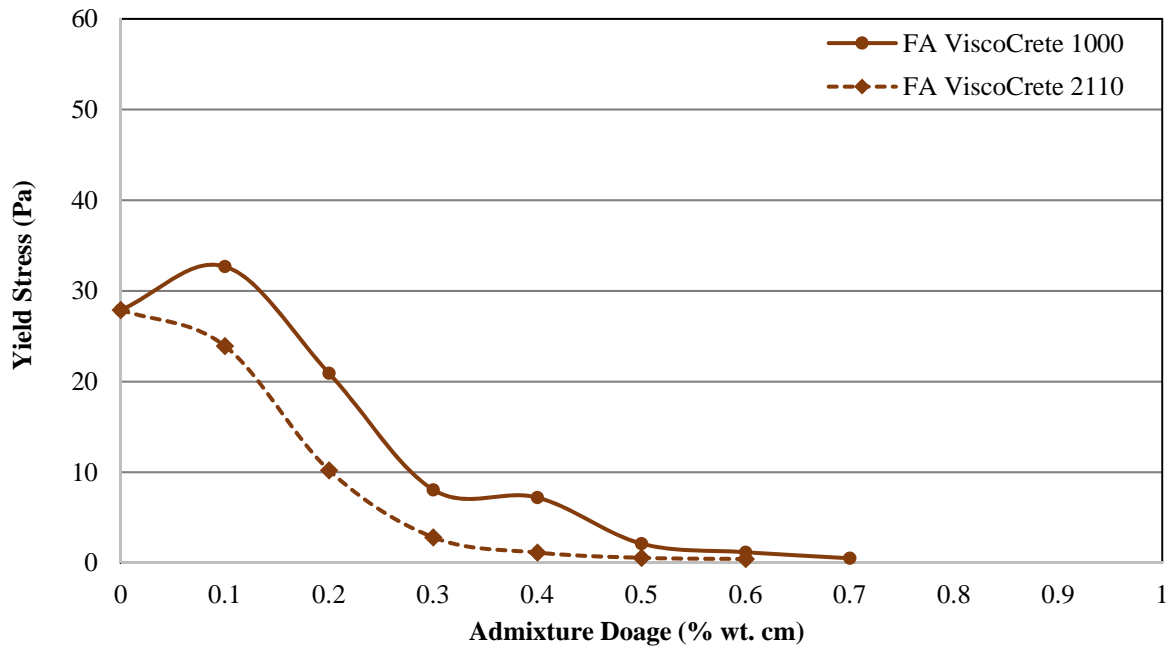

Figure D.1: Admixture Interaction of OPC

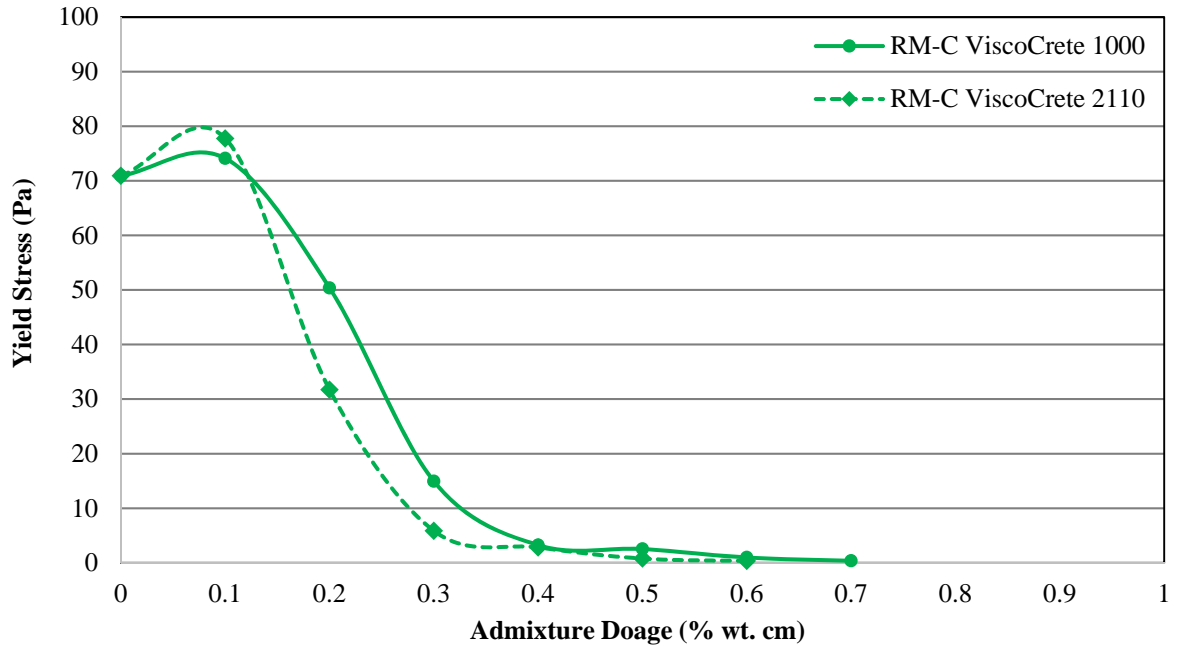*Figure D.2: Admixture Interaction of FA*

Figure D.3: Admixture Interaction of RM-C
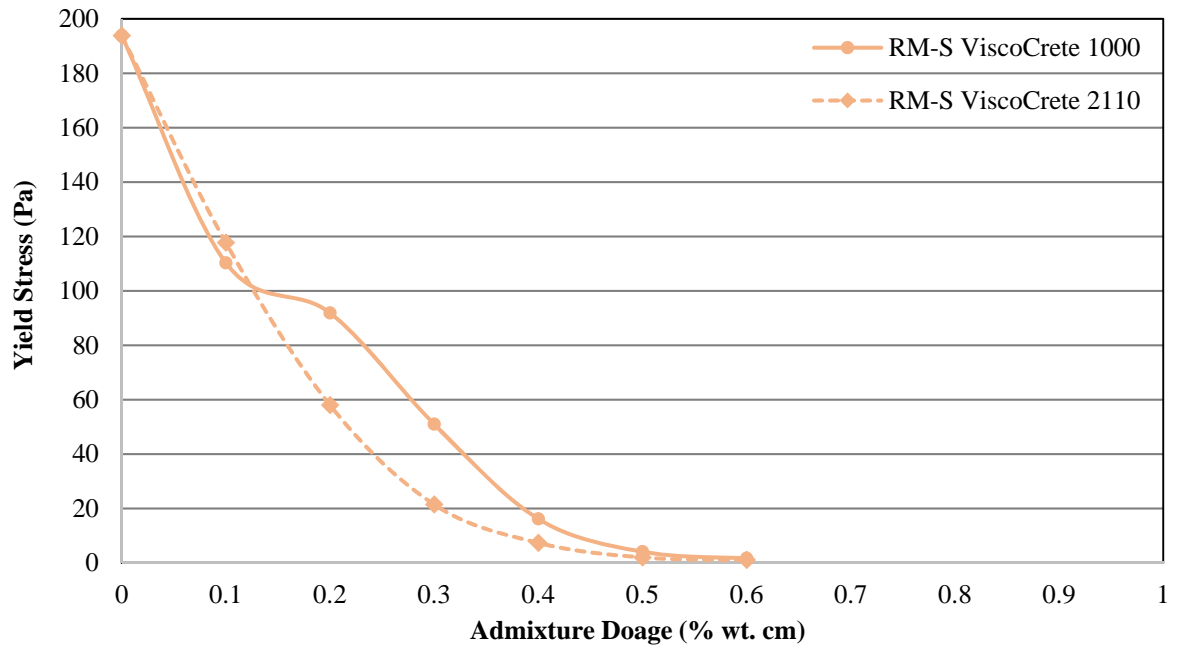
Figure D.4: Admixture Interaction of RM-S
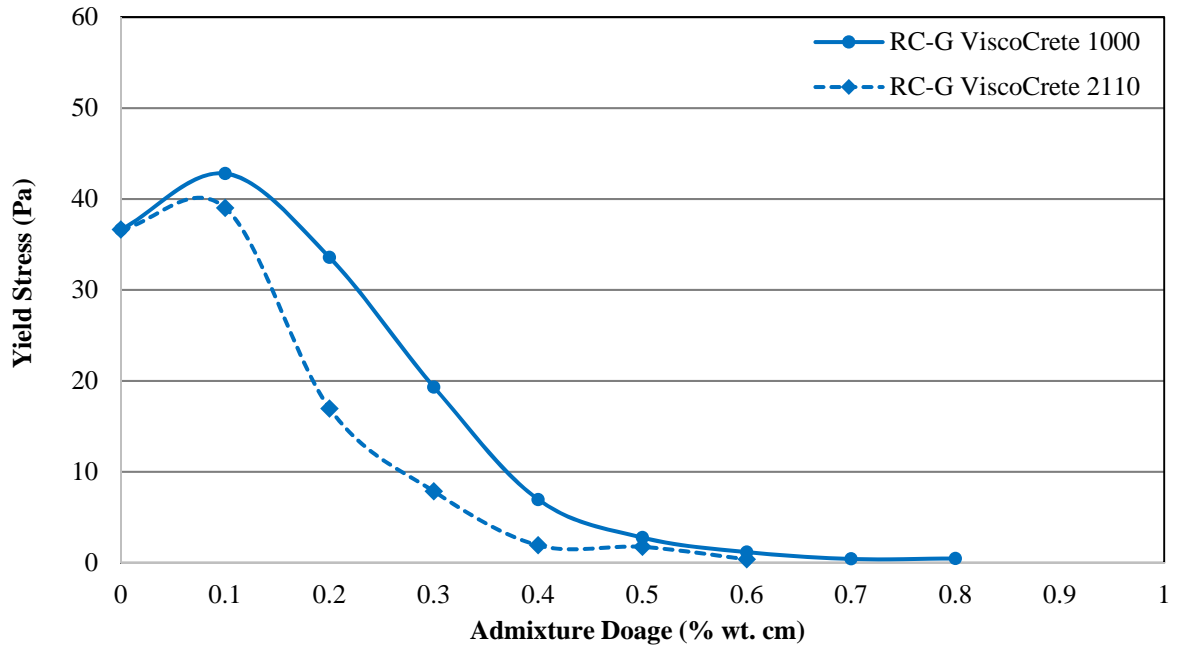
Figure D.5: Admixture Interaction of RC-G
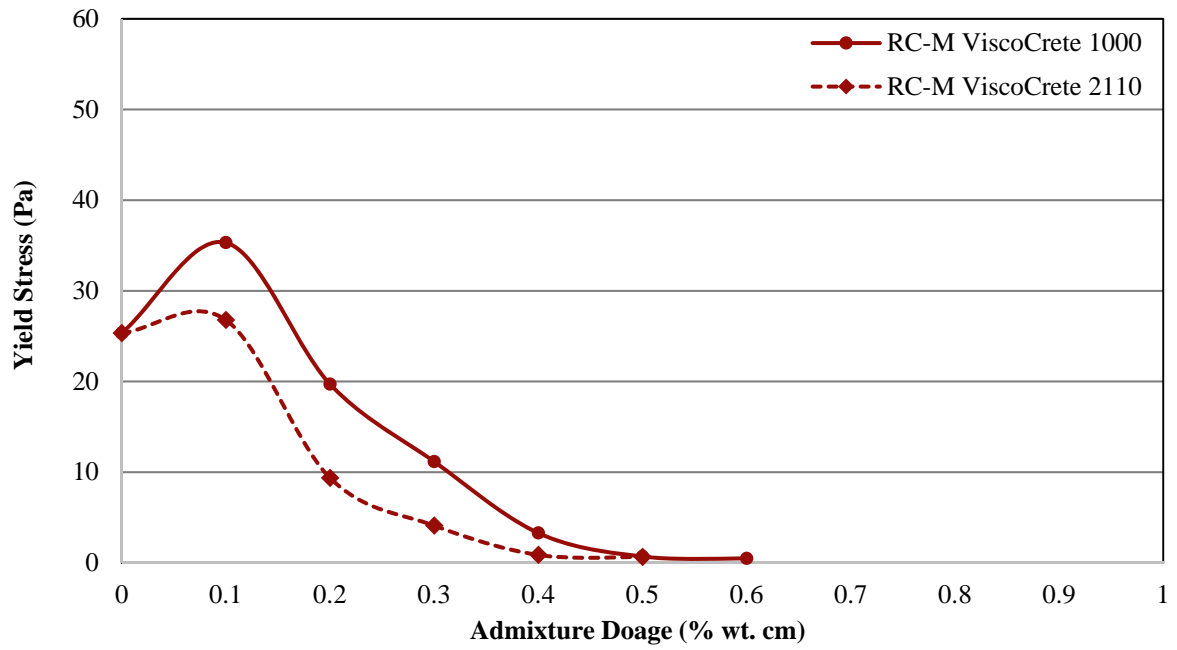
Figure D.6: Admixture Interaction of RC-M

Appendix E. Concrete Mixture Proportions

Table E.1: OPC Concrete Mixture Design

Component	Amount (lb/yd³)
OPC	564
Water	265
Coarse Aggregate	1807
Fine Aggregate	1342
Air	2 vol. %

Table E.2: FA Concrete Mixture Design

Component	Amount (lb/yd³)
OPC	451
FA	113
Water	288
Coarse Aggregate	1806
Fine Aggregate	1290
Air	2 vol. %

Table E.3: Q Concrete Mixture Design

Component	Amount (lb/yd³)
OPC	451
Q	113
Water	289
Coarse Aggregate	1805
Fine Aggregate	1301
Air	2 vol.%

Table E.4: D-S Concrete Mixture Design

Component	Amount (lb/yd³)
OPC	451
D-S	113
Water	288
Coarse Aggregate	1806
Fine Aggregate	1311
Air	2 vol.%

Table E.5: NS-I Concrete Mixture Design

Component	Amount (lb/yd³)
OPC	451
NS-I	113
Water	289
Coarse Aggregate	1806
Fine Aggregate	1309
Air	2 vol.%

Table E.6: NS-S Concrete Mixture Design

Component	Amount (lb/yd³)
OPC	451
NS-S	113
Water	289
Coarse Aggregate	1805
Fine Aggregate	1305
Air	2 vol.%

Table E.7: R-O Concrete Mixture Design

Component	Amount (lb/yd³)
OPC	451
R-O	113
Water	289
Coarse Aggregate	1805
Fine Aggregate	1310
Air	2 vol.%

Table E.8: RM-C Concrete Mixture Design

Component	Amount (lb/yd^3)
OPC	451
RM-C	113
Water	289
Coarse Aggregate	1805
Fine Aggregate	1295
Air	2 vol.%

Table E.9: RM-L Concrete Mixture Design

Component	Amount (lb/yd^3)
OPC	451
RM-L	113
Water	287
Coarse Aggregate	1803
Fine Aggregate	1300
Air	2 vol.%

Table E.10: RM-S Concrete Mixture Design

Component	Amount (lb/yd^3)
OPC	451
RM-S	113
Water	284
Coarse Aggregate	1804
Fine Aggregate	1302
Air	2 vol.%

Table E.11: P-B Concrete Mixture Design

Component	Amount (lb/yd^3)
OPC	451
P-B	113
Water	288
Coarse Aggregate	1803
Fine Aggregate	1302
Air	2 vol.%

Table E.12: P-W Concrete Mixture Design

Component	Amount (lb/yd^3)
OPC	451
P-W	113
Water	292
Coarse Aggregate	1803
Fine Aggregate	1291
Air	2 vol.%

Table E.13: RC-G Concrete Mixture Design

Component	Amount (lb/yd^3)
OPC	451
RC-G	113
Water	292
Coarse Aggregate	1803
Fine Aggregate	1296
Air	2 vol.%

Table E.14: RC-M Concrete Mixture Design

Component	Amount (lb/yd^3)
OPC	451
RC-M	113
Water	293
Coarse Aggregate	1802
Fine Aggregate	1303
Air	2 vol.%

Table E.15: RM-M Concrete Mixture Design

Component	Amount (lb/yd^3)
OPC	451
RM-M	113
Water	292
Coarse Aggregate	1803
Fine Aggregate	1302
Air	2 vol.%